eCAM Evidence-Based Complementary and Alternative Medicine

Biotechnological and Therapeutic Application of Useful Plants in Endocrinal Disorder

Lead Guest Editor: Na-Hyung Kim
Guest Editors: Vishal Chandra, Shruti Shukla, and Pradeep Kumar

Biotechnological and Therapeutic Application of Useful Plants in Endocrinal Disorder

Evidence-Based Complementary and Alternative Medicine

Biotechnological and Therapeutic Application of Useful Plants in Endocrinal Disorder

Lead Guest Editor: Na-Hyung Kim
Guest Editors: Vishal Chandra, Shruti Shukla, and Pradeep Kumar

Editorial Board

Contents

Hindawi
Evidence-Based Complementary and Alternative Medicine
Volume 2017, Article ID 3140683, 2 pages
https://doi.org/10.1155/2017/3140683

Editorial

Biotechnological and Therapeutic Application of Useful Plants in Endocrinal Disorder

Na-Hyung Kim,[1] Vishal Chandra,[2] Shruti Shukla,[3] and Pradeep Kumar[4]

[1]*Department of Oriental Pharmacy, Wonkwang University, Iksan 02404, Republic of Korea*
[2]*Department of Obstetrics and Gynecology, Stephenson Cancer Center (SCC), University of Oklahoma Health Sciences Center (OUHSC), Oklahoma City, OK, USA*
[3]*Department of Energy and Materials Engineering, Dongguk University, Seoul 100-715, Republic of Korea*
[4]*School of Biotechnology, Yeungnam University, Gyeongsan, Gyeongbuk, Republic of Korea*

Correspondence should be addressed to Na-Hyung Kim; knahyung@wku.ac.kr

Received 27 August 2017; Accepted 27 August 2017; Published 12 October 2017

The use of natural products in the remedies for health care and various diseases or traditional medicine has been around for a long time in many countries. Recent advances in the fields of natural products including various plants have been widely utilized in an aspect of biotechnology together with therapeutic applications. The active constitutes isolated or characterized from natural products have been developed as the lead ingredients of novel pharmaceuticals, alternative medicines, and nutraceuticals. Consistent efforts are being paid on treating metabolic diseases, cardiovascular diseases, carcinoma, inflammatory diseases, and infection around the world using natural products. In the current issue, we will deal with recent investigations of endocrinal disorder related to a network of glands which produce or release hormones that regulate in cell and organ of body. Endocrinal disorder in human can be induced by alterations of genetic factors and the exposure to endocrine disrupting chemicals as environmental factors has an impact on human life. We hope that biotechnological and therapeutic application of useful plants and their active constitutes may have efficacy to be developed as alternative remedies in curing endocrinal disorder in human disease.

For this special issue we invited global investigators to submit their original research and review articles involving biotechnological and therapeutic application using useful plants of natural products for controlling endocrine diseases including obesity/diabetes/hyperlipidemia related to metabolic syndrome, osteoporosis related to bone, thyroid disease, cardiovascular, or renal diseases, and hormonal growth disorders. In addition, we also invited the articles that investigate physiologic effects of the plants, its composition, and nutrients, using both *in vitro* and *in vivo* animal models, together with clinical trials. After a rigorous peer-review process, various studies on biotechnological and therapeutic application using useful plants of natural products for controlling endocrine diseases were accepted as the articles in this special issue.

Goiter, an enlargement of the thyroid gland, was reported which can be associated with a number of thyroid diseases such as thyroid dysfunction (hyperthyroidism and hypothyroidism), autoimmune thyroid disease (Graves' disease and Hashimoto's thyroiditis), thyroiditis, and thyroid cancer. L. Xiu et al. showed that HYDf and HYDp, which are two different species of Haizao Yuhu Decoction (HYD), have been widely used to treat thyroid-related diseases especially goiter with few side effects in traditional Chinese medicine (TCM), including herb pair *Sargassum* (HZ) and Glycyrrhizae Radix et Rhizoma (GC), could exhibit antigoitrous effect through alterations in hypothalamus-pituitary-thyroid (HPT) axis and inhibition of the TPO gene expression in goiter rat model.

Endometriosis is reported as a common benign disorder characterized by the ectopic growth of endometrium, affecting approximately 15% of women of reproductive age, causing chronic pelvic pain, dysmenorrheal, irregular menstrual cycle, and infertility. R.-N. Liang et al. demonstrated that Ping-Chong-Jiang-Ni formula (PCJNF), a Chinese herbal medicine (CHM), was shown to be clinically effective on endometriosis. They explored the effect of PCJNF on the

ectopic endometrial stromal cells (EESCs) from endometriosis. PCJNF could suppress cell proliferation, migration, and invasion, while increasing apoptosis in EESCs, and the suppressed proliferation and enhanced apoptosis were mediated by JNK signaling.

X. Wang et al. demonstrated that compounds from Cynomorium songaricum (CS) exhibited phytoestrogenic and phytoandrogenic activities using MCF-7 or LNCaP cells and HeLa or AD293 cells, which may contribute to inhibiting the oestrogen/androgen-induced BPH development. Y. Zhang et al. showed that Pingmu Decoction could reduce orbital preadipocytes viability, induce apoptosis of mature adipocyte via Fas/Fas L signaling pathway, and reduce lipid accumulation and downregulated the expression of PPAR γ and C/EBP α in preadipocytes of Graves' Ophthalmopathy (GO) patients from differentiating into mature adipocytes and medicinal serum which was prepared from rats.

In an aspect of osteoporosis, S.-W. Choi et al. demonstrated that barley seedling extracts (BSE) dose-dependently inhibited RANKL-induced osteoclast differentiation with alteration of IκB degradation, c-Fos, and NFATc1 molecules in the early-to-middle stages of osteoclastogenesis. Additionally, in the late phase of osteoclastogenesis, BSE also prevented DC-STAMP and cathepsin K, which are required for cell fusion and bone degradation, such as osteoclast function.

A variety of studies in this special issues could provide new insights to treat and prevent endocrinal disorders.

Acknowledgments

The editors would like to express great gratitude to all authors for their contributions and reviewers for their great help. We thanks the Editorial Board for their approval on this topic and continuous support of successful publication of this special issue.

Na-Hyung Kim
Vishal Chandra
Shruti Shukla
Pradeep Kumar

Hindawi
Evidence-Based Complementary and Alternative Medicine
Volume 2017, Article ID 3526186, 10 pages
https://doi.org/10.1155/2017/3526186

Research Article

Comparative Efficacy and Toxicity of Different Species of *Sargassum* in Haizao Yuhu Decoction in PTU-Induced Goiter Rats

Linlin Xiu, Gansheng Zhong, Dianna Liu, Shaohong Chen, Haiyan Liu, and Feng Chen

Beijing University of Chinese Medicine, Beijing, China

Correspondence should be addressed to Gansheng Zhong; 1206284369@qq.com

Received 18 November 2016; Accepted 18 May 2017; Published 21 June 2017

Academic Editor: Shruti Shukla

Background. Haizao Yuhu Decoction has been widely used to treat thyroid-related diseases especially goiter with few side effects in traditional Chinese medicine (TCM), including herb pair *Sargassum* (HZ) and Glycyrrhizae Radix et Rhizoma (GC), as one of "eighteen antagonistic medicaments." The two different species of *Sargassum*, *Sargassum fusiforme* (Sf) and *Sargassum pallidum* (Sp), are not clearly differentiated in clinical use, so that herb pair Sf-GC and Sp-GC could show different effect and toxicity. *Methods*. We investigated the antigoitrous effect and toxicity and clarified the potential underlying mechanism of the two different species of *Sargassum* in HYD (HYDf and HYDp) in PTU-reduced goiter rats. *Results*. The results demonstrated that both HYDf and HYDp could exhibit antigoitrous effect through alterations in hypothalamus-pituitary-thyroid (HPT) axis and inhibition of the TPO gene expression; there is no difference in the antigoitrous effects between the two different species of *Sargassum* application in HYD. *Conclusion*. This study evaluated the safety and efficacy of herb pair HZ-GC applied in HYD in goiter rats at molecular, cellular, and whole level and compared the two species of *Sargassum* further. We provide a reliable way to clarify the possible mechanism of the antagonistic medicament herb pair HZ-GC for its application.

1. Introduction

Goiter, an enlargement of the thyroid gland, is a common problem in clinical practice [1]. It can be associated with a number of thyroid diseases such as thyroid dysfunction (hyperthyroidism and hypothyroidism), autoimmune thyroid disease (Graves' disease and Hashimoto's thyroiditis) [2, 3], thyroiditis, and thyroid cancer [4, 5]. Regardless of varies clinical manifestation, the etiology of goiter is essentially the same: the thyroid attempting to adapt to circumstances of changes in the thyroid's ability to secrete adequate amounts of hormones [1], of which hypothyroidism is the most common in recent decade [6]. Hypothyroidism, abnormalities in thyroid hormone synthesis or thyroid dyshormonogenesis, is a common endocrine disorder [7] involved with multiple organs. The single most common cause of hypothyroidism worldwide was undoubtedly iodine deficiency. Where it is not a problem, the most common causes are chronic autoimmune thyroiditis and previous thyroid surgery or ^{131}I therapy. Its clinical characteristics are complex. Internationally, conventional drugs, such as potassium iodide and levothyroxine, are recommended for patients with hypothyroidism. However, their respective curative effects remain controversial [8].

According to traditional Chinese medicine (TCM) theory, goiter is mainly due to "Qi" stagnation and "phlegm" stasis [9]. Haizao Yuhu Decoction (HYD), which is described in a famous TCM monograph Waike Zhengzong (Summary of Surgical Medicine) in Ming Dynasty of China, has been used for approximately 500 years and famous for its efficacy in treating thyroid-related diseases especially goiter based on the clinical study [10]. It is worthwhile to mention that there is a herb pair *Sargassum* (Haizao, HZ) and Glycyrrhizae Radix et Rhizoma (Gancao, GC), one of the so-called "eighteen antagonistic medicaments" in TCM documents, indicating that the two herbs should not be applied simultaneously, whereas the herb pair HZ-GC has been widely used in HYD for the treatment of thyroid dysfunction, galactophorous hyperplasia, and ovarian cyst [11]. In recent decades, some

Table 1: Compositions of HYD.

HYDf/HYDp	海藻玉壶汤羊栖菜组/海藻玉壶汤海蒿子组		
Latin name	Chinese name	Source	Daily adult dose (g)
Glycyrrhiza uralensis Fisch.	生甘草	Root and rhizome	24
Sargassum fusiforme (Harv.) Setch. /Sargassum pallidum (Turn.) C.Ag.	羊栖菜 /海蒿子	Frond	24
Pinellia ternata (Thunb.) Breit.	法半夏	Tuber	9
Fritillaria thunbergii Miq.	浙贝母	Bulb	9
Laminaria japonica Aresch.	海带	Thallus	9
Forsythia suspensa (Thunb.) Vahl.	连翘	Fruit	9
Ligusticum chuanxiong Hort.	川芎	Rhizome	9
Angelica pubescens Maxim. *f. biserrata Shan et* Yuan	独活	Root	9
Laminaria japonica Aresch./Ecklonia kurome Okam.	昆布	Thallus	9
Citrus reticulata Blanco	青皮	Fruitlet	9
Citrus reticulata Blanco	陈皮	Pericarp	9
Angelica sinensis (Oliv.) Diels.	当归	Root	9

literature research, clinical study, and animal experiment have been carried out to evaluate the efficacy and safety of the combination [12, 13]. However, their respective curative effects and mechanisms remain controversial and there is limited scientific evidence to establish the safety and efficacy of these herbal products.

Additionally, *Sargassum fusiforme* (Yangqicai, Sf) and *Sargassum pallidum* (Haihaozi, Sp) are two different species of *Sargassum* officially recorded in the Chinese Pharmacopoeia but not clearly differentiated in clinical use. The pharmacological effects of them have been extensively studied [14], but there are few comparative studies between them.

What roles do these two different species of *Sargassum* play in the herb pair HZ-GC, and whether the different species are related to impact effects of HYD? Accordingly, we proposed the present study to systematically evaluate antigoitrous effect and toxicity and to clarify the underlying mechanism of the two different species of *Sargassum* in HYD in PTU-reduced goiter rats at molecular, cellular, and whole level.

2. Materials and Methods

2.1. Preparation of Haizao Yuhu Decoction. HYD is a decoction of 12 Chinese herbs as listed in Table 1.

As there are two species of *Sargassum*, Haizao Yuhu Decoction with the species of *Sargassum fusiforme* (HYDf) and Haizao Yuhu Decoction with the species of *Sargassum pallidum* (HYDp) were prepared separately. The rat equivalent doses were selected based on the clinical adult dosage provided by the Chinese Pharmacopoeia and calculated according to the ratio of body-surface area between human and rat.

All herbs used in the study were purchased from Beijing Shuangqiao Co., Ltd. (Beijing, China) and Anhui Tongling Co., Ltd. (Tongling, China) and authenticated in accordance with the standard of the Chinese Pharmacopoeia by Professor Li (School of Basic Medical Science, Beijing University of Chinese Medicine). The mixtures were soaked in distilled water in a ratio of 1/10 (g/ml) for 2 h and then subsequently boiled for a further 60 min. After saving the supernatant collected by filtering, the residue was added with a ratio of 1/8 (g/ml) distilled water and boiled again for a further 30 min. Finally, the two portions of aqueous extracts were pooled together and concentrated to a density of 1.0 g/ml crude herb by means of heating evaporation.

2.2. Experimental Reagents. Propylthiouracil (PTU) was purchased from Zhaohui Pharmaceutical Technology Corporation (Shanghai, China); Euthyrox was purchased from MerkKGaA (Darmstadt, Germany).

2.3. Preparation of Goiter Model and Grouping. 50 Male and female Wistar rats (180–220 g) were purchased from Charles River Laboratories, Beijing, China (Certificate of Conformity: SCXK (Beijing) 2012-0001). The animals had free access to drinking water and regular chow with a standard commercial rat feed every day and were housed in a room under controlled conditions (temperature 22 ± 2°C, humidity 50 ± 10%, and light illumination 12 h/d) (Certificate of Conformity: SCXK (Beijing) 2011-0024). Experimental protocols were approved by the Experimental Animal Care and Ethics Committees of Beijing University of Chinese Medicine.

After 3 days of acclimatization, the rats were randomly divided into 5 groups: normal, model, Euthyrox, HYDf, and HYDp groups; all rats except those in the normal control group received intragastric administration of PTU at a dosage of 0.01 g/kg daily for 14 days to induce the goitrous model according to previously reports [15] and were given different treatments for 28 days, as shown in Table 2.

2.4. Sample Collection. After 28 days of treatment, diets were removed from the cages 12 h before the animals were sacrificed. Blood samples were collected and centrifuged at 3000 ×g for 12 min to obtain serum.

Table 2: Experimental schema.

Groups	Dose	Treatment
Normal	10 ml/kg/d	Rats received only normal feeds, distilled water, and gavage normal saline (1 ml/100 g body weight/day)
Model	0.01 g/kg/ml	Rats received PTU every two days, distilled water, and gavage distilled water (1 ml/100 g/day)
Euthyrox	0.01 g/kg/ml	Rats received Euthyrox and distilled water
HYDf	12.06 g/kg/d	Rats received HYDf (1 ml/100 g/day)
HYDp	12.06 g/kg/d	Rats received HYDp (1 ml/100 g/day)

Thyroid glands, liver, and kidney were isolated, weighed, and stored at −80°C for pathological observation.

2.5. General Observations. Clinical signs and mortality were recorded twice a day (before and after treatment) throughout the study period. The body weight (BW) and rectal temperature of each rat were measured at the initiation of treatment and once a week during the study period.

2.6. Thyroid Function Assessment, Relative Organ Weights Assessment, and Biochemical Analysis. Absolute organ (thyroid gland, liver, and kidney) weights were measured and relative organ weights (organ-to-body weight ratios, g/100 g BW) were calculated.

The levels of serum free triiodothyronine (FT3), free thyroxine (FT4), thyroid stimulating hormone (TSH), and thyrotropin releasing hormone (TRH) were determined by radioimmunoassay using commercially available kits (purchased from Biosino. Inc., Beijing, China) according to manufacturer's instructions.

Serum alanine aminotransferase (ALT), aspartate aminotransferase (AST), alkaline phosphatase (ALP), blood urea nitrogen (BUN), creatinine (Cr), and uric acid (UA) were determined to assess liver and kidney function using commercially available kits (purchased from Biosino. Inc., Beijing, China) according to manufacturer's instructions.

2.7. Histopathology. After all animals had been sacrificed, thyroid glands were removed and divided into two parts; one was put in a buffer solution of 10% formalin and embedded in paraffin. Six to ten 4 μm-thick sections were prepared in a noncontiguous way and dyed with hematoxylin-eosin (H-E); the stained areas were viewed using an optical microscope to assess the pathologic alterations of thyroid tissues in different groups and to evaluate the effects of the treatments.

Another one was immediately stored in liquid nitrogen at −80°C for real-time reverse transcription-polymerase chain reaction (RT-PCR) analysis.

2.8. RT-PCR Analysis. Thyroglobulin (Tg) mRNA and thyroid peroxidase (TPO) mRNA expression were determined using RT-PCR. Total RNA was extracted from thyroid glands using the Trizol reagent (Invitrogen, USA). RNA yields and purity were assessed by spectrophotometric analysis (Spectronic Unicam, USA). Total RNA (1 μg/μl) transcription was performed using an in vitro transcription Kit (PrimeScript RT reagent Kit Perfect Real Time, TaKaRa, Japan). RT-PCR reactions were performed with 20 μl reactions that consisted of 10 μl 2x Taq PCR MasterMix (Solalbio, Beijing, China), 0.5 μl PCR forward primer (10 μM), 0.5 μl PCR reverse primer (10 μM), 3 μl cDNA, 0.5 μl GAPDH forward primer, 0.5 μl GAPDH reverse primer, and 5 μl double-distilled water. The PCR cycling conditions comprised a denaturation step for 3 min at 94°C, followed by 34 cycles of denaturation (94°C for 30 s), annealing (65°C for TPO, 62°C for Tg and 56°C for GAPDH for 30 s), and extension (72°C for 1 min). After the last cycle, all PCR products were subjected to a final extension for 8 min at 72°C. The primer sequences were shown in Table 3.

Table 3: The primer sequences.

Primer	Sequence (5′ to 3′)	Length
TPO	FW: CTCCACGGATGCACTATCAG RV: TTCTACCGA CGGAGGACAGA	180 bp
Tg	FW: GTGAACGCCTCTGTGACAGA RV: ACGAAACCTGAGGACCGTCT	280 bp
GAPDH	FW: TTCACCACCATGGAGAAGGC RV: ACTGTACGGCGGACCTCTTT	430 bp

PCR products were combined and then electrophoresed on 1.5% agarose gels containing ethidium bromide; data analysis was carried out using Alpha Ease FC software (Alpha Intech, USA). Values obtained for Tg and TPO were normalized against values obtained for GAPDH, and the results were expressed as relative integrated intensity.

2.9. Statistical Analysis. The data was analyzed using the SPSS 21.0 software and expressed as the mean ± standard deviation (SD). Differences between groups were examined for statistical significance using one-way analysis of variance (ANOVA; SPSS 20.0 for Windows; SPSS Inc., USA). The results were considered statistically significant when $P < 0.05$.

3. Results

3.1. Body Weight and Temperature Changes in PTU-Induced Goiter Rats. Body weight of rats was increased in a time-dependent manner (Figure 1(a)). PTU treatment for 14 days resulted in marked decreases in body weight and rectal temperature (Figure 1).

There were statistical increases of body weight in Euthyrox, HYDf, and HYDp treatment groups compared to the model group after 28 days drug treatment ($P < 0.05$).

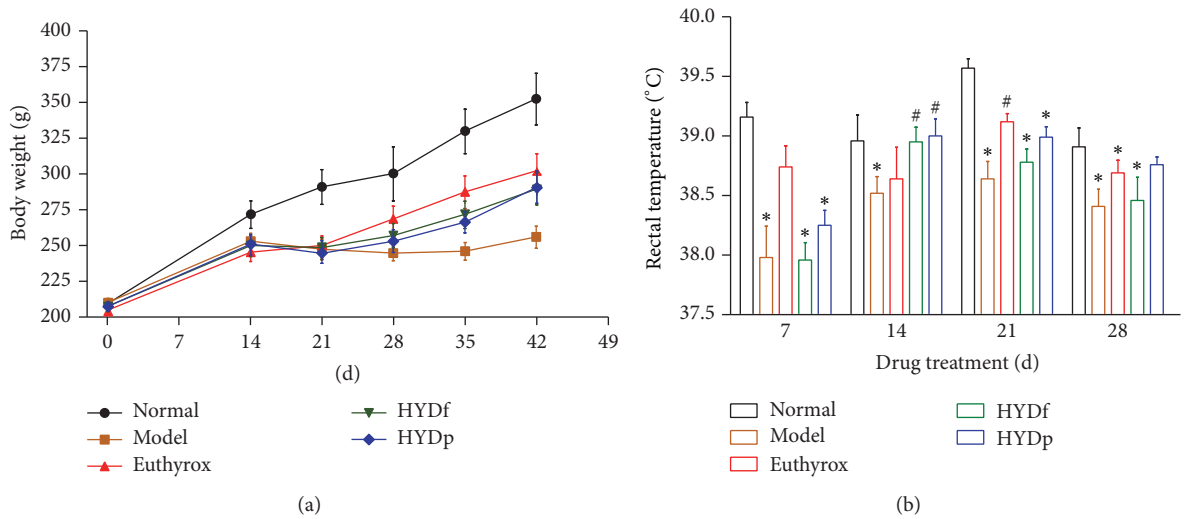

FIGURE 1: (a) Mean body weight changes in PTU-induced goiter rats. (b) Temperature changes in PTU-induced goiter rats after 28-day drug treatment. Data are presented as mean ± SD, $^{*}P < 0.05$ versus normal; $^{\#}P < 0.05$ versus model.

However, no difference was observed on body weight change in HYDf and HYDp.

After drug treatment for 28 days, there were obvious decreases of rectal temperature in the model, Euthyrox, and HYDf treatment groups compared to the normal group ($P < 0.05$). The rectal temperature of HYDp treatment group was statistically higher than that of HYDf treatment group ($P < 0.05$).

3.2. Comparison of Relative Thyroid Weights and Serum Levels of FT3, FT4, TSH, and TRH. Relative thyroid weights of model group were significantly increased ($P < 0.01$), its serum FT4 levels were significantly lower than those of the normal controls ($P < 0.01$), and serum TSH levels were higher than those of the normal controls ($P < 0.05$), indicating the successful production of PTU-induced hypothyroidism goiter model (Figure 2).

Euthyrox, HYDf, and HYDp showed a significant effect on the PTU-induced goiter rats after 28-day treatment (Figure 2(a)). In addition, thyroid enlargement was suppressed significantly in HYDf and HYDp treatment groups compared to Euthyrox group ($P < 0.01$).

The reduced levels of FT4 in the serum of goiter rats could be increased by Euthyrox, HYDf, and HYDp ($P < 0.01$; $P < 0.05$, Figure 2(c)). In addition, the elevated serum levels of TSH and TRH in goiter rats were decreased by their treatments ($P < 0.05$, Figures 2(d) and 2(e)).

3.3. Comparison of Some Liver/Renal Function Parameters. Compared to the normal controls, relative liver/kidney weights of model group were decreased ($P < 0.05$, Figure 3), and its serum activities of AST and Cr were obvious higher ($P < 0.05$); serum UA and Cr levels of Euthyrox treatment group were higher ($P < 0.01$; $P < 0.05$); relative liver/kidney weights of the HYDf treatment group were decreased ($P < 0.05$), and its serum UA and Cr levels were higher ($P < 0.05$).

The HYDp treatment group significantly improved the relative renal weights as well as the activities of AST, ALP, and Cr compared to the goiter model group ($P < 0.01$).

Besides, compared to the HYDf treatment group, the HYDp treatment group significantly improved the relative renal weights and the serum levels of AST, ALP, UA, and Cr ($P < 0.01$).

3.4. Histological Observations of the Thyroid Gland in Different Groups. Structurally, thyroid gland in PTU-induced goiter model group showed a diffuse homogeneous pattern of follicular epithelial cells hyperplasia with limited volumes of stored colloid compared to normal control group (Figure 4). Although the physiological parameters had returned to normal values, thyroid gland in the Euthyrox treatment group did not return to a morphologically euthyroid state (Figure 4(c)), which was consistent with the results of relative thyroid weights assessment. In contrast, follicular cell hyperplasia of the thyroid gland was obviously improved by HYDf and HYDp treatment (Figures 4(d) and 4(e)); no remarkable differences were found between the two groups.

3.5. Tg mRNA and TPO mRNA Levels of Different Groups. RT-PCR analysis showed that the mRNA levels of Tg and TPO expression in thyroid tissues of the goiter model group were both higher than those in normal group ($P < 0.05$). The administration of HYDf and HYDp could markedly decrease TPO expression compared to model group ($P < 0.05$, Figure 5).

4. Discussion

Haizao Yuhu Decoction has been widely used to treat thyroid-related diseases especially goiter with few side effects in TCM. Although the mechanisms are not clear so far, it is considered as a multistep process involving thyroid hormone

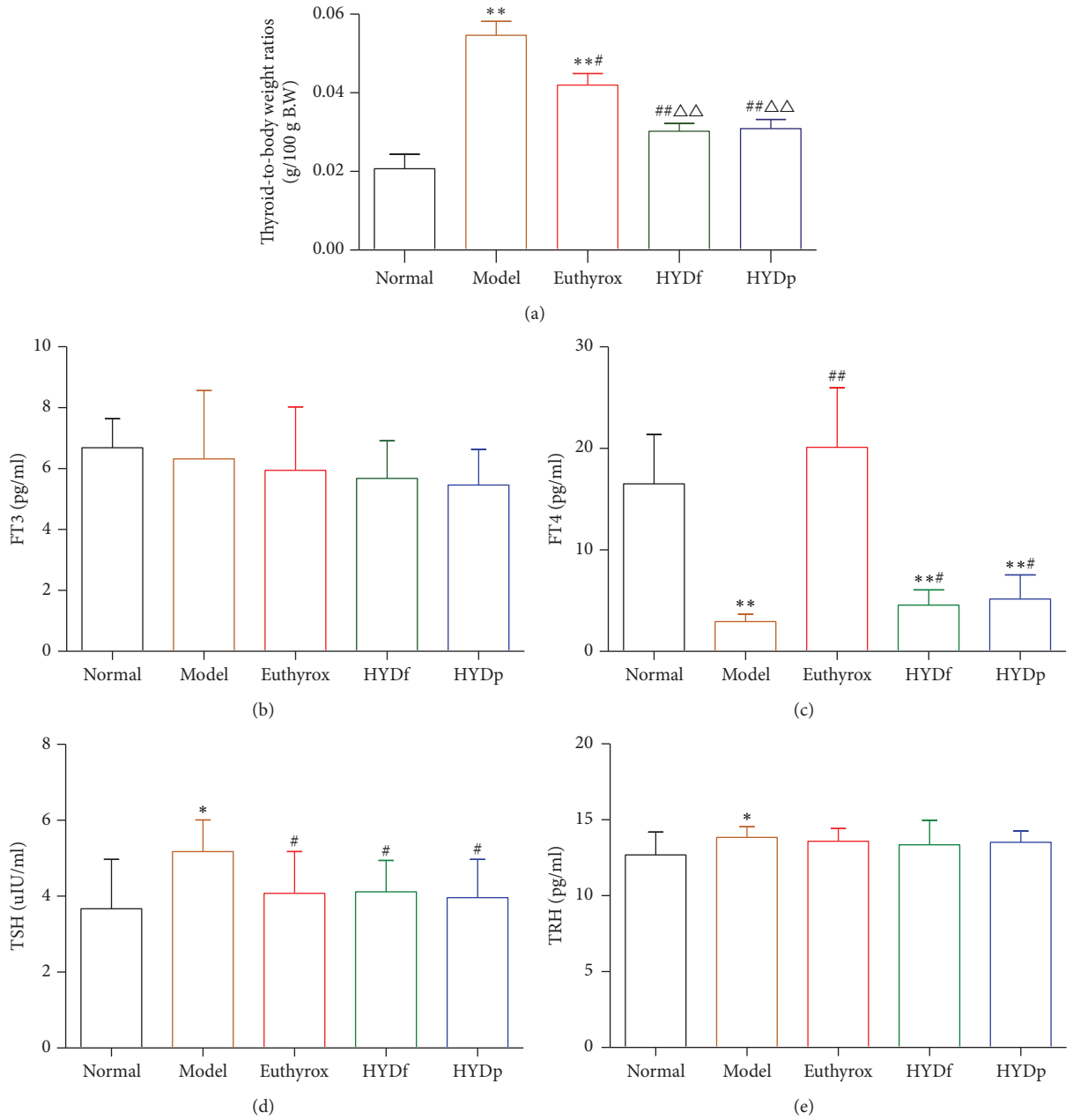

Figure 2: Comparison of relative thyroid weights (a), serum levels of FT3 (b), FT4 (c), TSH (d), and TRH (e). (a) Thyroid enlargement of goiter rats could be significantly suppressed by Euthyrox, HYDf, and HYDp treatment. HYDf and HYDp showed significant effect on the PTU-induced goiter rats, which were better than that of positive control Euthyrox. (b) No difference was observed on serum levels of FT3 change in different treatment groups. (c) The reduced serum levels of FT4 in goiter rats were increased in Euthyrox, HYDf, and HYDp treatment groups. (d), (e) The elevated serum levels of TSH and TRH in goiter rats were decreased by their treatment. Data are represented as the mean ± SD, $^{*}P < 0.05$ and $^{**}P < 0.01$ versus normal; $^{\#}P < 0.05$ and $^{\#\#}P < 0.01$ versus model; $^{\triangle\triangle}P < 0.01$ versus Euthyrox.

synthesis, antioxidative stress, and immunomodulatory effect [14, 16]. Notably, herb pair HZ-GC, as one of "eighteen antagonistic medicaments" which means that the two herbs should not be used in the same prescriptions in order to avoid mutually, has been demonstrated regulating targets into the synthesis of thyroid hormone [16], indicating the critical roles of this herb pair in HYD acting on goiter. The two different species of *Sargassum*, Sf and Sp, were studied for their pharmacological effects and acute toxicity [12]. The results of this initial study clearly demonstrated that there were marked differences in their chemical components and acute toxicity.

Therefore, we speculated that the use of different species of *Sargassum* in formula compound HYD (HYDf and HYDp) could have different pharmacological effects, accordingly, as for herb pair HZ-GC, the use of different species of

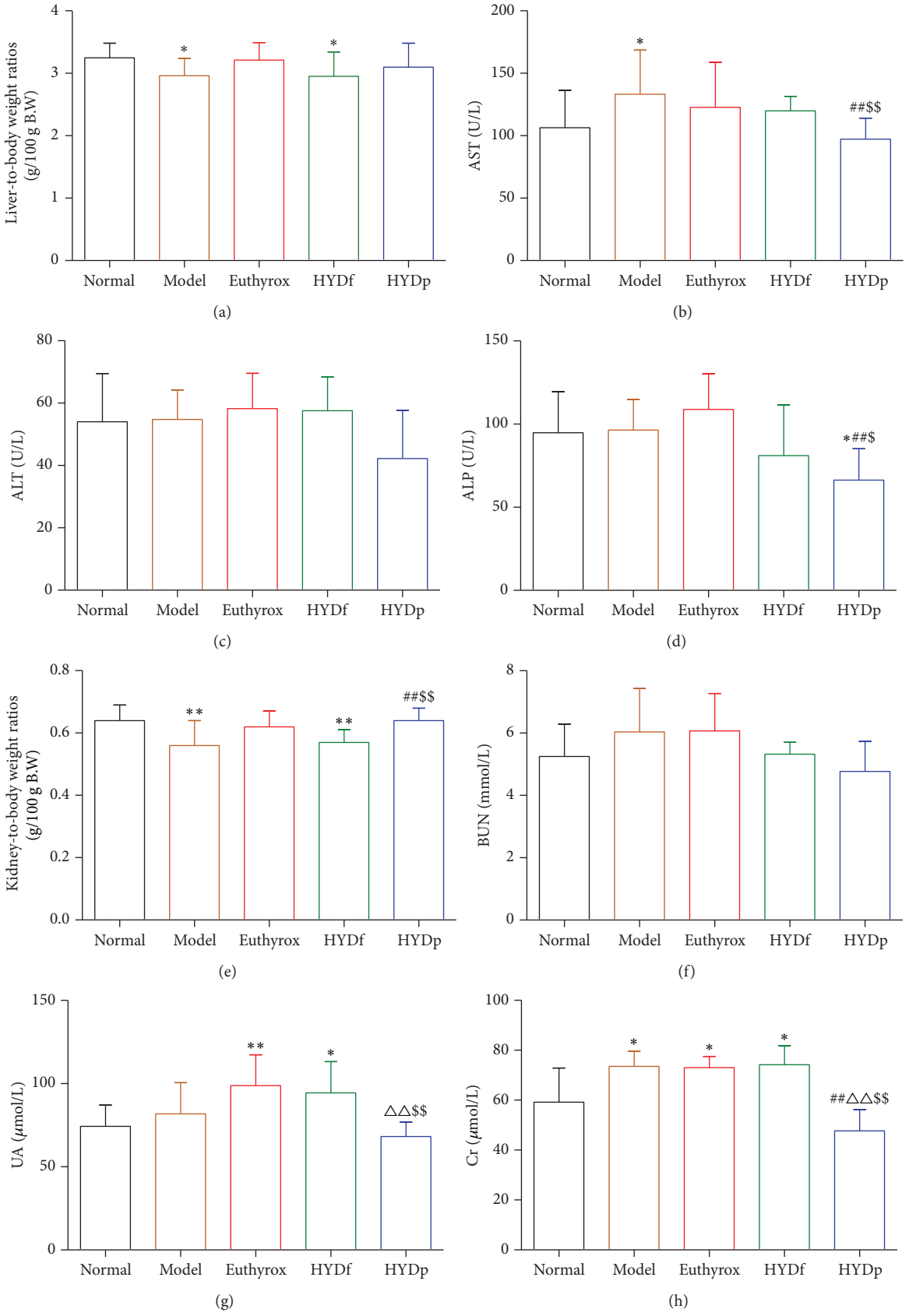

Figure 3: Comparison of relative liver weights (a), serum activities of AST (b), ALT (c), ALP (d), relative kidney weights (e), serum levels of BUN (f), UA (g), and Cr (h). Data are presented as mean ± SD, $^{*}P < 0.05$ and $^{**}P < 0.01$ versus normal; $^{\#\#}P < 0.01$ versus modle; $^{\triangle\triangle}P < 0.01$ versus Euthyrox; $^{\$}P < 0.05$ and $^{\$\$}P < 0.01$ versus HYDf.

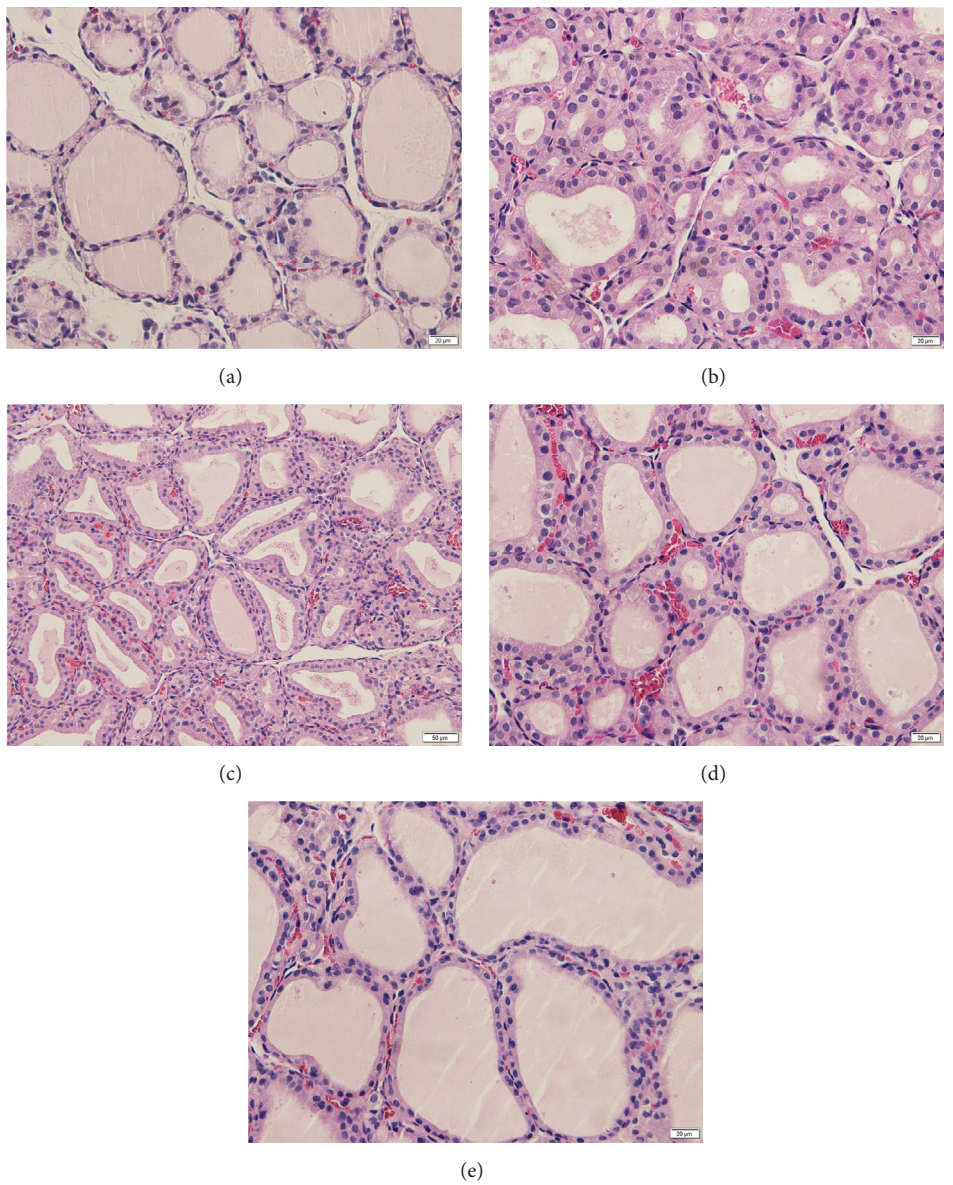

Figure 4: Histology of thyroid gland (H-E staining 400x). (a) Normal control. (b) Goiter model. (c) Goiter rats treated with Euthyrox. (d) Goiter rats treated with HYDf. (e) Goiter rats treated with HYDp.

Sargassum, herb pair Sf-GC, and herb pair Sp-GC could show different efficacy and toxicity, which might relate to the antagonistic medicament. To investigate whether the use of different species of *Sargassum* is related to antagonistic medicament, we proposed the present study to systematically evaluate antigoitrous effect (FT3, FT4, thyroid weight, and histological changes) and toxicity (liver/renal function parameters) and to clarify the potential underlying mechanism (TSH, TRH, Tg mRNA, and TPO mRNA) of the two different species of *Sargassum* in HYD (HYDf and HYDp) in PTU-reduced goiter rats.

This study showed that PTU-induced marked decreases in body weight and rectal temperature with rough hair, slow response, and impaired liver function in goiter rats, with the characteristic of thyroid enlargement and hypothyroidism. Positive control Euthyrox treatment of 28 days altered the disordered thyroid hormone of hypothyroidism but showed no antigoitrous effects accompanied with impaired renal function. In contrast, both HYDf and HYDp treatment showed antigoitrous effects by inhibition of follicular cell hyperplasia and altering the disordered thyroid hormone of hypothyroidism. However, HYDf treatment displayed liver and renal injury, whereas HYDp treatment could protect the liver and renal function.

TSH and FT4 constitute most standard thyroid function tests and play a central role in the process of diagnosis and treatment of thyroid diseases such as hypothyroidism and thyrotoxicosis [17]. The thyroid gland plays a crucial role, through thyroid hormones (TH) synthesis, in the regulation of various physiological processes, including growth,

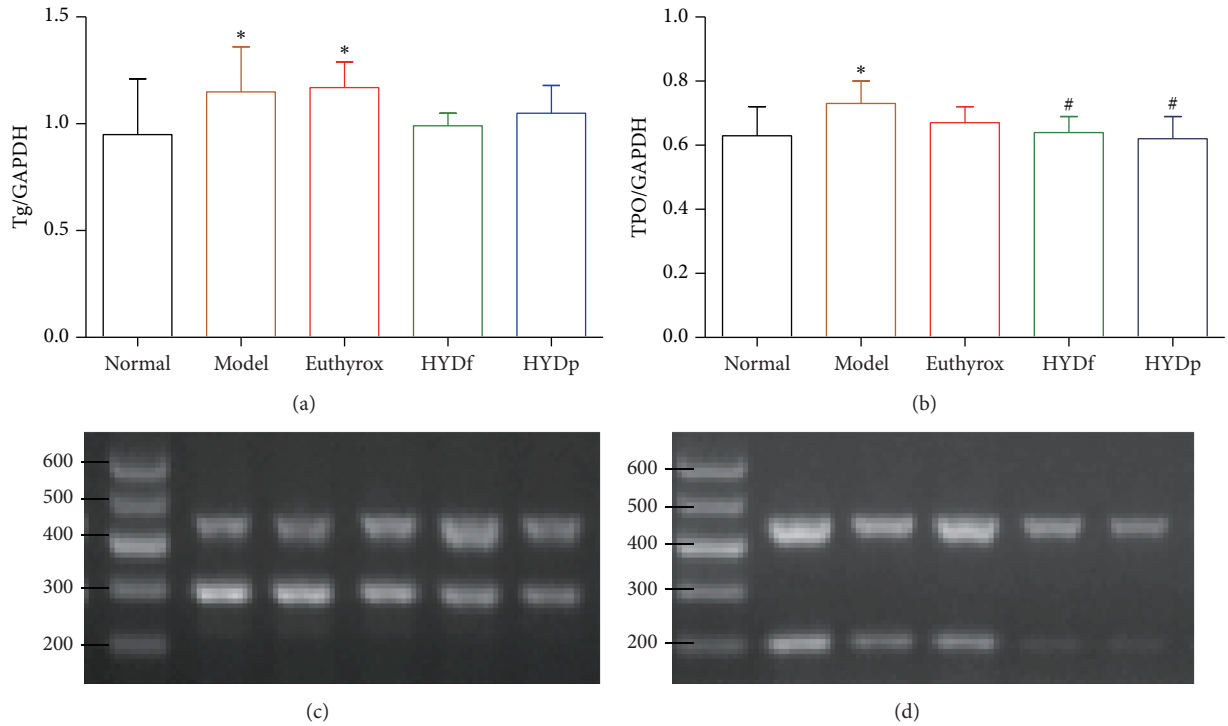

FIGURE 5: Tg mRNA (a, c) and TPO mRNA (b, d) levels of different groups. Data are presented as mean ± SD. $^{*}P < 0.05$ versus normal; $^{\#}P < 0.05$ versus model.

development, and metabolic stability. The synthesis of TH is regulated by hypothalamus-pituitary-thyroid (HPT) axis in the negative feedback loop [18]. The HPT axis constitutes the main pathogenesis of goiter, with TSH being the strongest stimulatory factor for thyroid hyperplasia and proliferation in thyroid development, growth, and function. TSH can induce the expression and activate the critical genes involved in thyroid hormone formation sodium iodide symporter (NIS), Tg, and TPO [19–21]. The initial precursor of TH is Tg. TPO catalyzes the coupling of these iodotyrosine residues to form TH [22]. It was shown in the rat thyroid that Tg stored in the follicular lumen was a potent regulator of thyroid-specific gene expression to maintain the function of individual follicles [23]. Variants in the Tg gene or TPO gene have been linked to goiter, autoimmune thyroid diseases, and thyroid cancer [24–29].

In PTU-reduced goiter rats, TH levels are reduced and TRH levels are elevated. The TRH stimulates the pituitary to produce TSH, which in turn stimulates the thyroid gland to produce thyroid hormones [30] and induces the expression of TPO and Tg gene, and eventually leads to thyroid hyperplasia and proliferation. HYDf and HYDp could exhibit antigoitrous effects by regulating TH levels through alterations in HPT axis, reducing the evaluated TSH level. TSH plays a central role in promoting thyroid cell proliferation involved in the progress of thyroid growth [31]. The decreased TSH could inhibit the expression of TPO gene, one of the causes of thyroid dyshormonogenesis leading to hypothyroidism characterized by normal synthesis of TH and aberrant protein expression as reported [32, 33].

The decrease in relative organ weights is an indication of cell constriction [34] implying that PTU and HYDf could cause cellular constriction in both liver and kidney, whereas HYDp could not produce any effect on relative liver/kidney weights investigated.

The transaminases (AST and ALT) are well-known enzymes used as biomarkers to predict possible toxicity to the liver [35]. The elevation of AST as observed in the model control suggested possible hepatic injury. Administration of HYDp lowered the elevated activities of AST comparable to the model control and indicated the liver protection effect of HYDp. Renal function indices such as serum urea, creatinine, and uric acid can be employed to assess the toxic effects of chemicals on the kidney [36]. The elevations of the indices as observed in the model, Euthyrox, and HYDf treatment rats suggested possible renal injury; HYDp showed the nontoxic and kidney protection effect.

In summary, this study demonstrated that both HYDf and HYDp could exhibit antigoitrous effect through alterations in HPT axis and inhibition of the TPO gene expression; there was no difference in the antigoitrous effects between the two different species of *Sargassum* application in HYD. HYDp showed the nontoxic and liver/kidney protection effect, but HYDf could cause cellular constriction in both liver and kidney. The reason is unclear and further analysis is needed to clarify.

There are few published reports of experimental studies of antagonistic medicament herb pair HZ-GC; this study has evaluated the safety and efficacy of its application in HYD in goiter rats at the molecular, cellular, and whole

level and compared the two species of *Sargassum* further. We provide a reliable way to clarify the possible mechanism of the antagonistic medicament herb pair HZ-GC for its application. The research on the potential mechanism is underway in our laboratory and will be reported shortly.

Conflicts of Interest

The authors declare that they have no conflicts of interest.

Acknowledgments

This study was supported by the National Natural Science Foundation of China (81573630).

References

[1] L. Hegedüs, S. J. Bonnema, and F. N. Bennedbæk, "Management of simple nodular goiter: current status and future perspectives," *Endocrine Reviews*, vol. 24, no. 1, pp. 102–132, 2003.

[2] T. H. Brix, K. O. Kyvik, K. Christensen, and L. Hegedüs, "Evidence for a major role of heredity in Graves' disease: a population-based study of two Danish twin cohorts," *Journal of Clinical Endocrinology and Metabolism*, vol. 86, no. 2, pp. 930–934, 2001.

[3] R. M. Ruggeri, S. Sciacchitano, A. Vitale et al., "Serum hepatocyte growth factor is increased in Hashimoto's thyroiditis whether or not it is associated with nodular goiter as compared with healthy non-goitrous individuals," *Journal of Endocrinological Investigation*, vol. 32, no. 5, pp. 465–469, 2009.

[4] M. Knobel, "Etiopathology, clinical features, and treatment of diffuse and multinodular nontoxic goiters," *Journal of Endocrinological Investigation*, vol. 39, no. 4, pp. 357–373, 2016.

[5] H. Yamashita, S. Noguchi, S. Watanabe et al., "Thyroid cancer associated with adenomatous goiter: an analysis of the incidence and clinical factors," *Surgery Today*, vol. 27, no. 6, pp. 495–499, 1997.

[6] B. Biondi and D. S. Cooper, "The clinical significance of subclinical thyroid dysfunction," *Endocrine Reviews*, vol. 29, no. 1, pp. 76–131, 2008.

[7] M. N. Andersen, A.-M. S. Olsen, J. C. Madsen et al., "Levothyroxine substitution in patients with subclinical hypothyroidism and the risk of myocardial infarction and mortality," *PLoS ONE*, vol. 10, no. 6, Article ID e0129793, 2015.

[8] V. Fatourechi, "Mild thyroid failure [subclinical hypothyroidism]: to treat or not to treat?" *Comprehensive Therapy*, vol. 28, no. 2, pp. 134–139, 2002.

[9] X.-H. Song, R.-Z. Zan, C.-H. Yu, and F. Wang, "Effects of modified Haizao Yuhu Decoction in experimental autoimmune thyroiditis rats," *Journal of Ethnopharmacology*, vol. 135, no. 2, pp. 321–324, 2011.

[10] Y. X. Liu, G. S. Zhong, H. Y. Liu et al., "Therapeutic effect of HaizaoYuhu decoction with/without seaweed and liquorice anti-drug combination on goiter rats in preferred dosage conditions," *Science and technology review*, vol. 33, pp. 87–91, 2015.

[11] Y. W. Li, G. S. Zhong, Q. Wang et al., "Clinical application analysis of haizaoyuhu decoction with antagonistic medicinal compatibility," *Nanjing TCM University*, vol. 27, pp. 317–321, 2011.

[12] L. L. Xiu, S. R. Wang, G. S. Zhong et al., "Research on acute toxicity of Sargassum pallidum, Sargassumfusiforme, Radix Glycyrrhiaze and HaizaoYuhu Decoction in mice," *China Journal of Traditional Chinese Medicine and Pharmacy*, vol. 31, pp. 1933–1936, 2016.

[13] T. C. Qi and T. S. Gao, "Comparative study on intervention mechanisms of iodine and haizaoyuhu decoction for goiter caused by iodine defciency," *Chinese Archives of Traditional Chinese Medicine*, vol. 30, pp. 1211–1214, 2012.

[14] Y.-W. Li, X. Yu, G.-S. Zhong et al., "Effect of different compatibility of Sargassum and Glycyrrhizae Radix in Haizao Yuhu Decoction on goiter model rats and its mechanism," *Chinese Traditional and Herbal Drugs*, vol. 45, no. 21, pp. 3124–3130, 2014.

[15] C. Laezza, G. Mazziotti, L. Fiorentino et al., "HMG-CoA reductase inhibitors inhibit rat propylthiouracil-induced goiter by modulating the ras-MAPK pathway," *Journal of Molecular Medicine*, vol. 84, no. 11, pp. 967–973, 2006.

[16] Y. Zhang, Y. Li, X. Mao et al., "Thyroid hormone synthesis: a potential target of a Chinese herbal formula Haizao Yuhu Decoction acting on iodine-deficient goiter," *Oncotarget*, vol. 7, no. 32, pp. 51699–51712, 2016.

[17] R. W. V. Flynn, T. M. MacDonald, A. D. Morris, R. T. Jung, and G. P. Leese, "The thyroid epidemiology, audit, and research study: thyroid dysfunction in the general population," *Journal of Clinical Endocrinology and Metabolism*, vol. 89, no. 8, pp. 3879–3884, 2004.

[18] M. Nilsson, "Molecular and cellular mechanisms of transepithelial iodide transport in the thyroid," *BioFactors*, vol. 10, no. 2-3, pp. 277–285, 1999.

[19] P. Kopp, "Thyroid hormone synthesis, thyroid iodine metabolism," in *In Werner and Ingbar's the thyroid, a fundamental and clinical text*, 9thed., L. Braverman, and R. Utiger, Eds., pp. 52–76, Lippincott, Williams, Wilkins, Philadelphia, Pa, USA, 9th edition, 2005.

[20] N. S. Halmi, D. K. Granner, D. J. DoughmaN, B. H. Peters, and G. Muller, "Biphasic effect of TSH on thyroidal iodide collection in rats," *Endocrinology*, vol. 67, no. 1, pp. 70–81, 1960.

[21] M. Nilsson, "Iodide handling by the thyroid epithelial cell," *Experimental and Clinical Endocrinology and Diabetes*, vol. 109, no. 1, pp. 13–17, 2001.

[22] A. Taurog, M. L. Dorris, and D. R. Doerge, "Mechanism of simultaneous iodination and coupling catalyzed by thyroid peroxidase," *Archives of Biochemistry and Biophysics*, vol. 330, no. 1, pp. 24–32, 1996.

[23] Y. Ishido, K. Yamazaki, M. Kammori et al., "Thyroglobulin suppresses thyroid-specific gene expression in cultures of normal but not neoplastic human thyroid follicular cells," *Journal of Clinical Endocrinology and Metabolism*, vol. 99, no. 4, pp. E694–E702, 2014.

[24] A. S. Alzahrani, E. Y. Baitei, M. Zou, and Y. Shi, "Metastatic follicular thyroid carcinoma arising from congenital goiter as a result of a novel splice donor site mutation in the thyroglobulin gene," *Journal of Clinical Endocrinology and Metabolism*, vol. 91, no. 3, pp. 740–746, 2006.

[25] J. Corral, C. Martin, R. Pérez et al., "Thyroglobulin gene point mutation associated with non-endemic simple goitre," *The Lancet*, vol. 341, no. 8843, pp. 462–464, 1993.

[26] C. Pérez-Centeno, R. González-Sarmiento, M. T. Mories, J. J. Corrales, and J. M. Miralles-García, "Thyroglobulin exon 10 gene point mutation in a patient with endemic goiter," *Thyroid*, vol. 6, no. 5, pp. 423–427, 1996.

[27] Y. Ban, D. A. Greenberg, E. Concepcion, L. Skrabanek, R. Villanueva, and Y. Tomer, "Amino acid substitutions in the

thyroglobulin gene are associated with susceptibility to human and murine autoimmune thyroid disease," *Proceedings of the National Academy of Sciences of the United States of America*, vol. 100, no. 25, pp. 15119–15124, 2003.

[28] A. Hishinuma, S. Fukata, S. Nishiyama et al., "Haplotype analysis reveals founder effects of thyroglobulin gene mutations C1058R and C1977S in Japan," *Journal of Clinical Endocrinology and Metabolism*, vol. 91, no. 8, pp. 3100–3104, 2006.

[29] A. Hishinuma, S. Fukata, K. Kakudo, Y. Murata, and T. Ieiri, "High incidence of thyroid cancer in long-standing goiters with thyroglobulin mutations," *Thyroid*, vol. 15, no. 9, pp. 1079–1084, 2005.

[30] A. Gökhan Özgen, G. Keser, N. Erdem et al., "Hypothalamus-hypophysis-thyroid axis, triidothyronine and antithyroid antibodies in patients with primary and secondary Sjögren's syndrome," *Clinical Rheumatology*, vol. 20, no. 1, pp. 44–48, 2001.

[31] M. C. Eggo, V. M. Quiney, and S. Campbell, "Local factors regulating growth and function of human thyroid cells in vitro and in vivo," *Molecular and Cellular Endocrinology*, vol. 213, no. 1, pp. 47–58, 2003.

[32] G. Medeiros-Neto, H. M. Targovnik, and G. Vassart, "Defective thyroglobulin synthesis and secretion causing goiter and hypothyroidism," *Endocrine Reviews*, vol. 14, pp. 165–183, 1993.

[33] G. Medeiros-Neto, M. Knobel, and L. J. DeGroot, "Genetic disorders of the thyroid hormone synthesis," in *Genetics in Endocrinology*, J. D. Baxter, Ed., pp. 375–402, Lippincott, Williams, Wilkins, Philadelphia, Pa, USA, 2002.

[34] B. M. Schmidt, N. Ilic, A. Poulev, and I. Raskin, "Toxicological evaluation of a chicory root extract," *Food and Chemical Toxicology*, vol. 45, no. 7, pp. 1131–1139, 2007.

[35] M. F. Rahman, M. K. Siddiqui, and K. Jamil, "Effects of Vepacide (Azadirachta indica) on aspartate and alanine aminotransferase profiles in a subchronic study with rats," *Human and Experimental Toxicology*, vol. 20, no. 5, pp. 243–249, 2001.

[36] T. O. Sunmonu and O. B. Oloyede, "Biochemical assessment of the effects of crude oil contaminated catfish (Clarias gariepinus) on the hepatocytes and performance of rat," *African Journal of Biochemistry Research*, vol. 1, no. 5, pp. 83–89, 2007.

Hindawi
Evidence-Based Complementary and Alternative Medicine
Volume 2017, Article ID 6489427, 10 pages
https://doi.org/10.1155/2017/6489427

Research Article

Ping-Chong-Jiang-Ni Formula Induces Apoptosis and Inhibits Proliferation of Human Ectopic Endometrial Stromal Cells in Endometriosis via the Activation of JNK Signaling Pathway

Rui-Ning Liang,[1] Pei-Shuang Li,[2] Yang Zou,[3] Yu-Ling Liu,[2] Zhen Jiang,[4] Zhen Liu,[5] Pei Fan,[6] Ling Xu,[6] Jia-Hua Peng,[1] and Xue-Yan Sun[1]

[1]*Jiangxi University of Traditional Chinese Medicine, Nanchang, Jiangxi 330004, China*
[2]*Department of Gynecology, The Affiliated Hospital of Jiangxi University of Traditional Chinese Medicine, Nanchang, Jiangxi 330006, China*
[3]*Key Laboratory of Women's Reproductive Health of Jiangxi Province, Jiangxi Provincial Maternal and Child Health Hospital, Nanchang, Jiangxi 330006, China*
[4]*Department of Gynecology & Obstetrics, Yingtan Hospital of Traditional Chinese Medicine, Yingtan, Jiangxi 335000, China*
[5]*Department of Gynecology & Obstetrics, Nankang Maternal and Child Health Hospital, Nankang, Jiangxi 341400, China*
[6]*Department of Gynecology & Obstetrics, The Second Affiliated Hospital of Jiangxi University of Traditional Chinese Medicine, Nanchang, Jiangxi 330012, China*

Correspondence should be addressed to Rui-Ning Liang; jack169@sina.com

Received 23 December 2016; Revised 22 February 2017; Accepted 13 March 2017; Published 1 June 2017

Academic Editor: Vishal Chandra

Endometriosis is a common gynecological condition in childbearing age women and its therapy in modern medicine achieves usually temporary cure. Ping-Chong-Jiang-Ni formula (PCJNF), a Chinese herbal medicine (CHM), was shown to be clinically effective on endometriosis. Meanwhile, c-Jun N-terminal kinase (JNK) signaling pathway was involved in the therapeutic process of CHM on endometriosis. Here, we explored the effect of PCJNF on the ectopic endometrial stromal cells (EESCs) from endometriosis and test whether JNK signaling was involved. After being treated with PCJNF-containing serum obtained from Sprague Dawley rat, cell proliferation, migration, invasion, and apoptosis were evaluated in EESCs, and the total and phosphorylated JNK, ERK, and p38 proteins were detected. Our results showed that PCJNF could suppress cell proliferation, migration, and invasion and induce apoptosis in EESCs. The suppressed proliferation and increased apoptosis were dependent on JNK activation. Additionally, PCJNF caused cell cycle arrest at G2/M phase and this effect was mediated by JNK signaling, while the decreased cell migration and invasion treated by PCJNF were independent of JNK signaling. In summary, our results provided the first evidence that PCJNF could suppress cell proliferation, migration, and invasion, while increasing apoptosis in EESCs, and the suppressed proliferation and enhanced apoptosis were mediated by JNK signaling.

1. Introduction

Endometriosis is a common benign disorder characterized by the ectopic growth of endometrium, affecting approximately 15% of women of reproductive age, causing chronic pelvic pain, dysmenorrheal, irregular menstrual cycle, and infertility [1]. The common therapy strategies for this disorder are involved in hormone therapy and surgical removal of endometriotic lesions, depending mainly on the patients' symptoms and desire of future fertility [2, 3]. However, these therapeutic strategies could only achieve a temporary cure; it is thus urgent to search for novel alternative therapy for this disease.

Endometriosis exhibits several features such as aberrant growth and metastasis; the development of this disorder includes a course of cell proliferation, apoptosis, invasion, and migration [4, 5]. Among which, the disrupted balance between cell proliferation and apoptosis are crucial for the development of endometriosis; furthermore, the enhanced cell invasion and migration are also crucial for the

development of this disorder [6, 7]. On the other hand, the endometrial tissue contains mainly epithelial and stromal components, among which, stroma supports and provides a regulatory role for the development and differentiation of the overlying epithelium. Furthermore, increasing studies have also suggested that endometrial stromal cells (ESCs) play essential roles in the initiation and development of endometriosis [7, 8]. For example, the stromal cells, rather than the epithelia cells, can be affected by the estradiol and progesterone, suggesting a crucial role of stromal cells played in the endometrial functions [7, 8]. It thus attracted increasing attention to explore the possible therapeutic effect of alternative therapy via targeting ESCs of endometriosis.

Accumulated evidences have shown that CHM possessed good therapeutic effects on multiple human diseases [9–11]. Also, multiple Chinese formulas have been used to treat endometriosis [1, 12–15]. Among which, PCJNF, a Chinese herbal formula, composed of eight herbs including *Ramulus Cinnamomi*, *Sanguis Draconis*, *Faeces Trogopterori*, *Pollen Typhae*, *Chinese Eaglewood*, *Whitmania pigra* Whitman, *Liriope spicata*, and *Glycyrrhiza uralensis* Fisch, had been shown to have good therapeutic effect on endometriosis in our multicentered clinical trial research [16], where we enrolled a total of 113 women with moderate/severe endometriosis and gave them PCJNF each day, continuous for 3 months without intervals; our results showed that the ratio of dysmenorrheal relief in these women was 93.81% (106/113), and the serum levels of cancer antigen 125 (CA125) and prolactin (PRL) decreased significantly after the administration.

The JNK signaling pathway can be activated by multiple stress stimuli, including drug treatments and cellular stresses, and involved in the adaptation to these stresses [17–20]. The molecular mechanisms of Traditional Chinese Medicine (TCM) therapy in human diseases usually included activation and deactivation of diverse signaling pathways [21–23], and JNK signaling pathway was found to be frequently involved in the process of TCM therapy in diverse diseases, including endometriosis [2, 24]. In the present study, we attempt to explore whether there is actual effect of PCJNF on EESCs in endometriosis and whether JNK signaling pathway is involved in the therapeutic process.

2. Materials and Methods

2.1. Animals and Ethics Statement. Forty healthy female SD rats weighing 200 ± 25 g were obtained from the Experimental Animal Center of Jiangxi University of Traditional Chinese Medicine. They were kept under specific pathogen-free conditions and fed with a standard diet and given water ad libitum, in accordance with the guidelines of the association for Assessment and Accreditation of Laboratory Animal Care, and all procedures were approved by the Animal Care and Use Committee of Jiangxi University of Traditional Chinese Medicine.

2.2. Preparation of Physiological Saline Control and PCJNF-Containing Serums. PCJNF was obtained from the Affiliated Hospital of Jiangxi University of Traditional Chinese Medicine (Nanchang, Jiangxi, China). An extract of PCJNF was obtained by decocting the dried prescription of herbs (15 g *Ramulus Cinnamomi*, 3 g *Sanguis Draconis*, 10 g *Faeces Trogopterori*, 6 g *Pollen Typhae*, 6 g *Chinese Eaglewood*, 3 g *Whitmania pigra* Whitman, 10 g *Liriope spicata*, and 6 g *Glycyrrhiza uralensis* Fisch) in 12 volumes of water (v/w) for 30 minutes and extracted twice; the suspension was collected by filtration and condensed to a concentration of 1.82 g/ml solution and stored at 4°C for experimental use. The dose of 18.2 g/kg once per day was equal to that of clinical used.

After 5 days of acclimation, these female SD rats were randomly divided into a PCJNF group ($N = 20$) and a physiological saline control group ($N = 20$). Rats were treated for 2 weeks: each rat in the PCJNF group was orally given PCJNF extract at doses of 18.2 g/kg twice per day for 7 successive days, respectively. The physiological saline control group received the equal volume of saline within the same time. After 2 hours of the final administration, rats were anesthetized with pentobarbital sodium and the blood samples were collected through the abdominal aorta. The serums were collected by centrifugation at 3,000 rpm for 10 minutes at 4°C. The serums were then isolated and subject to a 0.22 μm Millipore filter, stored at −80°C until use.

2.3. Cell Isolation and Culture. Human ectopic endometrial tissues during the luteal phase of the menstrual cycle were obtained from endometriosis samples who received no hormone treatment for >3 months, according to the guidelines of the Declaration of Helsinki, after informed consent had been obtained and with approval by the Institutional Review Board from Jiangxi University of Traditional Chinese Medicine. A total of 2 endometrial samples (35- and 42-year-old women) undergoing surgical resection were recruited and the ectopic endometrial tissues were minced into small pieces and incubated with 1 mg/mL type IV collagenase dissolved in complete culture medium for 2 hours at 37°C; the resultant digest was filtrated and centrifuged at 2,000 rpm for 10 minutes; the obtained pellets were collected and grown in complete culture medium, as described previously [5, 25]. The isolated primary EESCs were cultured in DMEM/F12 with 10% FBS, containing 100 IU/mL penicillin and 50 mg/mL streptomycin. Cells were treated with DMSO, saline control serum (NS), NS plus the selective JNK inhibitor SP600125 (300 μM, dissolved in DMSO), PCJNF serum (PCJNF), and PCJNF plus JNK inhibitor SP600125 (300 μM, dissolved in DMSO) 48 h prior to the experiment, respectively.

2.4. Immunocytochemistry. Cells seeded on 6-well chamber slides were firstly fixed with 4% paraformaldehyde; 0.75% H_2O_2 dissolved in methanol was used to block the endogenous peroxidase activity for 15 minutes at room temperature. Cell characterization of the isolated cells were evaluated by using immunostaining of mouse anti-vimentin (sc-73258, 1 : 500) (Santa Cruz Biotechnology, Santa Cruz, CA, USA) and cytokeratin (sc-53264, 1 : 500) (Santa Cruz Biotechnology, Santa Cruz, CA, USA). The purity of the isolated EESC was assessed with light microscopy.

2.5. Immunoblot Analysis. Cells were lysed by NP-40 with protease inhibitors and phosphatase inhibitors; the

proteins were separated via SDS-PAGE electrophoresis, transferred onto nitrocellulose membranes, and then incubated with primary and secondary antibodies, respectively. Primary antibodies against JNK1/2/3 (YT2441) (1 : 1000) and phospho-JNK1/2/3 (phospho Thr183/Y185) (1 : 1000) were obtained from ImmunoWay Biotechnology (Newark, DE, USA). Primary antibodies against ERK (ab196883, 1 : 1000), p-ERK (ab50011, 1 : 5000), p38 (ab27986, 1 : 1000), and p-p38 (ab45381, 1 : 5000) were purchased from Abcam (Abcam, Cambridge, MA, United States). The JNK inhibitor SP600125 was obtained from Santa Cruz Biotechnology (Santa Cruz, CA, USA). The immunoreactive bands were detected with an enhanced chemiluminescence detection system from Pierce (Thermo Fisher Scientific Inc., Rockford, IL, USA). Protein band was analyzed with Quantity One software (Bio-Rad Laboratories, Life Science Research, CA, USA). Protein levels were normalized to that of the internal control β-actin purchased from Abcam (Cambrige, MA, USA) (ab8226, 1 : 1000).

2.6. Cell Proliferation Assays. The Cell Counting Kit-8 (CCK8) assay was used to assess cell proliferation according to the manufacturer's instructions (Dojindo Laboratories, Tokyo, Japan). Briefly, 2×10^3 cells/well were seeded in 96-well plates, and 10 μL of CCK8 reagent was added to each well. After incubation of 3 hours, optical density (OD) value was determined with a spectrophotometry at wave length of 450 nm. Each assay group was performed in triplicate.

2.7. Transwell Cell Migration and Invasion Assays. The transwell assays were used to evaluate the migrative and invasive capacities of EESCs. The transwell chambers with 8 μm pores were obtained from Corning (Corning, NY, USA). Aliquots of 2×10^3 cells in serum-free DMEM (100 μL) were seeded into the upper compartments of the 24-well plate; the lower chambers were filled with DMEM containing 10% FBS. After 24 hours of incubation, the migrated cells were fixed with methanol, stained with crystal violet, and counted under a light microscope (Olympus IX71, Japan). An average of five visual fields was examined. For the invasion assay, the upper chamber was precoated with 60 μL Matrigel (1 : 8 dilution; BD Bioscience San Jose, CA, USA) and performed the same protocol as described above.

2.8. Cell Apoptosis Assay. Cell apoptosis was evaluated using Annexin V-fluorescein isothiocyanate (FITC) Apoptosis Detection Kit (556547, BD Biosciences, Franklin Lakes, NJ, USA) with flow cytometry (FCM). Briefly, cells were pretreated with JNK inhibitor (SP600125, 300 μM, dissolved in DMSO) for 1 hour and then treated with PCJNF-containing serums. After 24 hours, cells were stained with 5 μL FITC-conjugated Annexin V and 5 μL propidium iodide (PI) for 15 minutes in the dark. Cell apoptosis was analyzed by Cytomics™ FC500 flow cytometer (Beckman Coulter, Miami, FL, USA). A collection of 10,000 events were analyzed in three independent experiments.

2.9. Cell Cycle Analysis. EESCs were treated with PCJNF and different controls for 48 h in complete medium. The cells were trypsinized into single cells and then fixed in 70% (v/v) ethanol at 4°C overnight. After centrifugation, cells were washed with cold PBS and stained with propidium iodide (PI) according to the manufacturer's protocol with minor revision. After incubation for 30 min in a dark room, cell cycle distribution was analyzed by flow cytometry (Beckman Coulter, Miami, FL, USA) using MultiCycle software (Beckman Coulter).

2.10. Statistical Analysis. All data were presented as mean ± SD. Statistical analysis was performed using SPSS version 18.0 (SPSS Inc., Chicago, IL, USA). Student's t-test was used for comparisons between the two groups, and one-way ANOVA was used for multiple comparisons. P values < 0.05 were considered statistically significant.

3. Results

3.1. Primary EESC Isolation and Characterization. The primary EESCs were stained positive with anti-vimentin, a specific marker of stromal cells [5, 26], while they were stained negative with anti-cytokeratin by immunocytochemistry, a specific molecular marker for epithelial cells (Figure 1). The purity of isolated EESCs was >95% and cells between passages 4 to 12 were adopted in the current study.

3.2. PCJNF Suppressed Proliferation of EESCs through Activation of p-JNK. EESCs were exposed to culture medium containing 5%, 10%, 20%, and 40% (v/v) concentrations of PCJNF-containing serum, respectively, to determine the potential suppressed effect and activation of JNK signaling pathway. Our results showed that 20% and 40% of PCJNF-containing serum had the best suppressed effect on cell proliferation, when compared with the untreated cells (CONT), while cell proliferation decreased after 120 hours of PCJNF-containing serum treatment in EESCs (Figure 2). Meanwhile, the level of p-JNK treated with 20% and 40% PCJNF-containing serum resulted in an obvious activation of JNK pathway when compared with several lower concentration (5% and 10%) and NS (Figure 3). We thus adopt 20% concentrations of PCJNF-containing serum in subsequent cellular functional assays. Noted that, for 6-hour pretreatment with the JNK inhibitor SP600125, it could significantly attenuate cell proliferation suppression induced by PCJNF-containing serum (Figure 4(a)) and resulted in the decrease of p-JNK level (Figure 4(b)), suggesting that PCJNF-containing serum suppressed cell proliferation of EESCs through activation of p-JNK. Furthermore, the total and phosphorylated ERK and p38 in PCJNF-treated EESCs were not affected markedly when compared with that of different controls (Figure 4(c)).

3.3. PCJNF Induced Cell Apoptosis of EESCs through Activation of p-JNK. Cell apoptosis of EESCs induced by PCJNF-containing serum was assessed by Annexin V-fluorescein isothiocyanate (FITC) Apoptosis Detection Kit with FCM. Our results showed that 20% PCJNF-containing serum significantly increased cell apoptosis when compared with "NS" group ($P < 0.01$) (Figures 5(a) and 5(b)). In addition, the

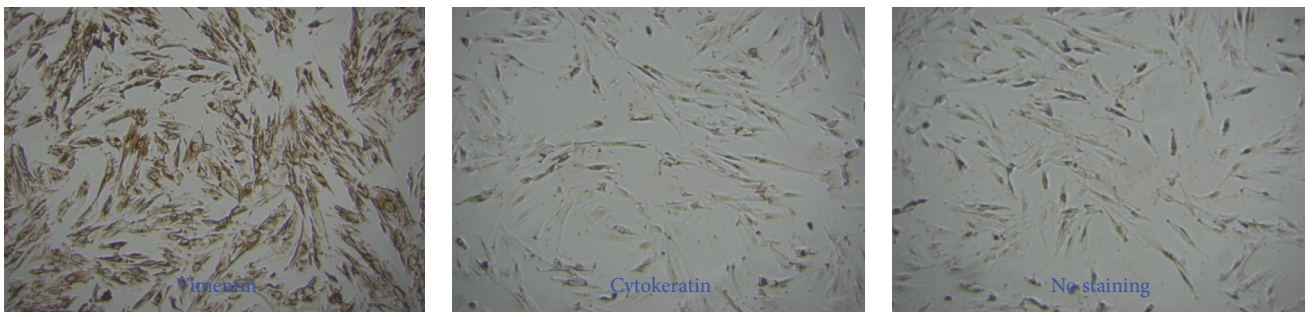

(a) (b) (c)

Figure 1: Morphological and molecular characterization of EESCs with inverted microscope and immunocytochemistry. The morphology of primary EESCs isolated from ectopic endometria of samples with endometriosis (×100) (a). Vimentin (b) and cytokeratin (c) were positively and negatively expressed in primary EESCs (×100), respectively.

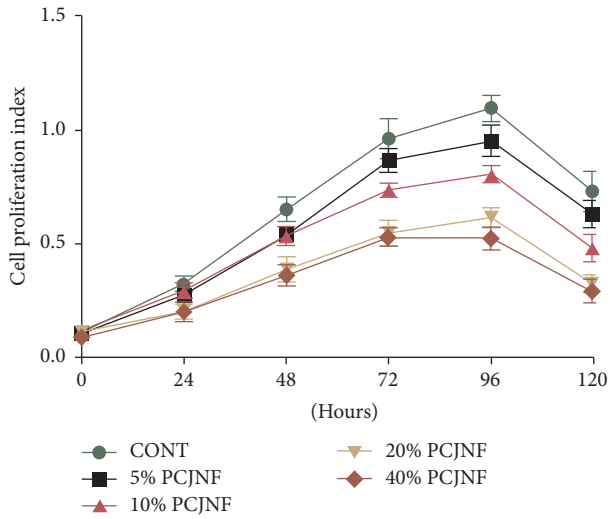

Figure 2: PCJNF suppressed cell proliferation in a concentration-dependent manner in EESCs. EESCs were exposed to different concentration of PCJNF-containing serum (5%, 10%, 20%, and 40%) for 0, 24, 48, 72, 96, and 120 h, respectively. The cell viability was assessed by CCK8 assay. Compared with the CONT group, PCJNF-containing serum suppressed cell proliferation in a concentration-dependent manner: 5% and 10% PCJNF-containing serum had low or medium suppressive effects on cell proliferation, while 20% and 40% PCJNF-containing serum resulted in significantly suppressed proliferation in EESCs. The experiment was performed in triplicate. CONT: EESCs cultured with complete medium. Data are presented as means ± SD of three independent tests.

blockage of JNK signaling with SP600125 inhibitor could significantly reverse cell apoptosis treated by PCJNF-containing serum, suggesting that PCJNF induces cell apoptosis through activation of p-JNK in EESCs ($P < 0.01$) (Figures 5(a) and 5(b)).

3.4. PCJNF Inhibited Migration and Invasion of EESCs Independent of JNK Signaling Pathway. We evaluated the migrative and invasive effects of EESCs treated by 20% of PCJNF-containing serums with transwell assays. PCJNF-containing serums could significantly inhibit the migration (Figure 6(a)) ($P < 0.01$) and invasion (Figure 6(b)) ($P < 0.01$) of EESCs relative to that of "NS" group. However, the JNK inhibitor SP600125 did not attenuate the apoptotic level of EESCs treated with PCJNF-containing serums ($P < 0.05$). These results showed that PCJNF could inhibit migration and invasion of EESCs, while these effects were independent of JNK signaling pathway.

3.5. EESCs Underwent Increased G2/M Phase Arrest after PCJNF Treatment. To evaluate whether the inhibitory cell proliferation effect of PCJNF will affect cell cycle distribution in EESCs, we applied FCM to analyze the cell cycle distribution. At 48 h after PCJNF treatment, the percentage of G2/M phase cells was significantly increased when compared with the different controls; furthermore, the JNK inhibitor SP600125 could attenuated the G2/M arrest (Figure 7). The results suggest that treatment of PCJNF on EESCs could increase G2/M phase arrest and this effect was mediated by JNK pathway.

4. Discussion

TCMs and their ingredients have been regarded as the most important therapeutic agents in China for more than 2,000 years. Based on the systematic intervention strategy, TCMs are often used in a combined form which usually composed of multiple chemical components from several herbs, which usually could strengthen the therapeutic effects or minimize the potential adverse effects of certain components [27–29]. For example, we have shown that PCJNF had good therapeutic effects in endometriosis in our prior clinical study [16]. In spite of the clinical observations, the underlying molecular mechanisms remain unexplored. The present study characterized the antiproliferation and proapoptotic properties of PCJNF in EESCs in endometriosis; moreover, we also wondered whether JNK signaling pathway was involved in the therapeutic effect of PCJNF on endometriosis.

Previous study has shown that *Ramulus Cinnamomi* might induce cell apoptosis in diabetic peripheral neuropathy [30]. Similarly, we observed that PCJNF-containing *Ramulus Cinnamomi*, the king herb of this formula, also increased cell apoptosis in EESCs markedly when compared with that

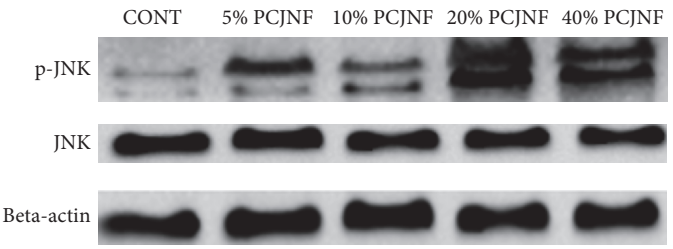

Figure 3: PCJNF induced the activation of JNK signaling pathway in EESCs. EESCs were exposed to different concentration of PCJNF-containing serum (5%, 10%, 20%, and 40%). Representative Western blot of beta-actin, total JNK, and phospho-JNK was shown. Different concentration of PCJNF-containing serum increased the expression of p-JNK but not the total JNK, indicating the activation of JNK signaling pathway. Compared with CONT group, 5% and 10% PCJNF-containing serum had certain effect on the activation of JNK pathway, while 20% and 40% PCJNF-containing serum resulted in obvious activation of JNK pathway. The experiment was performed in triplicate. CONT: complete medium.

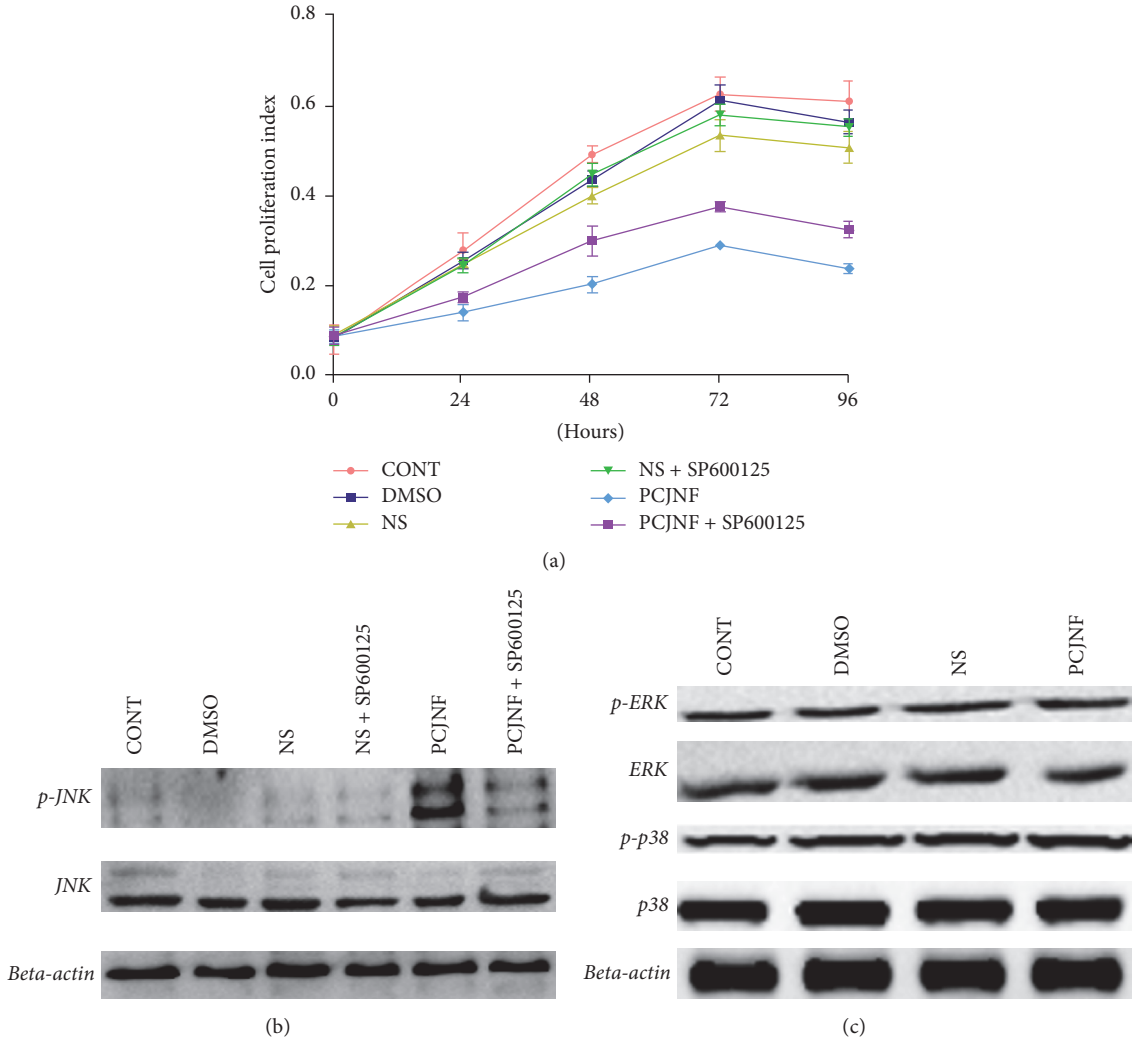

Figure 4: The suppressive effect of PCJNF-containing serum was mediated by JNK signaling pathway in EESCs. (a) EESCs were treated with 20% PCJNF-containing serum and different controls for 0, 24, 48, 72, and 96 h, respectively. The cell viability was assessed by CCK8 assay. Compared with different control groups (CONT, DMSO, and NS), 20% PCJNF-containing serum had significant suppressed effect on cell viability after 24 h, while the JNK inhibitor SP600125 attenuated this effect only after 48 h. The experiment was performed in triplicate. (b) Meanwhile, JNK inhibitor SP600125 deactivates the JNK signaling pathway in EESCs, when compared with different controls (CONT, DMSO, and NS). While there was no significant difference of cell proliferation in EESCs between the "NS" and "NS + SP600125" group ($P > 0.05$). (c) The total and phosphorylated ERK and p38 of EESCs did not change markedly, when compared with different controls. The experiment was performed in triplicate. NS: rat serum from saline treatment; PCJNF: rat serum with PCJNF treatment.

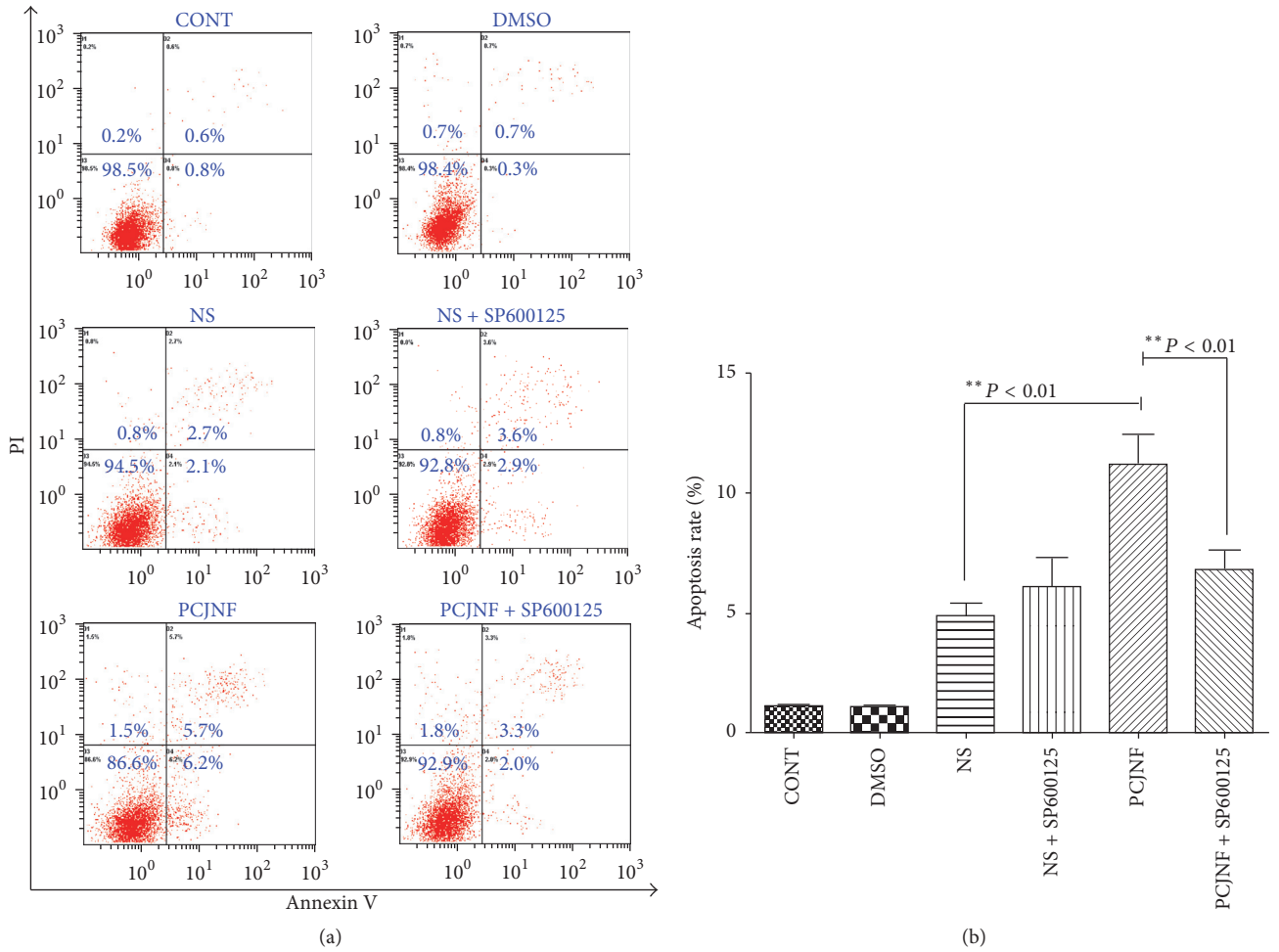

Figure 5: PCJNF induced cell apoptosis and this effect was dependent on the activation of JNK signaling pathway in EESCs. (a) Compared with different control group (CONT, DMSO, and NS), the percentage of apoptotic cells treated with PCJNF-containing serum increased significantly ($P < 0.01$), and JNK inhibitor SP600125 could significantly abrogate this effect ($P < 0.01$). There was no significant difference of cell apoptosis between the "NS" and "NS + SP600125" group ($P > 0.05$). (b) Analysis of apoptosis rates using bar graphs. Cell apoptosis was assessed by flow cytometry. Data are presented as means ± SD of three independent tests.

treated with control saline serum. Furthermore, this effect was dependent on the activation of JNK signaling pathway, which was usually involved in cell apoptosis induction under diverse stimulus. It should be noted that *Ramulus Cinnamomi* did not affect cell apoptosis in human non-small-cell lung carcinoma cell line A549 [31]; we speculated that this differential effect of *Ramulus Cinnamomi* on cell apoptosis might be cell line-specific; alternatively, the differential components between these formulas could be responsible for this discrepancy.

Previous study has shown that *Ramulus Cinnamomi* could inhibit cell proliferation in A549 lung carcinoma cell line, via inducing cell cycle arrest in G1 and G2 phases [32]. Similarly, we here showed that PCJNF inhibited significantly cell proliferation of EESCs relative to that treated with saline control serum. Here, we further showed that the suppression of cell proliferation treated with PCJNF in EESCs was JNK signaling-dependent, which showed that blockage of JNK signal could attenuate the inhibitor of cell proliferation. Furthermore, our FCM analysis results showed that PCJNF could cause significant cell cycle arrest in G2/M phase in EESCs when compared with different control groups, and JNK inhibitor SP600125 could attenuate this arrest.

Clinically, endometrial tissues might metastasize both locally and distantly and thus inhibit endometriotic cell invasion and migration might be crucial for the management of endometriosis [32–34]. Here we showed that PCJNF could effectively inhibit the migration and invasion of EESCs in vitro, suggesting that this Chinese herbal formula could be a potential alternative option for the treatment of patients with endometriosis. Furthermore, the effect of inhibitory invasion and migration effects of PCJNF on EESCs did not activate the JNK signaling pathway, implicating that some other signaling, rather than JNK signaling, was involved in the inhibitory process. It should be noted that prior studies have shown that JNK signaling pathway was involved in the process of cell invasion and migration in human disorders: it was either activated or inhibited in different cancers and/or

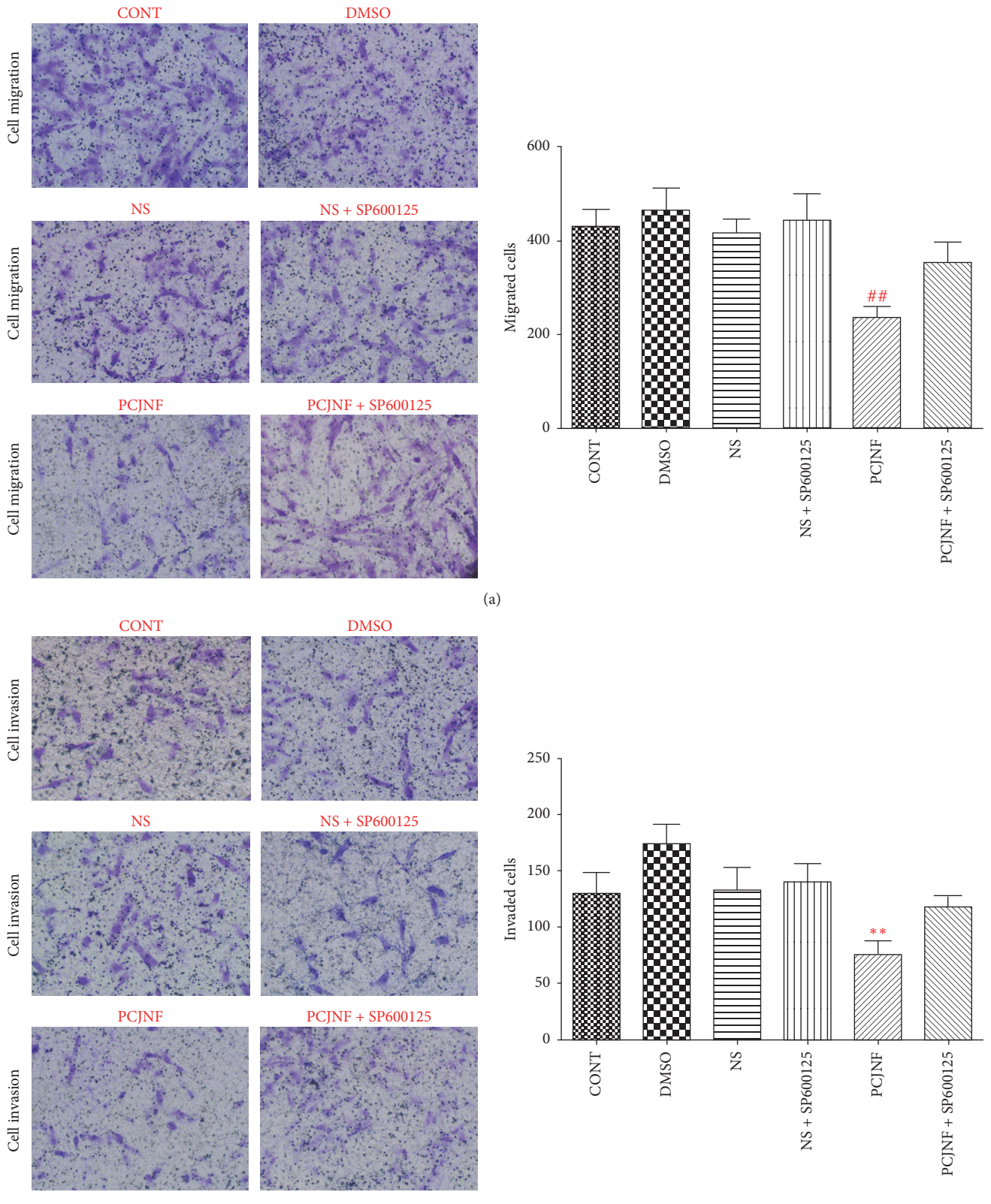

Figure 6: PCJNF decreased cell migration and invasion, while this effect was independent of the activation of JNK signaling pathway in EESCs. EESCs were exposed to different control groups (CONT, DMSO, and NS) and 20% PCJNF-containing serum, respectively. Compared with different control group (CONT, DMSO, and NS), 20% PCJNF-containing serum inhibited significantly the cell migration ($P < 0.01$) (a) and invasion ($P < 0.01$) (b) capacities in EESCs, respectively. Furthermore, JNK inhibitor SP600125 attenuated these effects obviously. Data are presented as means ± SD of three independent tests. ## and ** mean that the p values are less than 0.01 and the statistical differences are significant.

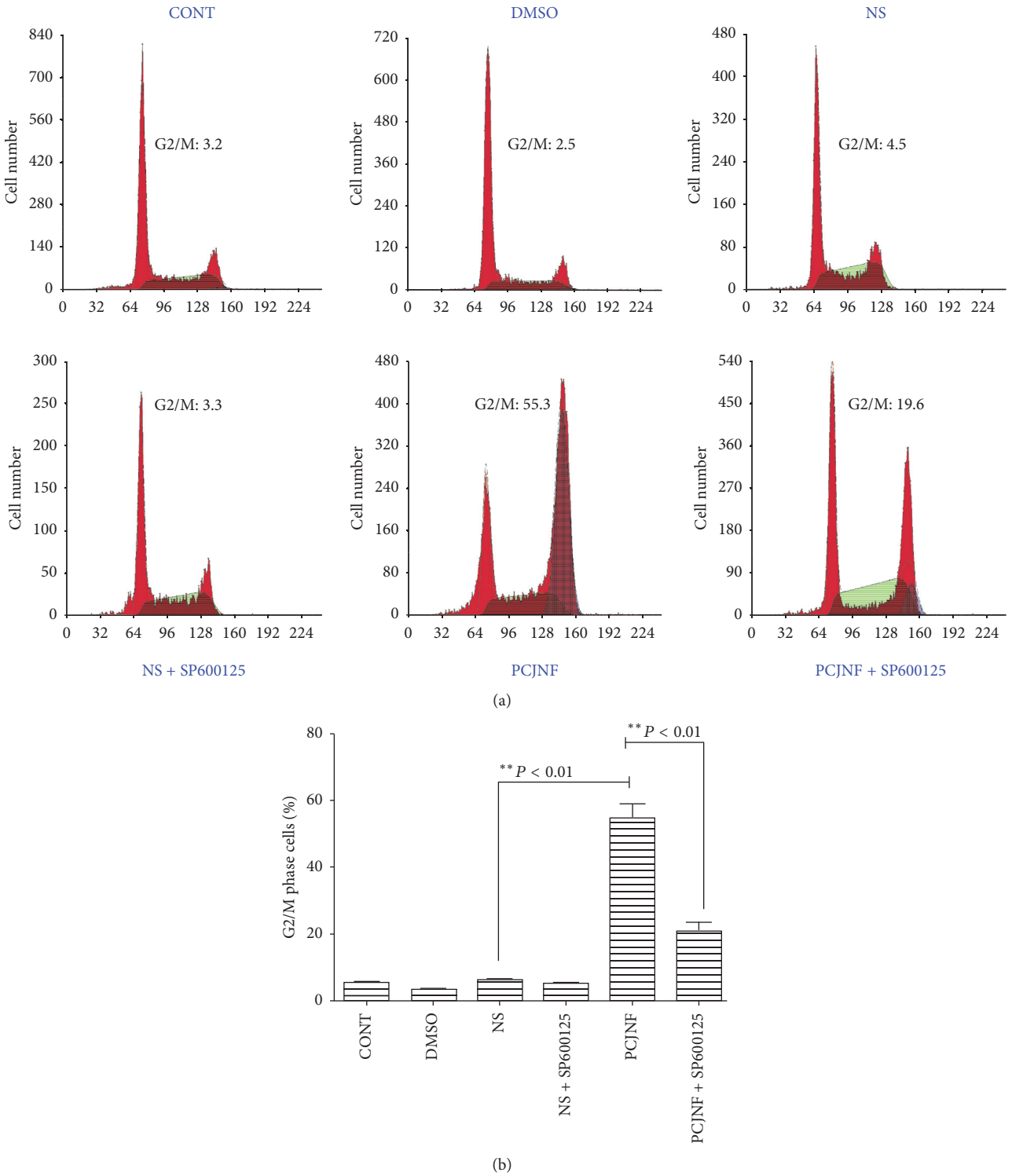

Figure 7: Effect of PCJNF on cell cycle distribution in EESCs. Cell cycle distribution was determined by flow cytometry. (a) PI staining assay was performed after treatment with PCJNF, PCJNF plus SP600125, and different controls, after treatment for 48 h. (b) Statistical analysis of cell cycle phase distribution. Data are presented as means ± SD of three independent tests.

under different extra- and intracellular stimuli [35–38]. Even though in the process of TCM therapy of human diseases, the activation or inhibition of JNK signaling pathway was inconsistent: it was activated in the decreased migration and invasion in HepG2 cells treated by the Chinese herbal formula QHF [39], while being inhibited in the inhibitory cell migration and invasion of MDA-MB-231 cells treated with the Chinese herbal formula PC-SPESII [40]; it thus seemed that

the potential roles of JNK signaling pathway in cell migration and invasion were more complex than previously thought.

5. Conclusions

We showed that PCJNF could promote apoptosis and suppress proliferation of EESCs, at least partly, via activation of JNK signaling pathway for the first time. In addition, PCJNF could also effectively suppress cell invasion and migration in vitro, while this effect was independent of JNK signaling pathway. These results provide experimental evidences supporting the rationality of use of PCJNF in the administration of endometriosis.

Conflicts of Interest

The authors declare no conflicts of interest.

Authors' Contributions

Rui-Ning Liang, Pei-Shuang Li, and Yang Zou contributed equally to this work.

Acknowledgments

This work was supported by the grants of National Natural Science Foundation of China (nos. 81160447 and 81560783).

References

[1] S. Kong, Y. H. Zhang, C. F. Liu et al., "The complementary and alternative medicine for endometriosis: a review of utilization and mechanism," *Evidence-Based Complementary and Alternative Medicine*, vol. 2014, Article ID 146383, 16 pages, 2014.

[2] B. D. McKinnon, V. Kocbek, K. Nirgianakis, N. A. Bersinger, and M. D. Mueller, "Kinase signalling pathways in endometriosis: potential targets for non-hormonal therapeutics," *Human Reproduction Update*, vol. 22, no. 3, pp. 382–403, 2016.

[3] U. L. R. Maggiore, S. Ferrero, G. Mangili et al., "A systematic review on endometriosis during pregnancy: Diagnosis, misdiagnosis, complications and outcomes," *Human Reproduction Update*, vol. 22, no. 1, pp. 70–103, 2016.

[4] P. Rai and S. Shivaji, "The role of DJ-1 in the pathogenesis of endometriosis," *PLoS ONE*, vol. 6, no. 3, Article ID e18074, 2011.

[5] L. Wan, Y. Zou, L.-H. Wan et al., "Tanshinone IIA inhibits the proliferation, migration and invasion of ectopic endometrial stromal cells of adenomyosis via 14-3-3ζ downregulation," *Archives of Gynecology and Obstetrics*, vol. 292, no. 6, pp. 1301–1309, 2015.

[6] C. G. T. Silveira, J. Krampe, B. Ruhland, K. Diedrich, D. Hornung, and A. Agic, "Cold-shock domain family member YB-1 expression in endometrium and endometriosis," *Human Reproduction*, vol. 27, no. 1, pp. 173–182, 2012.

[7] J.-J. Zhang, Z.-M. Xu, C.-M. Zhang et al., "Pyrrolidine dithiocarbamate inhibits nuclear factor-κB pathway activation, and regulates adhesion, migration, invasion and apoptosis of endometriotic stromal cells," *Molecular Human Reproduction*, vol. 17, no. 3, pp. 175–181, 2011.

[8] X.-X. Hou, W.-J. Zhou, X.-Q. Wang, and D.-J. Li, "Fractalkine/CX3CR1 is involved in the pathogenesis of endometriosis by regulating endometrial stromal cell proliferation and invasion," *American Journal of Reproductive Immunology*, vol. 76, 318, no. 4, p. 325, 2016.

[9] W. Liu, X. Xiong, X. Yang, F. Chu, and H. Liu, "The Effect of Chinese Herbal Medicine Gualouxiebaibanxia Decoction for the Treatment of Angina Pectoris: A Systematic Review," *Evidence-Based Complementary and Alternative Medicine*, vol. 2016, Article ID 8565907, 14 pages, 2016.

[10] L. Zhang, G. Wang, W. Hou, P. Li, A. Dulin, and H. L. Bonkovsky, "Contemporary clinical research of traditional Chinese medicines for chronic hepatitis B in China: an analytical review," *Hepatology*, vol. 51, no. 2, pp. 690–698, 2010.

[11] A. F. Ceylan-Isik, R. M. Fliethman, L. E. Wold, and J. Ren, "Herbal and traditional Chinese medicine for the treatment of cardiovascular complications in diabetes mellitus," *Current Diabetes Reviews*, vol. 4, no. 4, pp. 320–328, 2008.

[12] S.-Y. Su, C.-H. Muo, F.-C. Sung, and D. E. Morisky, "Reduction of surgery rate in endometriosis patients who take Chinese medicine: a population-based retrospective cohort study," *Complementary Therapies in Medicine*, vol. 22, no. 4, pp. 632–639, 2014.

[13] Z. Zhang, C. Hu, W. Tang et al., "Therapeutic potential of Wenshen Xiaozheng Tang, a traditional chinese medicine prescription, for treating endometriosis," *Reproductive Sciences*, vol. 20, no. 10, pp. 1215–1223, 2013.

[14] Z. Z. Zhang, C. P. Hu, W. W. Tang et al., "Wenshen Xiaozheng Tang suppresses the growth of endometriosis with an antiangiogenic effect," *Climacteric*, vol. 16, no. 6, pp. 700–708, 2013.

[15] R.-C. Fang, Y.-T. Tsai, J.-N. Lai, C.-H. Yeh, and C.-T. Wu, "The traditional chinese medicine prescription pattern of endometriosis patients in Taiwan: A population-based study," *Evidence-based Complementary and Alternative Medicine*, vol. 2012, Article ID 591391, 9 pages, 2012.

[16] R. N. Liang, W. H. Li, M. Xia, X. X. Niu, L. P. Zhang, and P. S. Li, "A multiple-centered clinical study of the effect of PCJNF on dysmenorrheal in patients with endometriosis," *Journal of New Chinese Medicine*, vol. 44, no. 1, pp. 66–68, 2012, (Chinese).

[17] G. Verma and M. Datta, "The critical role of JNK in the ER-mitochondrial crosstalk during apoptotic cell death," *Journal of Cellular Physiology*, vol. 227, no. 5, pp. 1791–1795, 2012.

[18] Z. Shaukat, D. Liu, R. Hussain, M. Khan, and S. L. Gregory, "The role of JNK signalling in responses to oxidative DNA damage," *Current Drug Targets*, vol. 17, no. 2, pp. 154–163, 2016.

[19] X. Sui, N. Kong, L. Ye et al., "P38 and JNK MAPK pathways control the balance of apoptosis and autophagy in response to chemotherapeutic agents," *Cancer Letters*, vol. 344, no. 2, pp. 174–179, 2014.

[20] Y.-H. Li, C.-H. Zhang, J. Qiu et al., "Antidepressant-like effects of Chaihu-Shugan-San via SAPK/JNK signal transduction in rat models of depression," *Pharmacognosy Magazine*, vol. 10, no. 39, pp. 271–277, 2014.

[21] D. C. Hao and P. G. Xiao, "Network pharmacology: A rosetta stone for traditional chinese medicine," *Drug Development Research*, vol. 75, no. 5, pp. 299–312, 2014.

[22] W. Liu, X. Liang, and D. Yang, "The Effects of Chinese Medicine on Activation of Wnt/ β -Catenin Signal Pathway under High Glucose Condition," *Evidence-based Complementary and Alternative Medicine*, vol. 2015, Article ID 295135, 6 pages, 2015.

[23] Y. Tu, W. Sun, Y.-G. Wan et al., "Dahuang Fuzi Decoction ameliorates tubular epithelial apoptosis and renal damage via inhibiting TGF-β1-JNK signaling pathway activation in vivo," *Journal of Ethnopharmacology*, vol. 156, pp. 115–124, 2014.

[24] K. H. Kim, J. K. Park, Y. W. Choi et al., "Hexane extract of aged black garlic reduces cell proliferation and attenuates the expression of ICAM-1 and VCAM-1 in TNF-α-activated human endometrial stromal cells," *International Journal of Molecular Medicine*, vol. 32, no. 1, pp. 67–78, 2013.

[25] J. C. Irwin, D. Kirk, R. J. B. King, M. M. Quigley, and R. B. L. Gwatkin, "Hormonal regulation of human endometrial stromal cells in culture: an in vitro model for decidualization," *Fertility and Sterility*, vol. 52, no. 5, pp. 761–768, 1989.

[26] L. I. Mambelli, R. C. Mattos, G. H. Z. Winter et al., "Changes in expression pattern of selected endometrial proteins following mesenchymal stem cells infusion in mares with endometrosis," *PLoS ONE*, vol. 9, no. 6, Article ID e97889, 2014.

[27] F. Y. Fung and Y. C. Linn, "Developing traditional Chinese medicine in the era of evidence-based medicine: current evidences and challenges," *Evidence-Based Complementary and Alternative Medicine*, vol. 2015, Article ID 425037, 9 pages, 2015.

[28] Y.-Y. Wang, X.-X. Li, J.-P. Liu, H. Luo, L.-X. Ma, and T. Alraek, "Traditional Chinese medicine for chronic fatigue syndrome: a systematic review of randomized clinical trials," *Complementary Therapies in Medicine*, vol. 22, no. 4, pp. 826–833, 2014.

[29] X. Zhou, Y. Li, Y. Peng et al., "Clinical phenotype network: the underlying mechanism for personalized diagnosis and treatment of traditional Chinese medicine," *Frontiers of Medicine in China*, vol. 8, no. 3, pp. 337–346, 2014.

[30] N. Zhao, J. Li, L. Li et al., "Molecular network-based analysis of Guizhi-Shaoyao-Zhimu decoction, a TCM herbal formula, for treatment of diabetic peripheral neuropathy," *Acta Pharmacologica Sinica*, vol. 36, no. 6, pp. 716–723, 2015.

[31] T.-C. Wang, C.-N. Fang, C.-C. Shen et al., "Yang-Dan-Tang, identified from 15 Chinese herbal formulae, inhibits human lung cancer cell proliferation via cell cycle arrest," *Evidence-based Complementary and Alternative Medicine*, vol. 2012, Article ID 276032, 12 pages, 2012.

[32] K. L. Bruner, L. M. Matrisian, W. H. Rodgers, F. Gorstein, and K. G. Osteen, "Suppression of matrix metalloproteinases inhibits establishment of ectopic lesions by human endometrium in nude mice," *Journal of Clinical Investigation*, vol. 99, no. 12, pp. 2851–2857, 1997.

[33] Y.-T. Guan, Y.-Q. Huang, J.-B. Wu et al., "Overexpression of chloride channel-3 is associated with the increased migration and invasion ability of ectopic endometrial cells from patients with endometriosis," *Human Reproduction*, vol. 31, no. 5, pp. 986–998, 2016.

[34] J.-J. Yu, H.-T. Sun, Z.-F. Zhang et al., "IL15 promotes growth and invasion of endometrial stromal cells and inhibits killing activity of NK cells in endometriosis," *Reproduction*, vol. 152, no. 2, pp. 151–160, 2016.

[35] H.-J. Lin, S.-T. Kao, Y.-M. Siao, and C.-C. Yeh, "The Chinese medicine Sini-San inhibits HBx-induced migration and invasiveness of human hepatocellular carcinoma cells," *BMC Complementary and Alternative Medicine*, vol. 15, no. 1, article no. 348, 2015.

[36] X. Dai, L. Wang, A. Deivasigamni et al., "A novel benzimidazole derivative, MBIC inhibits tumor growth and promotes apoptosis via activation of ROS-dependent JNK signaling pathway in hepatocellular carcinoma," *Oncotarget*, vol. 8, pp. 12831–12842, 2017.

[37] H.-L. Cheng, C.-W. Lin, J.-S. Yang, M.-J. Hsieh, S.-F. Yang, and K.-H. Lu, "Zoledronate blocks geranylgeranylation not farnesylation to suppress human osteosarcoma U2OS cells metastasis by EMT via Rho A activation and FAK-inhibited JNK and p38 pathways," *Oncotarget*, vol. 7, no. 9, pp. 9742–9758, 2016.

[38] Y. Chikano, T. Domoto, T. Furuta et al., "Glycogen synthase kinase 3β sustains invasion of glioblastoma via the focal adhesion kinase, Rac1, and c-Jun N-terminal kinase-mediated pathway," *Molecular Cancer Therapeutics*, vol. 14, no. 2, pp. 564–574, 2015.

[39] T. Chen, Q. Wang, Y. Li, H. Huang, and W. Hu, "Chinese herbal formula QHF inhibits liver cancer cell invasion and migration," *Experimental and Therapeutic Medicine*, vol. 11, no. 6, pp. 2413–2419, 2016.

[40] X.-F. Wang, J. Du, T.-L. Zhang, Q.-M. Zhou, Y.-Y. Lu, and S.-B. Su, "Inhibitory effects of PC-SPESII herbal extract on human breast cancer metastasis," *Evidence-Based Complementary and Alternative Medicine*, vol. 2013, Article ID 894386, 11 pages, 2013.

Hindawi
Evidence-Based Complementary and Alternative Medicine
Volume 2017, Article ID 6438013, 12 pages
https://doi.org/10.1155/2017/6438013

Research Article

Compounds from *Cynomorium songaricum* with Estrogenic and Androgenic Activities Suppress the Oestrogen/Androgen-Induced BPH Process

Xueni Wang,[1] Rui Tao,[2] Jing Yang,[3] Lin Miao,[1,2] Yu Wang,[1,3] Jose Edouard Munyangaju,[1] Nuttapong Wichai,[1,2] Hong Wang,[1,2] Yan Zhu,[1] Erwei Liu,[1,2] Yanxu Chang,[1,2] and Xiumei Gao[1,2,3]

[1]*Tianjin State Key Laboratory of Modern Chinese Medicine, 312 Anshanxi Road, Nankai District, Tianjin 300193, China*
[2]*Institute of Traditional Chinese Medicine, Tianjin University of Traditional Chinese Medicine, 312 Anshanxi Road, Nankai District, Tianjin 300193, China*
[3]*Key Laboratory of Pharmacology of Traditional Chinese Medical Formulae, Ministry of Education, Tianjin University of Traditional Chinese Medicine, Tianjin 300193, China*

Correspondence should be addressed to Lin Miao; mmmlin@tjutcm.edu.cn and Xiumei Gao; gaoxiumei@tjutcm.edu.cn

Received 2 February 2017; Accepted 9 April 2017; Published 15 May 2017

Academic Editor: Pradeep Kumar

Objective. To investigate the phytoestrogenic and phytoandrogenic activities of compounds isolated from CS and uncover the role of CS in prevention of oestrogen/androgen-induced BPH. *Methods*. Cells were treated with CS compounds, and immunofluorescence assay was performed to detect the nuclear translocation of ERα or AR in MCF-7 or LNCaP cells; luciferase reporter assay was performed to detect ERs or AR transcriptional activity in HeLa or AD293 cells; MTT assay was performed to detect the cell proliferation of MCF-7 or LNCaP cells. Oestrogen/androgen-induced BPH model was established in rat and the anti-BPH, anti-estrogenic, and anti-androgenic activities of CS in vivo were further investigated. *Results*. The nuclear translocation of ERα was stimulated by nine CS compounds, three of which also stimulated AR translocation. The transcriptional activities of ERα and ERβ were induced by five compounds, within which only ECG induced AR transcriptional activity as well. Besides, ECG stimulated the proliferation of both MCF-7 cells and LNCaP cells. CS extract suppressed oestrogen/androgen-induced BPH progress in vivo by downregulation of E2 and T level in serum and alteration of the expressions of ERα, ERβ, and AR in the prostate. *Conclusion*. Our data demonstrates that compounds from CS exhibit phytoestrogenic and phytoandrogenic activities, which may contribute to inhibiting the oestrogen/androgen-induced BPH development.

1. Introduction

Cynomorium songaricum (CS) is a traditional Chinese medicine (TCM) that has been practically used for treatment of hormone deficient diseases, including sexual dysfunction, infertility, deficient kidney function, and prostatic diseases for hundreds of years [1–3]. A variety of compounds isolated from CS have been identified and classified as pentacyclic triterpene, flavonoid, flavonoid glycoside, and anthraquinones (Figure 1) [4, 5]. However, the mechanism by which CS and its compounds regulate estrogen and/or androgen signaling remains unclear.

It has been reported that natural compounds may exhibit phytoestrogenic activity through multiways such as induction of estrogen receptor (ER) nuclear translocation, stimulation of ER transcriptional activity, and promotion of estrogen-dependent cell proliferation, thereby behaving like estradiol [6, 7]. Phytoestrogens participate in estrogen-related signaling as either ER antagonists or agonists and thus are called selective estrogen receptor modulators (SERMs). It has been reported that phytoestrogens have protective effects against breast cancer, prostate cancer, and cardiovascular diseases [8]. Comparison to that of phytoestrogens identification of phytoandrogenic activity from natural compounds

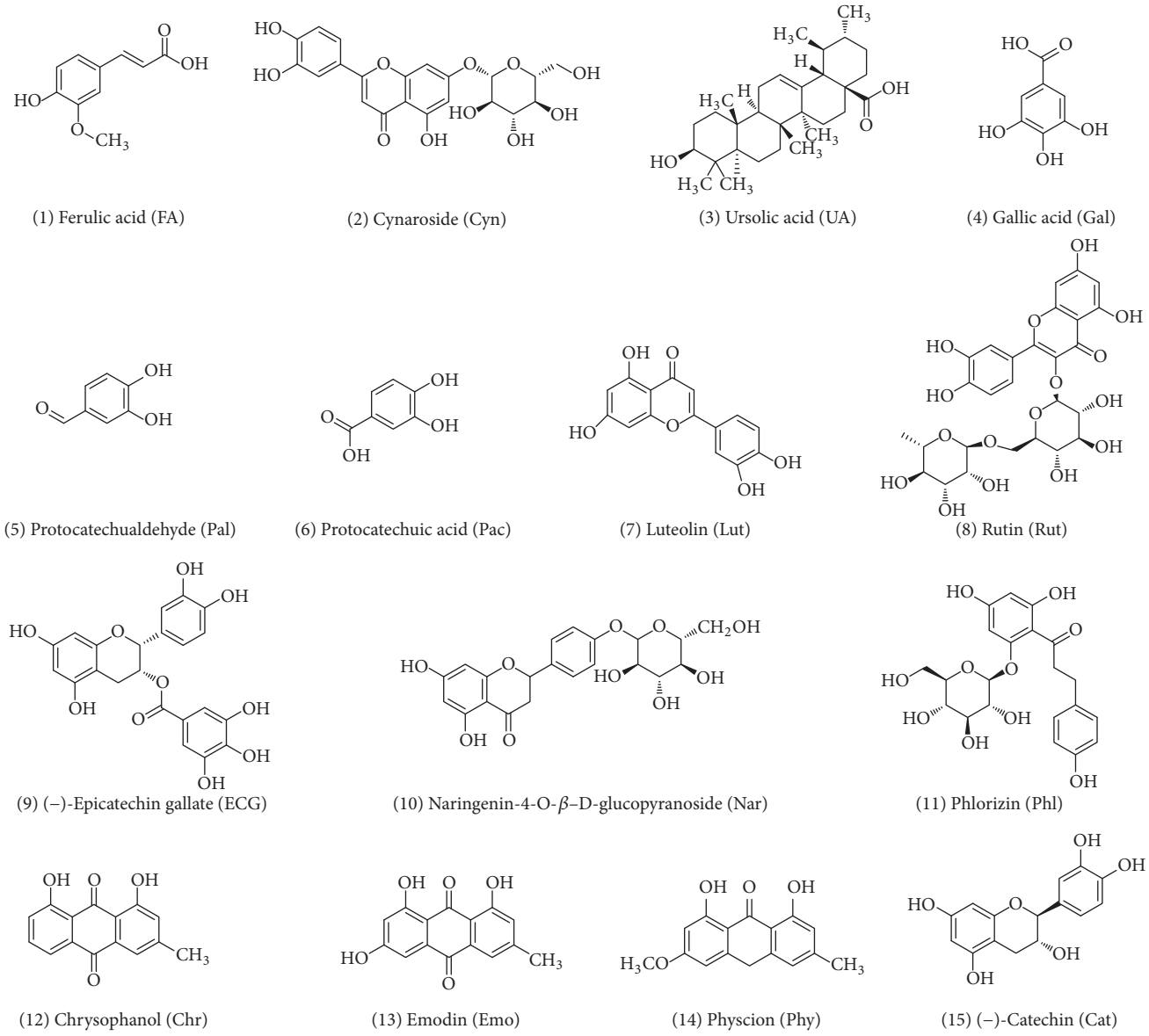

Figure 1: Chemical structures of compounds isolated from *Cynomorium songaricum* (CS).

is arising recently [9]. Concerning the potential treatment for androgen-regulated diseases like benign prostatic hyperplasia and prostate cancer, several natural compounds have been recognized as agonists or antagonists against androgens [10–15], and display the tissue-selective activation of androgenic signaling [16], which are so called selective androgen receptor modulators (SARMs) by competitively binding to androgen receptor (AR).

Benign prostatic hyperplasia (BPH) is an age-related common disease in older men [17], in which both androgen and estrogen signaling [18, 19] are involved via their specific receptors. Studies from different groups have showed that ERα (one subtype of ER) and AR are overexpressed in BPH tissues and knocking down either of them significantly blocks BPH progression in vivo [20, 21], indicating their positive roles for BPH development [22, 23]. On the other hand, ERβ (the other subtype of ER) exhibits antiproliferation activity that suppresses BPH development as a negative factor in the prostate [24]. Therefore, downregulation of ERα and AR or upregulation of ERβ could become effective ways and hopeful targets that contribute to BPH therapeutics.

CS is an important anti-BPH herbal medicine in China [25], while the mechanism is still uncovered well. Here we first analyzed the phytoestrogenic and phytoandrogenic activities of compounds isolated from CS and then investigated whether the anti-BPH effect of CS in oestradiol/testosterone (1 : 100)-induced BPH was due to interference with androgen and/or estrogen signaling.

2. Materials and Methods

2.1. Extract and Compounds. *Cynomorium songaricum* extract was prepared by desiccation after reflux with 70% ethanol. Ferulic acid (FA), cynaroside (Cyn), ursolic acid (UA), gallic acid (Gal), protocatechualdehyde (Pal), protocatechuic acid (Pac), luteolin (Lut), rutin (Rut), epicatechin gallate (ECG), naringenin-4-O-b-D-glucopyranoside (Nar), phlorizin (Phl), chrysophanol (Chr), emodin (Emo), physcion (Phy), catechin (Cat) were isolated from the extract as previously described [26]. Chemical structures of compounds were shown in Figure 1.

2.2. Reagents and Plasmids. Dihydrotestosterone (DHT) was purchased from Solarbio (Beijing China). 17β-estradiol (E2) and Tamoxifen (Tam) were obtained from Sigma-Aldrich. Lipofectamine® 2000 Transfection Reagent was from life technologies (USA). Hoechst 33342 was purchased from Cell Signaling Technology (USA). RPMI 1640 was purchased from Sigma (USA). Fetal Bovine Serum was from Hyclone (New Zealand). Charcoal stripped FBS was from Biological Industries (USA). Dual-Luciferase® Reporter Assay was from Promega (USA).

Mammalian ERα, ERβ, and AR expression vectors and the estrogen response element (ERE) and the androgen response element luciferase reporter plasmids pTk-ERE-luc and pTk-ARE-luc were gifts from Dr. ZhuYan (Tufts Medical Center, Boston, USA) and Dr. J. Zhang (Nankai University, Tianjin, China) separately. pTk-Renilla was purchased from Promega.

2.3. Cell Culture. MCF-7 cells were obtained from professor Zhang (Peking University, Beijing). Hela cells were purchased from Institute of Biochemistry and Cell Biology (Shanghai, China). MCF-7 cells and HeLa cells were maintained in DMEM supplemented with 10%, 100 units/mL penicillin, and 100 μg/μL streptomycin. LNCaP and AD293 cells were obtained from professor Zhang Ju (Nankai University, Tianjin) and maintained in RPMI 1640 supplemented with 10% (v/v) fetal bovine serum (FBS) (HyClone, New Zealand), 100 units/mL penicillin, and 100 μg/μL streptomycin. In experiments requiring androgen or estrogen or compound stimulation, cells were cultured in phenol red-free medium supplemented with 10% charcoal stripped FBS.

2.4. Immunocytofluorescence Imaging. MCF-7 cells were plated into 96-well plates and cultured in phenol red-free DMEM plus 1% charcoal-treated FBS. After culture for 24 h, cells were treated with Tam (100 nM) or compounds (100 nM) for 6 h. And then cells were fixed, permeabilized, and incubated with an ERα-antibody (SC-8002, Santa Cruz, dilution 1/200), and Alexa Fluor® 488 anti-mouse antibody [27]. LNCaP cells were cultured on poly-D-lysine-coated cover wells in phenol red-free RPMI 1640 plus 1% cs-FBS overnight and treated with compounds for 1 h. DHT was added to a final concentration of 10 nM. After 1 h, cells were fixed, permeabilized, and incubated with an anti-AR antibody (ab3510, Abcam, dilution 1/1000) and an Alexa Fluor 488 donkey anti-rabbit IgG (H+L) antibody [28, 29]. Nuclei were counterstained with Hoechst 33342. Images were captured at 20x magnification using a PerkinElmer High content screening system.

Table 1: The experimental treatments on each group.

Group	E2/T (in coin oil, s.c.)	Drugs
Sham-operated	0.1 mL coin oil	Normal saline
BPH Model	0.1 mL E2/T	Normal saline
CS extract treatment	0.1 mL E2/T	CS extract (6 g/kg/d)

2.5. Transient Transfection and Luciferase Reporter Assay. Hela cells were seeded in 24-well plates at a density to become 70–90% confluent when they are attached. Transient transfection was performed by using the Lipofectamine and plus reagents following the manufacturer's instructions. Cells were cotransfected either with 0.2 μg ERα plasmid, 0.4 μg pERE-luc, and 0.2 μg pTk-Renilla or 0.2 μg ERβ plasmid, 0.4 μg pERE-luc, and 0.2 μg pTk-Renilla per well. After incubating for 6 h, cells were treated with compounds. AD293 cells were plated in 96-well plates in growth medium of 1% CD-FBS without antibiotics at a density to reach 90% to 95% confluence at transfection. After attachment and growth for 24 h, the cells were cotransfected with the reporter plasmid pTk-ARE-Luc and AR. Transfection was carried out for 18 h in serum-free, antibiotic-free RPMI 1640 media using Lipofectamine. Luciferase activity was then assayed after additional 24 h incubation by using the Luciferase Assay System (Promega). The Renilla luciferase activity was used to normalize that of firefly luciferase.

2.6. MTT Assay. Cell proliferation was studied by using MTT assay. Cells were seeded (MCF-7 cells, 10^4/well in 24-well plates; LNCaP cells, 8000/well in 96 wells plate) and, after attachment, cells were treated with various concentrations of compounds in DMSO for 72 h. OD570 values of compounds were detected using a TECAN Infinite® 200 PRO NanoQuant multimode microplate reader.

2.7. Animals and Hormonal Manipulations. A total number of 18 Wistar male rats (250–300 g) were obtained from Beijing Vital River Laboratory Animal Technology Co., Ltd. in China. The experiments and animal care were conducted in accordance with the guidelines of the Chinese Council on Animal Care and approved by the Tianjin University of Traditional Chinese Medicine Animal Care and Use Committee.

BPH rat model was conducted as the previous method [30]. In brief, 6 rats were randomly separated into a sham-operated group, and the other 12 rats were castrated and randomly assigned to two experimental groups with 6 rats per group. All rats were maintained in an animal facility under standard laboratory conditions for 3 weeks. The specific experimental treatments on each group were listed in Table 1. The ratio of oestradiol benzoate and testosterone propionate was 1 : 100 (E/T = 10 μg/1000 μg) [30, 31], subcutaneous daily injection of the mixed solutions to the castrated 12 rats. As vehicle, the sham-operated rats were daily subcutaneously injected with 0.1 mL of corn oil. CS extract was orally given

Table 2: List of primer sequences.

Primer name	Primer sequence (5′-3′)	Annealing temperature
PCNA Forward	GAGCAACTTGGAATCCCAGAACAGG	60°C
PCNA Reverse	CCAAGCTCCCCACTCGCAGAAAACT	
AR Forward	GCCGGACATGACAACAACCAGCC	60°C
AR Reverse	AGTGAAGGACCGCCAACCCATGG	
ERα Forward	GGTCATAACGATTACATGTG	60°C
ERα Reverse	TCTGTCCAAGACCAAGTTAG	
ERβ Forward	GAGGCAGAAAGTAGCCGGAA	53°C
ERβ Reverse	CGTGAGAAAGAAGCATCAGGA	
GAPDH Forward	ATGATTCTACCCACGGCAAG	53°C
GAPDH Reverse	CTGGAAGATGGTGATGGGTT	

for 45 days. Rats were under the chloral hydrate anesthesia and weighed 24 h after the last injection. The whole prostates were dissected and weighed for calculating the prostatic index (PI). One ventral lobe of the prostate was fixed in phosphate-buffered formalin and embedded in paraffin for histological and immunohistochemical studies. And the other ventral lobe was stored at −80°C for the protein and RNA extraction.

2.8. Calculation of PI. The formula for calculating the prostatic index (PI) was as follows [30]:

$$\text{PI} = \frac{\text{gross wet weight of prostate}}{\text{body weight of the whole rat}} \times 100\%. \quad (1)$$

2.9. Histological and Immunohistochemical Studies. Haematoxylin and eosin (H&E) staining and immunohistochemical (IHC) staining were performed as previously described [30]. Briefly, 5 μm sections of one ventral lobe of the prostate were deparaffinized in xylene and rehydrated in a graded series of alcohol. One 5-μm section was stained with haematoxylin and eosin (H&E) for histological examination. Another 5-μm section was using the avidin–biotin–peroxidase complex method to process immunohistochemistry. The endogenous peroxidase activity was blocked with 0.3% hydrogen peroxide at room temperature for 10 min, followed by incubation with 10% serum at 37°C for 1 hour. Sections were incubated with primary antibody at 4°C overnight. The primary antibody was anti-PCNA antibody (proliferating cell nuclear antigen, 1/200, Pro-tech,). Then the sections were added the biotinylated secondary antibody at 37°C for 1 hour, followed by peroxidase-labelled streptavidin. The secondary antibody was biotinylated goat anti-rabbit IgG (1/200, ZSGB-BIO). Finally the sections were stained by the DAB (boster) and hematoxylin, followed by dehydration and transparency in a graded series of alcohol and dimethylbenzene.

2.10. Determination of Estradiol and Testosterone Level in Serum. The blood samples of rats were centrifuged at 3,000 rpm for 10 min at room temperature. The supernatant of the blood samples was collected and then stored at ultra-low temperature freezer. The concentrations of estradiol and testosterone in serum were determined by the enzyme-linked immunosorbent assay [30].

2.11. Real-Time Quantitative PCR Analysis. Total RNA was extracted from the frozen ventral lobe of the prostate tissue using Trizol reagent (TIANGEN) according to the manufacturer's protocol. Real-time quantitative PCR was carried out with the PCR primers as Table 2. The conditions of Real-time quantitative PCR included preheating at 95°C for 5 min, and then followed by 39 cycles of 95°C for 30 s, 55°C for 30 s, and 72°C for 30 s. The mRNA level of relative gene expression was determined by the comparative CT method and normalized to the housekeeping gene GAPDH.

2.12. Western Blot Assay. Protein was extracted from the ventral lobe of prostate for each group, and the concentration was determined according to the manufacturer's instructions (BCA Protein Assay Kit, Thermo Fisher). 40 μg proteins were loaded into the SDS-PAGE. Following gel electrophoresis (SDS-PAGE), gel was transferred onto PVDF membrane (Millipore, Billerica, MA, USA) and incubated in TBST buffer, supplemented with 5% milk as the blocking buffer for 1 h. Next the membrane was incubated with primary antibodies under the 4°C rotating overnight. The primary antibodies were PCNA (10205-Z-AP, Pro-tech, dilution 1/2000), AR (ab3510, Abcam, dilution 1/500), ERα (SC-8002, Santa Cruz, dilution 1/500), ERβ (SC-8974, Santa Cruz, dilution 1/500), and GAPDH (B0004-1-lg, Pro-tech, dilution 1/2000). The PVDF membrane was washed five times with TBST and then incubated with the appropriate secondary antibodies conjugated to horseradish peroxidase and detected next by Enhanced chemiluminescence.

2.13. Statistical Analysis. All results were presented as mean ± standard deviation (SD). Statistical significance was determined with One-Way ANOVA. $^{*}P < 0.05$, $^{**}P < 0.01$, and $^{***}P < 0.001$ were considered statistically significant.

3. Results

3.1. Compounds of CS Extract Showed Phytoestrogenic Activity In Vitro. In the absence of estrogen, ERα was distributed throughout the cell. Following stimulation with Tam, the nuclear staining of ERα was increased dramatically. Similarly, when treating with compounds FA, Cyn, UA, Gal, Pal, Pae, Lut, Rut, or ECG, ERα locations in the nucleus were

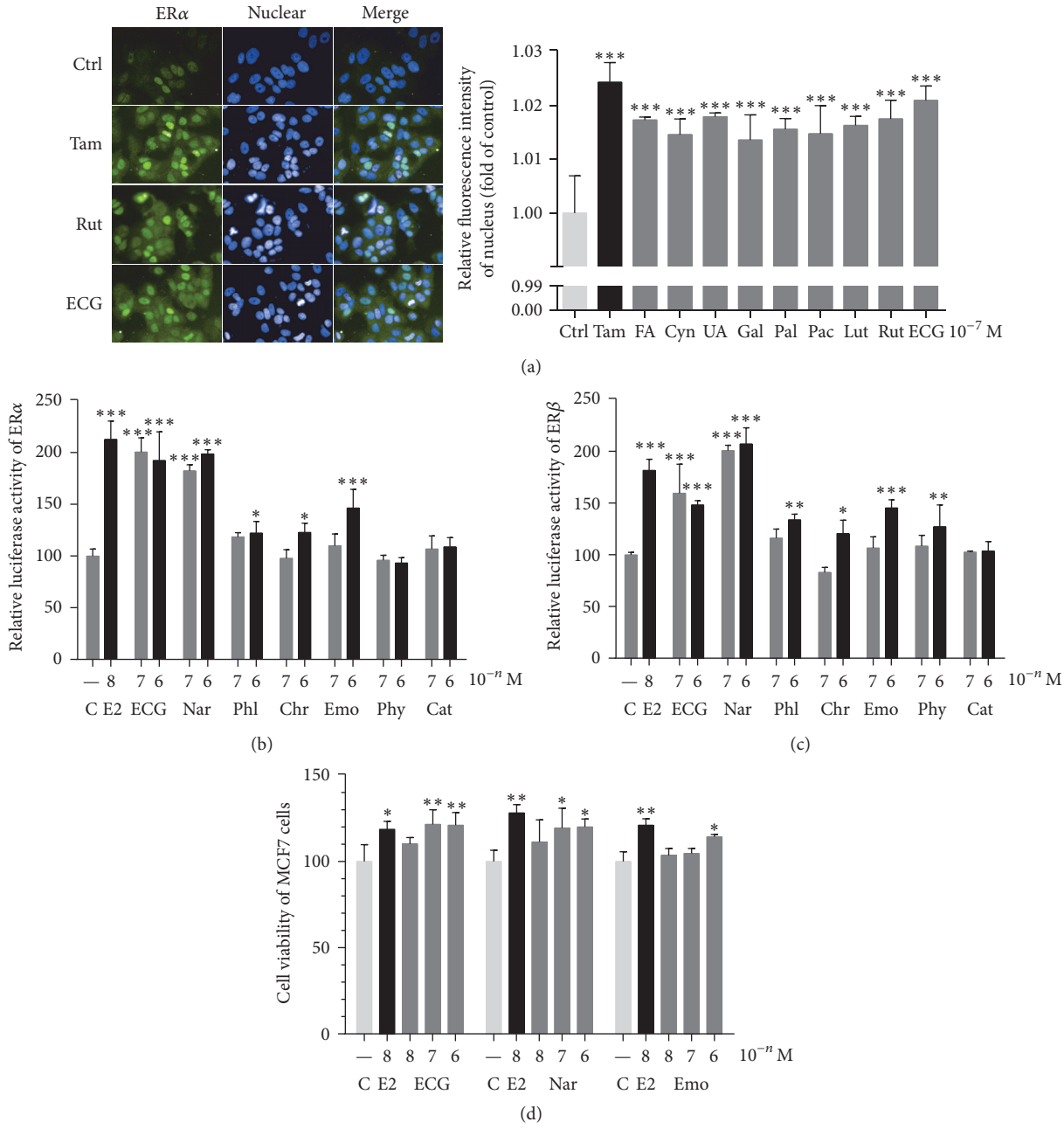

Figure 2: Compounds from CS extract showed phytoestrogenic activity in vitro. (a) Visualization of intracellular ERα in MCF-7 cells (left) and quantification of fluorescence intensity after treatment with compounds (right). (b), (c) ERα and ERβ transcriptional activity were activated after treatment with compounds. (d) The proliferation of MCF-7 cells was induced after treatment with compounds. Compare with control, $^{*}P < 0.05$, $^{**}P < 0.01$, and $^{***}P < 0.001$.

also significantly increased in MCF-7 cells (Figure 2(a)), indicating their possible phytoestrogenic activities. Further investigation by dual-luciferase assay showed that ECG and Nar upregulated ERα transcriptional activity at 10^{-7} M and 10^{-6} M, while Phl, Chr, and Emo promoted ERα transcription activity at 10^{-6} M (Figure 2(b)). These results suggest that compounds of CS extract exhibit estrogenic like activity by facilitating ERα translocation to nuclear and activated ERα transcriptional activity. Since not only ERα, but also ERβ plays a role in estrogen-stimulated genomic effects, we also detected the ERβ transcriptional activities after treatment with compounds. ECG and Nar upregulated ERβ transcriptional activity at 10^{-7} M and 10^{-6} M, and Phl, Chr, Emo, and Phy promoted ERβ transcription activity at 10^{-6} M (Figure 2(c)). Considering the selectivity of ERα and ERβ and different affinities to ERα and ERβ with different concentrations, we thought that compounds from CS exhibit estrogenic activities depending on different conditions. To further confirm the effect of compounds on estrogenic like function, we did MTT assay. As shown in Figure 2(d), ECG,

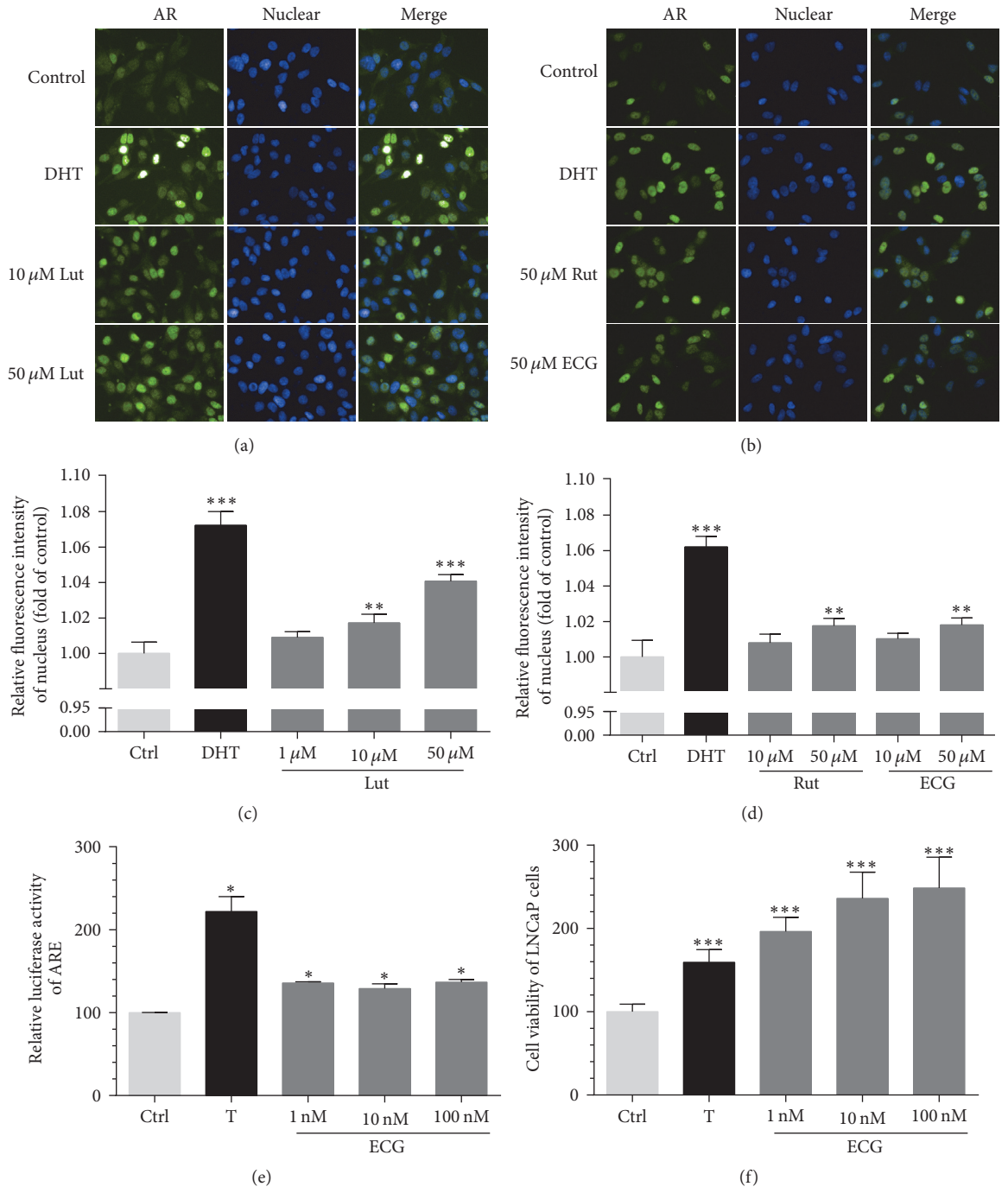

Figure 3: Compounds from CS extract showed phytoandrogenic activities in vitro. (a) Visualization of intracellular AR in LNCaP cells when incubated with DHT or Lut. (b) Visualization of intracellular AR in LNCaP cells when incubated with DHT, Rut, or ECG. (c), (d) The relative fluorescence intensity of AR in nuclear was quantified after treatment with Lut, Rut, or ECG. (e) AR transcriptional activity was activated by ECG in AD293 cells. (f) The proliferation of LNCaP cells was induced by ECG. Compare with control, $^{*}P < 0.05$, $^{**}P < 0.01$, and $^{***}P < 0.001$.

Nar, and Emo accelerated proliferation of MCF-7 cells as estradiol did.

3.2. Compounds of CS Extract Showed Phytoandrogenic Activity In Vitro. We also investigated the phytoandrogenic activities of compounds from CS. In the absence of androgen, AR was mainly distributed in the cytoplasm of LNCaP cells. After 1 h stimulation with DHT, the nuclear staining of AR was increased obviously. AR locations in the nucleus were also highly increased in a dose-dependent manner when treated with compounds Lut, Rut, and ECG (Figures 3(a), 3(b), 3(c), and 3(d)), while FA, Cyn, UA, Gal, Pal, and Pac have no

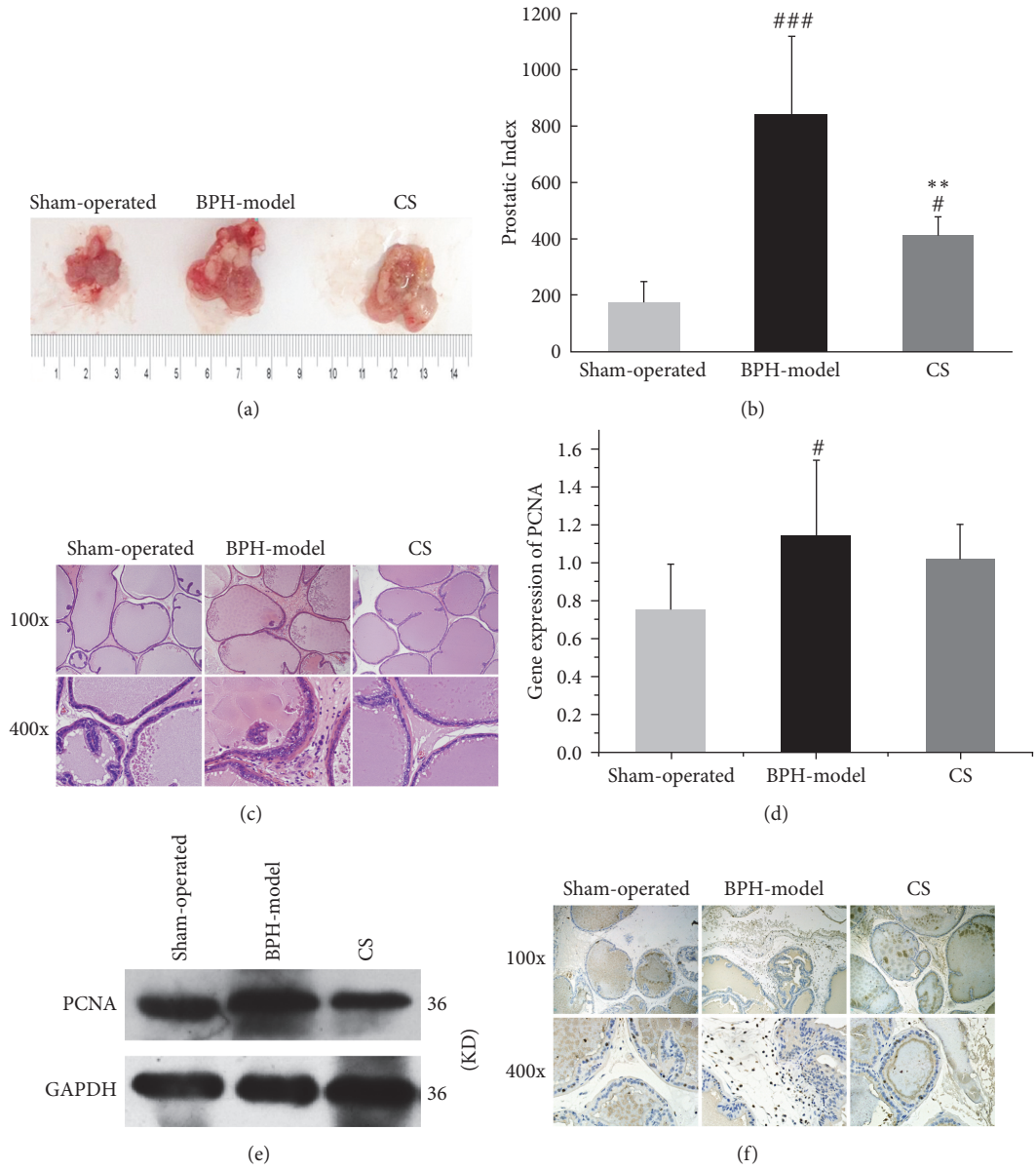

Figure 4: CS extract inhibited the estrogen-androgen induced-BPH progress in vivo. (a) The prostatic morphologies and (b) the prostatic index of rats were shown and calculated in sham-operated group, BPH model, and CS groups. (c) The pathophysiology of rat prostate was analyzed by HE staining in sham-operated group, BPH model, and CS groups. (d) The mRNA and (e) protein expressions and (f) distributions of PCNA in prostate tissues were investigated and quantified by RT-qPCR, western blot, and immunohistochemical staining. Compare with sham-operated group, $^{\#}P < 0.05$, $^{\#\#\#}P < 0.001$; Compare with BPH model, $^{**}P < 0.01$.

obvious effects (data not shown). We also found ECG induced ARE luciferase activity and androgen-dependent LNCaP proliferation in a dose-dependent manner as testosterone did (Figures 3(e) and 3(f)), while Lut and Rut have no obvious effects (data not shown).

3.3. CS Extract Inhibited the Estrogen-Androgen Induced-BPH Progress In Vivo. Compared with those in the sham-operated group, the sizes and weights of the prostate in BPH model group were significantly increased, which was further decreased by CS administration (Figures 4(a) and 4(b)). By pathological analysis, thickness of the periglandular smooth muscle layer and the height of the luminal cells were significantly increased in BPH model group, which was decreased after CS administration (Figure 4(c)). The mRNA and protein expressions and distribution of PCNA in the prostate were also upregulated in the BPH model group comparing with the sham-operated group, which were then suppressed in CS group (Figures 4(d), 4(e), and 4(f)).

3.4. Effects of CS Extract on AR and ER. Since compounds from CS have phytoestrogenic and phytoandrogenic activities, and estrogen and androgen play important roles in

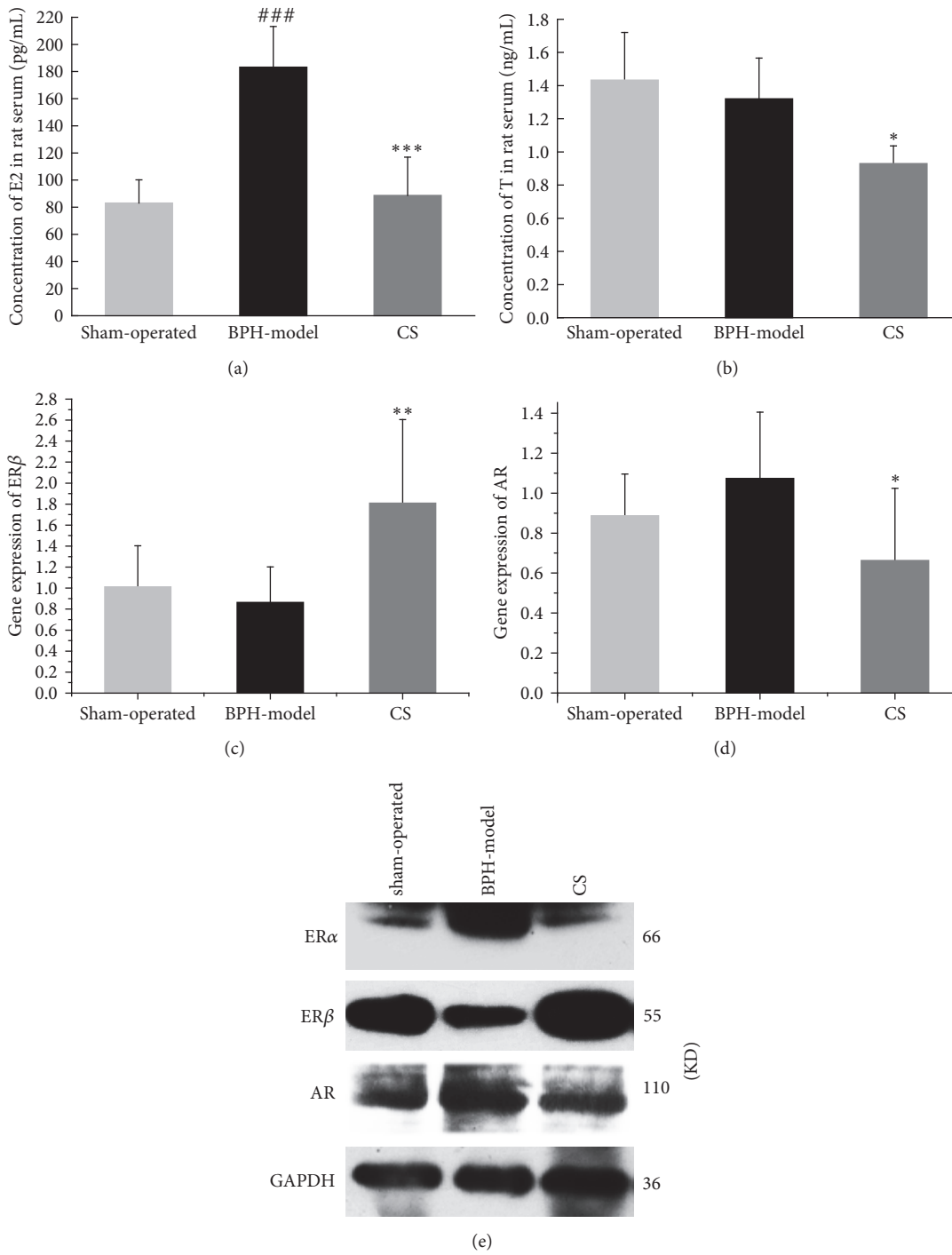

Figure 5: Effects of CS extract on AR and ER in vivo. (a), (b) The levels of estradiol (E2) and testosterone (T) in serum were detected by ELISA in sham-operated group, BPH model, and CS groups. (c), (d) Gene expressions of ERβ and AR in prostate of rats were tested by RT-qPCR in sham-operated group, BPH model, and CS groups. (e) Protein expressions of ERα, ERβ, and AR were determined by western blot in sham-operated group, BPH model, and CS groups. Compare with sham-operated group, $^{###}P < 0.001$; compare with BPH model, $^{*}P < 0.05$, $^{**}P < 0.01$, and $^{***}P < 0.001$.

BPH development, we wondered whether the suppression of BPH by CS is mediated by interfering with the estrogen and/or androgen signaling. As shown in Figures 5(a) and 5(b), E2 and T levels in serum CS group were significantly lower than those in BPH model group. ERα expression was suppressed at protein level in CS extract treatment group. Besides, ERβ expressions were increased and AR expressions were decreased in CS extract treatment group compared

Table 3: Summary of results on cellular level.

Number	Abb.	Androgenic activity			Estrogen activity				
		AR N.T.	AR T.A.	LNCaP Prol.	ERα N.T.	ERα T.A.	ERβ N.T.	ERβ T.A.	MCF7 Prol.
(1)	FA	−	−	N.D.	+	N.D.	N.D.	N.D.	N.D.
(2)	Cyn	−	−	N.D.	+	N.D.	N.D.	N.D.	N.D.
(3)	UA	−	−	N.D.	+	N.D.	N.D.	N.D.	N.D.
(4)	Gal	−	−	N.D.	+	N.D.	N.D.	N.D.	N.D.
(5)	Pal	−	−	N.D.	+	N.D.	N.D.	N.D.	N.D.
(6)	Pac	−	−	N.D.	+	N.D.	N.D.	N.D.	N.D.
(7)	Lut	+	−	N.D.	+	N.D.	N.D.	N.D.	N.D.
(8)	Rut	+	−	N.D.	+	N.D.	N.D.	N.D.	N.D.
(9)	ECG	+	+	+	+	+	N.D.	+	+
(10)	Nar	N.D.	N.D.	N.D.	N.D.	+	N.D.	+	+
(11)	Phl	N.D.	N.D.	N.D.	N.D.	+	N.D.	+	−
(12)	Chr	N.D.	N.D.	N.D.	N.D.	+	N.D.	+	−
(13)	Emo	N.D.	N.D.	N.D.	N.D.	+	N.D.	+	+
(14)	Phy	N.D.	N.D.	N.D.	N.D.	−	N.D.	+	−
(15)	Cat	N.D.	N.D.	N.D.	N.D.	−	N.D.	−	−

Note. "N.T.": nuclear translocation, "T.A.": transcriptional activity, "Prol.": proliferation, "−": negative, "+": positive, and "N.D.": has not been detected.

with BPH model group at levels of both mRNA and protein (Figures 5(c), 5(d), and 5(e)).

4. Discussion

Phytoestrogens are a diverse group of natural compounds that have the abilities to act as estrogenic or/and antiestrogenic functions [32]. Studies have shown that lots of traditional medicines produce compounds that may mimic estrogenic effect and thus considered as typical phytoestrogens [7, 33, 34]. In our study, we first showed that several compounds from CS have phytoestrogenic activities (Table 3) by increasing ERα translocation to nucleus, inducing ERE luciferase activity, and/or enhancing MCF-7 proliferation (Figure 2), indicating that CS is such kind of traditional medicines that may participate in the estrogen signaling pathway and regulate the abnormal signaling involved in the estrogen-induced diseases. Meanwhile, it is also worth noting that compounds that were used in our distinct assays did not overlap with each other. We found that all of the nine detected compounds (FA, Cyn, UA, Gal, Pal, Pae, Lut, Rut, and ECG) promoted ERα nuclear translocation (Figure 2(a)) in the concentration of 100 nM, whereas only two of seven detected compounds (ECG and Nar) significantly induced ERα transcriptional activities at 100 nM (Figure 2(b)), which further confirmed their phytoestrogenic effects by proliferation of MCF-7 cells (Figure 2(d)). Our finding indicated that ER translocation to nucleus is the necessary step induced by compounds to mimic estradiol genomic effects, but it is not sufficient. The competitive ability with estradiol by ER recruitment and selective manner of the target genes involved in certain biofunctions such as cell proliferation are also worth noting. Therefore, we cannot exclude that compounds with positive results from one assay may have different effects or may behave negative readouts from other assays. ECG is one of the important compounds from CS, and our results first proved that ECG has strong and consistent results on the phytoestrogenic activity (Figures 2(a), 2(b), 2(c), and 2(d)). Previous study has reported that Lut has estrogenic activity [35]. Here we also found that Lut promoted ERα nuclear translocation. On the selectivity of ER subtypes, we did not observe the specific ERα or ERβ selectivity among seven detected compounds (ECG, Nar, Phl, Chr, Emo, Phy, and Cat) (Figures 2(b) and 2(c)).

Similar to phytoestrogens, the concept of phytoandrogen has also been recognized and valued [9]. Traditional medicines that were reported for treatment of syndromes including impotence, infertility, and erectile dysfunction in clinically are a large class of phytoandrogen pool containing hopeful candidates with androgenic activities, while the related reports are still not too much [36]. CS is a well-known and widely used traditional medicine applied to reinforce yang in TCM. Here, we first demonstrated that ECG, Lut, and Rut significantly induced AR translocation to nuclear (Figures 3(a) and 3(b)), and ECG upregulated AR transcriptional activities (Figure 3(e)) and stimulated androgen-dependent LNCaP cell proliferation in a dose-dependent manner (Figure 3(f)), providing evidence that CS contains potential phytoandrogens (Table 3).

Combining the results of estrogenic and androgenic activities, it is interesting and notable to find that ECG is the only one with dual activities of estrogen and androgen among all isolated compounds from CS (Table 3). Previously, ECG has been reported as a naturally occurring polyphenolic compound with putative antioxidant, anti-inflammatory, antibacterial, and antitumor activities [37–41]. Here, we

first demonstrated its function involved in hormone related signaling and regulation.

It has been well accepted that both estrogen and androgen play key roles during BPH development [42]. Here, we used estradiol and testosterone cooperatively induced rat BPH model [30, 43, 44] to detect the inhibitory effect of CS in BPH development. As we expected, the prostate volume, PI, and PCNA expression in BPH group were dramatically increased comparing with those in the sham-group, which were further inhibited in CS group (Figures 4(a), 4(b), 4(d), 4(e), and 4(f)), providing evidence that CS is an efficient administration for BPH treatment in accordance with the clinical experience in China. Recently, two publications showed that Lut and UA, two of the compounds isolated from CS, have significant effects in inhibiting prostate-related diseases. Lut inhibited cell proliferation and induced apoptosis in LNCaP human prostate cancer cells by mediated AR downregulation [45]. UA significantly decreased the prostate size, prostatic hyperplasia, and DHT levels in the serum and prostate of BPH rat, strongly suggesting it can be utilized as a useful agent in BPH treatment [46]. However, concerning the phytoestrogenic or/and phytoandrogenic activities of different compounds from CS, mainly compounds that are involved in and contributed to anti-BPH effects of CS still need to be studied in the future.

As we known, ERα, ERβ, and AR are nuclear receptors that mediate estrogen and androgen signaling. In prostatic stromal cells, ERα and AR are highly expressed and the increased levels of which are considered to contribute the BPH progression [47, 48], while, in contrast, ERβ and AR are highly expressed in prostatic epithelial cells; the upregulation of AR and downregulation of ERβ are related to BPH [49, 50]. In our study, we found the CS group significantly inhibited ERα and AR and induced ERβ, particularly in protein levels. These data suggested that CS exhibits antiestrogen and antiandrogen effects that finally inhibited BPH development.

Selective estrogen receptor modulators (SERMs) and selective androgen receptor modulators (SARMs) are two classes of drugs under development for a variety of diseases due to their high specificity for ER or AR, selective anabolic activity, lack of virilizing side effect, and ability to extend estrogen or androgen therapy [51]. Due to their unique abilities to selectively act as agonists or antagonists in a target gene and in a tissue-specific fashion [52], SERMs and SARMs are now being used as treatment for breast cancer, osteoporosis, postmenopausal symptoms, prostate cancer, and BPH [53–55]. We found that compounds from CS act as agonists of estrogen and/or androgen in HeLa, MCF-7, AD293, or LNCaP cells, while in vivo CS extract acted as antagonists for anti-BPH, indicating the potential role of CS and its active compounds as SERM or SARM.

Taken together, our findings demonstrated that CS inhibits rat BPH via interfering with estrogenic and androgenic signaling, thereby offering the potent candidates from CS as SERMs or SARMs for related diseases in the future.

Conflicts of Interest

The authors declare that there are no conflicts of interest.

Authors' Contributions

Xueni Wang, Rui Tao, and Jing Yang contributed equally to this research work.

Acknowledgments

This work was supported by the National Natural Science Foundation of China (81125024, 81303293), the National Key Basic Research Program of China (2012CB518400), the National Key Technology R&D Program of China (no. 2014BAI05B01), and the Technology Development Plan of Tianjin (14JCQNJC13400). The authors thank Professor Zhang Ju of Nankai University for the kind contribution of LNCaP cell line, AD293 cell lines, and AR plasmids.

References

[1] H.-P. Liu, R.-F. Chang, Y.-S. Wu, W.-Y. Lin, and F.-J. Tsai, "The Yang-tonifying herbal medicine cynomorium songaricum extends lifespan and delays aging in drosophila," *Evidence-Based Complementary and Alternative Medicine*, vol. 2012, Article ID 735481, pp. 1–11, 2012.

[2] W. M. Yang, H. Y. Kim, S. Y. Park, H.-M. Kim, M. S. Chang, and S. K. Park, "Cynomorium songaricum induces spermatogenesis with glial cell-derived neurotrophic factor (GDNF) enhancement in rat testes," *Journal of Ethnopharmacology*, vol. 128, no. 3, pp. 693–696, 2010.

[3] J. S. Lee, H. A. Oh, and J. Y. Kwon et al., "The effects of cynomorium songaricum on the reproductive activity in male golden hamsters," *Development and Reproduction*, vol. 17, no. 1, pp. 37–43, 2013.

[4] C. Ma, N. Nakamura, H. Miyashiro, M. Hattori, and K. Shimotohno, "Inhibitory effects of constituents from *Cynomorium songaricum* and related triterpene derivatives on HIV-1 protease," *Chemical and Pharmaceutical Bulletin*, vol. 47, no. 2, pp. 141–145, 1999.

[5] S. Jin, Eerdunbayaer, and A. Doi et al., "Polyphenolic constituents of cynomorium songaricum rupr. and antibacterial effect of polymeric proanthocyanidin on methicillin-resistant staphylococcus aureus," *Journal of Agricultural and Food Chemistry*, vol. 60, no. 29, pp. 7297–7305, 2012.

[6] A. B. Dull, A. A. George, E. I. Goncharova et al., "Identification of compounds by high-content screening that induce cytoplasmic to nuclear localization of a fluorescent estrogen receptor α chimera and exhibit agonist or antagonist activity in vitro," *Journal of Biomolecular Screening*, vol. 19, no. 2, pp. 242–252, 2014.

[7] D. Xin, H. Wang, J. Yang et al., "Phytoestrogens from *Psoralea corylifolia* reveal estrogen receptor-subtype selectivity," *Phytomedicine*, vol. 17, no. 2, pp. 126–131, 2010.

[8] P. Y. Maximov, T. M. Lee, and V. Craig Jordan, "The discovery and development of selective estrogen receptor modulators (SERMs) for clinical practice," *Current Clinical Pharmacology*, vol. 8, no. 2, pp. 135–155, 2013.

[9] M. J. Edouard, L. Miao, G.-W. Fan et al., "Yang-tonifying traditional Chinese medicinal plants and their potential phytoandrogenic activity," *Chinese Journal of Natural Medicines*, vol. 12, no. 5, pp. 321–334, 2014.

[10] J.-J. Chen and H.-C. Chang, "By modulating androgen receptor coactivators, daidzein may act as a phytoandrogen," *Prostate*, vol. 67, no. 5, pp. 457–462, 2007.

[11] H. Y. Tian, X. F. Yuan, and L. Jin et al., "A bufadienolide derived androgen receptor antagonist with inhibitory activities against prostate cancer cells," *Chemico-Biological Interactions*, vol. 207, no. 3, pp. 16–22, 2014.

[12] W. Hessenkemper, J. Roediger, S. Bartsch et al., "A natural androgen receptor antagonist induces cellular senescence in prostate cancer cells," *Molecular Endocrinology*, vol. 28, no. 11, pp. 1831–1840, 2014.

[13] D. Xu, T.-H. Lin, S. Li et al., "Cryptotanshinone suppresses androgen receptor-mediated growth in androgen dependent and castration resistant prostate cancer cells," *Cancer Letters*, vol. 316, no. 1, pp. 11–22, 2012.

[14] D. Roell and A. Baniahmad, "The natural compounds atraric acid and N-butylbenzene-sulfonamide as antagonists of the human androgen receptor and inhibitors of prostate cancer cell growth," *Molecular and Cellular Endocrinology*, vol. 332, no. 1-2, pp. 1–8, 2011.

[15] S. Y. Jang, E. H. Jang, S. Y. Jeong, and J. Kim, "Shikonin inhibits the growth of human prostate cancer cells via modulation of the androgen receptor," *International Journal of Oncology*, vol. 44, no. 5, pp. 1455–1460, 2014.

[16] G. N. Brooke, S. C. Gamble, and M. A. Hough et al., "Antiandrogens act as selective androgen receptor modulators at the proteome level in prostate cancer cells," *Molecular and Cellular Proteomics*, vol. 14, no. 5, pp. 1201–1216, 2015.

[17] C. L. Eaton, "Aetiology and pathogenesis of benign prostatic hyperplasia," *Current Opinion in Urology*, vol. 13, no. 1, pp. 7–10, 2003.

[18] C. K. M. Ho and F. K. Habib, "Estrogen and androgen signaling in the pathogenesis of BPH," *Nature Reviews Urology*, vol. 8, no. 1, pp. 29–41, 2011.

[19] S. Gail, L. H. Prins, L. Birch, and P. Yongbing, "The role of estrogens in normal and abnormal development of the prostate glan," *Annals of the New York Academy of Sciences*, vol. 1089, pp. 1–13, 2006.

[20] K.-P. Lai, C.-K. Huang, L.-Y. Fang et al., "Targeting stromal androgen receptor suppresses prolactin-driven benign prostatic hyperplasia (BPH)," *Molecular Endocrinology*, vol. 27, no. 10, pp. 1617–1631, 2013.

[21] Z. Zhang, L. Duan, X. Du et al., "The proliferative effect of estradiol on human prostate stromal cells is mediated through activation of ERK," *Prostate*, vol. 68, no. 5, pp. 508–516, 2008.

[22] R. Shao, J. Shi, H. Liu et al., "Epithelial-to-mesenchymal transition and estrogen receptor α mediated epithelial dedifferentiation mark the development of benign prostatic hyperplasia," *Prostate*, vol. 74, no. 9, pp. 970–982, 2014.

[23] T. Lu, W.-J. Lin, K. Izumi et al., "Targeting androgen receptor to suppress macrophage-induced EMT and benign prostatic hyperplasia (BPH) development," *Molecular Endocrinology*, vol. 26, no. 10, pp. 1707–1715, 2012.

[24] S. J. McPherson, S. J. Ellem, V. Patchev, K. H. Fritzemeier, and G. P. Risbridger, "The role of Erα and ERβ in the prostate: insights from genetic models and isoform-selective ligands," *Ernst Schering Foundation Symposium Proceedings*, vol. 1, pp. 131–148, 2006.

[25] R. Tao, L. Miao, X. N. Wang, and N. Wichai, "Research progress of effects of *Cynomorium songaricum* Rupr. on the benignprostatic hyperplasia treatment," *The Chinese Journal of Clinical Pharmacology*, vol. 32, no. 12, pp. 1150–1152, 2016.

[26] Q.-H. Zhang, W.-B. Wang, J. Li et al., "Simultaneous determination of catechin, epicatechin and epicatechin gallate in rat plasma by LC-ESI-MS/MS for pharmacokinetic studies after oral administration of Cynomorium songaricum extract," *Journal of Chromatography B: Analytical Technologies in the Biomedical and Life Sciences*, vol. 880, no. 1, pp. 168–171, 2012.

[27] Q.-G. Gao, H.-Y. Chan, C. W.-Y. Man, and M.-S. Wong, "Differential ERα-mediated rapid estrogenic actions of ginsenoside Rg1 and estren in human breast cancer MCF-7 cells," *Journal of Steroid Biochemistry and Molecular Biology*, vol. 141, pp. 104–112, 2014.

[28] J. Li, B. Cao, X. Liu et al., "Berberine suppresses androgen receptor signaling in prostate cancer," *Molecular Cancer Therapeutics*, vol. 10, no. 8, pp. 1346–1356, 2011.

[29] M. A. Titus, J.-A. Tan, C. W. Gregory et al., "14-3-3η amplifies androgen receptor actions in prostate cancer," *Clinical Cancer Research*, vol. 15, no. 24, pp. 7571–7581, 2009.

[30] Y. Zhou, X.-Q. Xiao, L.-F. Chen et al., "Proliferation and phenotypic changes of stromal cells in response to varying estrogen/androgen levels in castrated rats," *Asian Journal of Andrology*, vol. 11, no. 4, pp. 451–459, 2009.

[31] X. Xiao, Q. Yuan, Y. Wang et al., "Establishment of rats prostatic stromal hyperplasia model," *Acta Scientiarum Naturalium Universitatis Nankaiensis*, vol. 39, no. 4, pp. 91–95, 2006.

[32] H. B. Patisaul and W. Jefferson, "The pros and cons of phytoestrogens," *Frontiers in Neuroendocrinology*, vol. 31, no. 4, pp. 400–419, 2010.

[33] J.-M. Zhang, J. Li, E.-W. Liu et al., "Danshen enhanced the estrogenic effects of Qing E formula in ovariectomized rats," *BMC Complementary and Alternative Medicine*, vol. 16, no. 1, article 181, 2016.

[34] C. Shi, X. Zhu, J. Wang, and D. Long, "Tanshinone IIA promotes non-amyloidogenic processing of amyloid precursor protein in platelets via estrogen receptor signaling to phosphatidylinositol 3-kinase/Akt," *Biomedical Reports*, vol. 2, no. 4, pp. 500–504, 2014.

[35] R. J. Miksicek, "Commonly occurring plant flavonoids have estrogenic activity," *Molecular Pharmacology*, vol. 44, no. 1, pp. 37–43, 1993.

[36] V. Y. C. Ong and B. K. H. Tan, "Novel phytoandrogens and lipidic augmenters from *Eucommia ulmoides*," *BMC Complementary and Alternative Medicine*, vol. 7, article 3, 2007.

[37] N. Caturla, E. Vera-Samper, J. Villalain, C. R. Mateo, and V. Micol, "The relationship between the antioxidant and the antibacterial properties of galloylated catechins and the structure of phospholipid model membranes," *Free Radical Biology and Medicine*, vol. 34, no. 6, pp. 648–662, 2003.

[38] C. Kürbitz, D. Heise, T. Redmer et al., "Epicatechin gallate and catechin gallate are superior to epigallocatechin gallate in growth suppression and anti-inflammatory activities in pancreatic tumor cells," *Cancer Science*, vol. 102, no. 4, pp. 728–734, 2011.

[39] S. J. Baek, J. S. Kim, F. R. Jackson, T. E. Eling, M. F. McEntee, and S. H. Lee, "Epicatechin gallate-induced expression of NAG-1 is associated with growth inhibition and apoptosis in colon cancer cells," *Carcinogenesis*, vol. 25, no. 12, pp. 2425–2432, 2004.

[40] S. Shah, P. D. Stapleton, and P. W. Taylor, "The polyphenol (-)-epicatechin gallate disrupts the secretion of virulence-related proteins by Staphylococcus aureus," *Letters in Applied Microbiology*, vol. 46, no. 2, pp. 181–185, 2008.

[41] C. S. Stevens, H. Rosado, R. J. Harvey, and P. W. Taylor, "Epicatechin gallate, a naturally occurring polyphenol, alters the course of infection with β-lactam-resistant Staphylococcus

aureus in the zebrafish embryo," *Frontiers in Microbiology*, vol. 6, Article ID 01043, 2015.

[42] T. M. Nicholson and W. A. Ricke, "Androgens and estrogens in benign prostatic hyperplasia: Past, present and future," *Differentiation; Research in Biological Diversity*, vol. 82, no. 4-5, pp. 184–199, 2011.

[43] C. Wang, X. Du, and R. Yang et al., "The prevention and treatment effects of tanshinone IIA on oestrogen/androgen-induced benign prostatic hyperplasia in rats," *The Journal of Steroid Biochemistry and Molecular Biology*, vol. 145, pp. 28–37, 2015.

[44] C. Wang, F. Luo, Y. Zhou et al., "The therapeutic effects of Docosahexaenoic acid on oestrogen/androgen-induced benign prostatic hyperplasia in rats," *Experimental Cell Research*, vol. 345, no. 2, pp. 125–133, 2016.

[45] F.-L. Chiu and J.-K. Lin, "Downregulation of androgen receptor expression by luteolin causes inhibition of cell proliferation and induction of apoptosis in human prostate cancer cells and xenografts," *Prostate*, vol. 68, no. 1, pp. 61–71, 2008.

[46] I. S. Shin, M. Y. Lee, D. Y. Jung, C. S. Seo, H. K. Ha, and H. K. Shin, "Ursolic acid reduces prostate size and dihydrotestosterone level in a rat model of benign prostatic hyperplasia," *Food and Chemical Toxicology*, vol. 50, no. 3-4, pp. 884–888, 2012.

[47] S. J. Ellem and G. P. Risbridger, "The dual, opposing roles of estrogen in the prostate," *Annals of the New York Academy of Sciences*, vol. 1155, pp. 174–186, 2009.

[48] S. Wen, H.-C. Chang, J. Tian, Z. Shang, Y. Niu, and C. Chang, "Stromal androgen receptor roles in the development of normal prostate, benign prostate hyperplasia, and prostate cancer," *American Journal of Pathology*, vol. 185, no. 2, pp. 293–301, 2015.

[49] M. Stanbrough, I. Leav, P. W. L. Kwan, G. J. Bubley, and S. P. Balk, "Prostatic intraepithelial neoplasia in mice expressing an androgen receptor transgene in prostate epithelium," *Proceedings of the National Academy of Sciences of the United States of America*, vol. 98, no. 19, pp. 10823–10828, 2001.

[50] S. J. McPherson, S. J. Ellem, E. R. Simpson, V. Patchev, K.-H. Fritzemeier, and G. P. Risbridger, "Essential role for estrogen receptor beta in stromal-epithelial regulation of prostatic hyperplasia," *Endocrinology*, vol. 148, no. 2, pp. 566–574, 2007.

[51] B. L. Clarke and S. Khosla, "New selective estrogen and androgen receptor modulators," *Current Opinion in Rheumatology*, vol. 21, no. 4, pp. 374–379, 2009.

[52] S. Martinkovich, D. Shah, S. L. Planey, and J. A. Arnott, "Selective estrogen receptor modulators: Tissue specificity and clinical utility," *Clinical Interventions in Aging*, vol. 9, pp. 1437–1452, 2014.

[53] R. T. Atawia, M. G. Tadros, A. E. Khalifa, H. A. Mosli, and A. B. Abdel-Naim, "Role of the phytoestrogenic, pro-apoptotic and anti-oxidative properties of silymarin in inhibiting experimental benign prostatic hyperplasia in rats," *Toxicology Letters*, vol. 219, no. 2, pp. 160–169, 2013.

[54] S. Gupta, F. Afaq, and H. Mukhtar, "Involvement of nuclear factor-kappa B, Bax and Bcl-2 in induction of cell cycle arrest and apoptosis by apigenin in human prostate carcinoma cells," *Oncogene*, vol. 21, no. 23, pp. 3727–3738, 2002.

[55] F. Ren, S. Zhang, S. H. Mitchell, R. Butler, and C. Y. F. Young, "Tea polyphenols down-regulate the expression of the androgen receptor in LNCaP prostate cancer cells," *Oncogene*, vol. 19, no. 15, pp. 1924–1932, 2000.

Hindawi
Evidence-Based Complementary and Alternative Medicine
Volume 2017, Article ID 6072573, 12 pages
https://doi.org/10.1155/2017/6072573

Research Article

Barley Seedling Extracts Inhibit RANKL-Induced Differentiation, Fusion, and Maturation of Osteoclasts in the Early-to-Late Stages of Osteoclastogenesis

Sik-Won Choi,[1] Shin-Hye Kim,[1,2] Kwang-Sik Lee,[1,3] Hyeon Jung Kang,[1] Mi Ja Lee,[1] Kie-In Park,[2] Jin Hwan Lee,[4] Ki Do Park,[1] and Woo Duck Seo[1]

[1]*Division of Crop Foundation, National Institute of Crop Science (NICS), Rural Development Administration (RDA), Jeonbuk 565-851, Republic of Korea*
[2]*Department of Biological Sciences, College of Natural Science, Chonbuk National University, Jeonbuk 561-756, Republic of Korea*
[3]*College of Crop Science and Biotechnology, Dankook University, Cheonan 330-714, Republic of Korea*
[4]*Division of Research Development and Education, National Institute of Chemical Safety, Ministry of Environment, Daejeon 305-343, Republic of Korea*

Correspondence should be addressed to Woo Duck Seo; swd2002@korea.kr

Received 7 March 2017; Revised 3 April 2017; Accepted 18 April 2017; Published 8 May 2017

Academic Editor: Vishal Chandra

The number of patients with osteoporosis is increasing worldwide, and a decrease in bone mass is a main risk factor for fracture. The prevention of bone loss is critical for improving the quality of life for patients. However, the long-term use of antiosteoporotic agents is limited due to their side effects. Barley has been traditionally ingested for thousands of years as a safe, natural food with pharmaceutical properties, and its seedling can enhance the biological activity of the medicinal components found in food. This study aimed to clarify the antiresorptive activity of barley seedling and its mode of action. Barley seedling extracts (BSE) dose-dependently inhibited RANKL-induced osteoclast differentiation with alteration of IκB degradation, c-Fos, and NFATc1 molecules in the early-to-middle stages of osteoclastogenesis. In the late phase of osteoclastogenesis, BSE also prevented DC-STAMP and cathepsin K, which are required for cell fusion and bone degradation, such as osteoclast function. In conclusion, barley seedling from natural foods may provide long-term safety and be useful for the prevention or treatment of osteoclast-mediated bone metabolic diseases, including osteoporosis.

1. Introduction

Bones are dynamic structures that are continually being formed and resorbed through the constant processes of remodeling and reorganisation. Bone homeostasis is sustained by a tight balance between osteoclast-mediated bone destruction and osteoblast-related bone formation. However, an imbalance of bone homeostasis by the induction of osteoclastic bone destruction or by the reduction of osteoblastic bone formation can lead to a variety of bone metabolic disorders, including osteoporosis, rheumatoid arthritis, and Paget's disease [1–3]. Most bone metabolic disorders induce the activation of osteoclasts; consequently, bone resorption can exceed bone formation and lead to pathological bone-resorbing activity resulting in osteopenic disorders with increased risk of fracture [4, 5]. The economic burdens for hospitalisation, skeletal deformity, and pain due to fractures have become a serious public health issue worldwide [6]. Therefore, protection against bone loss and the risk of bone fracture is an essential means of improving the quality of patients' lives with bone defects.

The differentiation of osteoclasts is a complex multistep process that involves cell differentiation, migration, fusion, and resorption. In bone marrow, osteoclasts are multinucleated giant cells that resorb mineralised tissues; they are differentiated from hematopoietic stem cells by key regulators, such as receptor activator of NF-κB ligand (RANKL) and macrophage colony-stimulating factor (M-CSF) [7]. M-CSF

and RANKL trigger the differentiation of osteoclast precursors into mononuclear osteoclasts (preosteoclasts) and increase them to migrate until they attach to the bone matrix. Mononuclear osteoclasts then fuse to form giant multinucleated osteoclasts that, subsequently, relate to bone resorption. In the initial stage, the binding of RANKL to its receptor RANK triggers osteoclast differentiation by the activation of mitogen-activated protein (MAP) kinases and transcription factor, NF-κB [8]. These essential signaling molecules contribute to the activation of c-Fos and nuclear factor of activated T cells, cytoplasmic 1 (NFATc1), which are known to be master regulators for osteoclast differentiation [7, 9, 10]. c-Fos is induced in the early-to-middle stages of osteoclastogenesis and NFATc1 is increased in the middle-to-late phases. These two transcription factors play a critical role in the expression of specific genes, such as tartrate-resistant acid phosphatase (TRAP), osteoclast-associated receptor (OSCAR), dendritic cell-specific transmembrane protein (DC-STAMP), and cathepsin K, which are required for osteoclast differentiation, cell fusion, and maturation. Thus, the regulation of osteoclast formation-mediated molecules is essentially responsible for the degradation of the mineralised matrix during physiological and pathological bone turnover [11].

For thousands of years, plant foods, including vegetables, fruit, wheat, rice, and barley, have been conventionally ingested in many countries around the world due to their nutritional support for the body. Moreover, plant foods contain naturally occurring bioactive components known as phytochemicals. Therefore, plants are a source of safe, healthy foods because they are suitable for long-term use, although the fact that ingesting plants might have therapeutic benefits is clearly not a new concept. Specifically, functional foods, and their bioactive compounds that play a role in improving skeletal health, have received noticeable attention. Recently, a number of studies have reported that functional foods and their phytochemicals prevent bone loss in both female and male osteoporotic animal models, as well as in postmenopausal women [12–15]. Therefore, dietary intake of natural bioactive plant foods is an adaptable habit that may play a key role in reducing the risk of diseases disorders, such as osteoporosis.

The various physiological functions of barley have been reported to exhibit antioxidative, anti-inflammatory, antiobesity, hair-growth stimulation, and cholesterol-lowering activities [16–21]. These studies have attracted considerable research attention focusing on the biological activity of barley, and its evident safety valuation has accelerated the commercial use of barley and its phytochemicals. Furthermore, researchers have shown an interest in developing natural ingredients that can increase the bioactive components in barley. Notably, the barley seedling (BS), grown for about 7 days from barley seed, contains high concentrations of various physiologically active ingredients that enable it to germinate and to protect itself from external attacks. In particular, BS contains policosanols with substantial levels of polyphenol and saponarin as a major flavonoid, which have a variety of biological activities [22, 23]. Accordingly, the pharmaceutical properties of BS have potential roles in the prevention and treatment of disease. Few studies have investigated barley seedling extracts (BSE), and it has not been elucidated as to whether or not BSE has antiresorptive activity. Therefore, we investigated the effect of BSE on RANKL-mediated osteoclast differentiation and the bone-resorbing activity of mature osteoclasts.

2. Materials and Methods

2.1. Preparation of the Barley Seedling Extracts. Barley (*Hordeum vulgare* L.) was cultivated in 2015 in the experimental field at the National Institute of Crop Science, Rural Development Administration, Jeonbuk, Korea. BS was prepared using the procedure reported in the literature [23]. Barley seeds were washed twice using deionized distilled water and imbibed in water at 18°C for 24 hr. The imbibed seeds were germinated in 65% humidity at 16°C in a normal light cycle (16/8 hr day/night). The germinating seeds and seedlings were harvested in liquid nitrogen 7 days after germination. The collected leaves were freeze-dried immediately after sampling. Prior to obtaining the BSE, the leaves were pulverised to 100 mesh. The masses of all the samples were based on dry weight. To determine the antiosteoporotic activities, the pulverised seeds (10 g) were extracted with 20 ml of the prethanol for 2 days at 4°C in the dark. The crude extracts were filtered through Whatman Number 42 filter paper to remove the sediment. The solvent was evaporated, and the prethanol extracts were obtained from the BS.

2.2. Reagents and Antibodies. Mouse soluble RANKL and M-CSF were purchased from R&D Systems (Minneapolis, MN, USA). Penicillin, streptomycin, cell culture medium, and foetal bovine serum (FBS) were purchased from Invitrogen Life Technologies (Carlsbad, CA, USA). Antibodies against NFATc1, actin, and IκB and secondary antibody conjugated to horseradish peroxidase (HRP) were purchased from Santa Cruz Biotechnology (Dallas, TX, USA). All of the other antibodies were obtained from Cell Signaling Technology (Beverly, MA, USA).

2.3. Ethics Statement. This study was conducted in strict accordance with the recommendations in the Standard Protocol for Animal Study of Gangnam Severance Hospital Biomedical Center (Permit Number 2016-0238). The protocol (ID Number 0238) was approved by the Institutional Animal Care and Use Committee (IACUC) of Yonsei University College of Medicine. Every effort was made to minimise the number of animals used in the study and minimise their suffering and stress/discomfort.

2.4. Preparation of Osteoclast Precursor Cells. All the experiments were carried out as described in a previous study, with modifications [24]. Five-week-old male Imprinting Control Region (ICR) mice (Damul Science Co., Daejeon, Korea) were maintained in a room illuminated daily from 07:00 to 19:00 (12 : 12 hr light/dark cycle), with controlled temperature (23 ± 1°C) and ventilation (10–12 times per hour); humidity was maintained at 55 ± 5% and the animals had free access to a standard animal diet and tap water.

Table 1: The primer sequences used in this study.

Target gene	Forward primer (5′–3′)	Reverse primer (5′–3′)
c-Fos	CCAGTCAAGAGCATCAGCAA	AAGTAGTGCAGCCCGGAGTA
NFATc1	GGGTCAGTGTGACCGAAGAT	GGAAGTCAGAAGTGGGTGGA
TRAP	GATGACTTTGCCAGTCAGCA	ACATAGCCCACACCGTTCTC
OSCAR	AGGGAAACCTCATCCGTTTG	GAGCCGGAAATAAGGCACAG
DC-STAMP	CCAAGGAGTCGTCCATGATT	GGCTGCTTTGATCGTTTCTC
Cathepsin K	GGCCAACTCAAGAAGAAAAC	GTGCTTGCTTCCCTTCTGG
GAPDH	ACCACAGTCCATGCCATCAC	TCCACCACCCTGTTGCTGTA
HPRT1	TGCTCGAGATGTCATGAAGG	AGAGGTCCTTTTCACCAGCA

Bone marrow cells were obtained from the five-week-old male ICR mice by flushing their femurs and tibias with alpha minimum essential medium- (α-MEM-) containing antibiotics (100 units/ml penicillin, 100 μg/ml streptomycin). The bone marrow cells were cultured on culture dishes for 1 day in α-MEM containing 10% FBS and M-CSF (10 ng/ml). The nonadherent bone marrow cells were plated into Petri dishes and cultured for 3 days in the presence of M-CSF (30 ng/ml). After the nonadherent cells were washed out, the adherent cells were used as bone marrow-derived macrophages (BMMs).

2.5. Osteoclast Cell Culture and Osteoclast Differentiation. The BMMs were maintained in α-MEM supplemented with 10% FBS, 100 units/ml penicillin, and 100 μg/ml streptomycin. The medium was changed every 3 days in a humidified atmosphere of 5% CO_2 at 37°C. To differentiate the osteoclasts from the BMMs, the BMMs (1×10^4 cells/well in a 96-well plate or 3×10^5 cells/well in a 6-well plate) were cultured with M-CSF (30 ng/ml) and RANKL (10 ng/ml) for 4 days, and then the multinucleated osteoclasts were observed.

2.6. TRAP Staining and Activity Assay. The mature osteoclasts were visualised using TRAP staining, a biomarker of osteoclast differentiation. Briefly, the multinucleated osteoclasts were fixed with 3.7% formalin for 10 min, permeabilised with 0.1% Triton X-100 for 10 min, and then stained with TRAP solution (Sigma-Aldrich, Saint Louis, MO, USA). The TRAP-positive multinucleated osteoclasts (MNC; nuclear $\geq$ 3 or nuclear $\geq$ 10) were counted. To measure TRAP activity, the multinucleated osteoclasts were fixed in 3.7% formalin for 5 min, permeabilised with 0.1% Triton X-100 for 10 min, and then treated with TRAP buffer (100 mM sodium citrate, pH 5.0, 50 mM sodium tartrate) containing 3 mM *p*-nitrophenyl phosphate (Sigma-Aldrich) at 37°C for 5 min. The reaction mixtures in the wells were transferred to new plates containing an equal volume of 0.1 N NaOH, and the optical density values were determined at 405 nm.

2.7. Cell Viability Assay. The BMMs were plated in a 96-well plate at a density of 1×10^4 cells/well, in triplicate. After treatment with M-CSF (30 ng/ml) and various concentrations of BSE, the cells were incubated for 3 days, and cell viability was measured using the Cell Counting Kit 8 (CCK-8) according to the manufacturer's protocol. The CCK-8 assay kit was purchased from Dojindo Molecular Technologies (Rockville, MD, USA).

2.8. RNA Isolation and Real-Time Polymerase Chain Reaction Analysis. Real-time polymerase chain reaction (PCR) was performed as described previously [25]. The primers were chosen using the online Primer3 design program [26]. The primer sets used in this study are shown in Table 1. Briefly, total RNA was isolated with TRIzol reagent, and the first-strand cDNA was synthesized with the RevertAid First-Strand cDNA Synthesis Kit (Thermo Scientific, Waltham, MA, USA) according to the manufacturer's recommended protocol. SYBR green-based quantitative PCR (qPCR) was performed using the Bio-Rad CFX96 Real-Time PCR Detection System (Hercules, CA, USA) and Topreal qPCR 2x PreMIX (Enzynomics, Daejeon, Korea). All reactions were run in triplicate, and the data were analysed using the $2^{-\Delta\Delta CT}$ method [27]. Hypoxanthine phosphoribosyltransferase 1 (HPRT1) and glyceraldehyde 3-phosphate dehydrogenase (GAPDH) were used as the internal standard genes. The statistical significance was determined using Student's *t*-test with HPRT1/GAPDH-normalised $2^{-\Delta\Delta CT}$ values; the differences were considered significant at $P < 0.05$.

2.9. Western Blot Analysis. Western blot analysis was performed as described previously [28]. Briefly, the cultured cells were washed with ice-cold phosphate-buffered saline (PBS) and lysed in lysis buffer (50 mM Tris-HCl, 150 mM NaCl, 5 mM EDTA, 1% Triton X-100, 1 mM sodium fluoride, 1 mM sodium vanadate, and 1% deoxycholate) supplemented with protease inhibitors. After centrifugation at 15,000 ×g for 15 min, the protein quantification in the supernatant was determined using the detergent compatible (DC) protein assay kit (Bio-Rad). The quantified proteins were denatured, separated on sodium dodecyl sulphate-polyacrylamide gel electrophoresis (SDS-PAGE) gels, and transferred onto a polyvinylidene difluoride (PVDF) membrane (Merck Millipore, Darmstadt, Germany). After incubation with an antibody, the membranes were developed using SuperSignal West Femto Maximum Sensitivity Substrate (Thermo Scientific) and visualised with the LAS-4000 luminescent image

analyser (GE Healthcare Life Sciences, Little Chalfont, UK). Actin was used as a loading control.

2.10. Bone Pit Formation Analysis. The mature osteoclasts were prepared by isolating osteoblasts from the calvariae of newborn mice by serial digestion in 0.1% collagenase (Gibco, Paisley, UK), as previously described [29]. The bone marrow cells were isolated as described above. The osteoblasts (3.5×10^5 cells/well) and BMMs (1×10^6 cells/well) were cocultured on a collagen-coated 90 mm dish in the presence of 1α,25-dihydroxyvitamin D_3 ($VitD_3$) and prostaglandin E_2 (PGE_2) for 6 days. The α-MEM complete medium with $VitD_3$ and PGE_2 was changed every 3 days. The cocultured cells were detached from the collagen-coated dishes using 0.1% collagenase and then replated on a bone biomimetic synthetic surface (Corning, NY, USA) in a 24-well plate. After 1 hr, each well was treated with RANKL (10 ng/ml) and BSE for 24 hrs. The cells on these plates were stained for TRAP and photographed under a light microscope at 10x magnification. To observe the resorption pits, the slides were washed with PBS and treated with 5% sodium hypochlorite for 5 min. After the plate was washed with PBS and dried, it was photographed under a light microscope. Quantification of the resorbed areas was performed using the ImageJ program.

2.11. Statistical Analysis. All quantitative values are presented as mean ± standard deviation. Each experiment in triplicate was performed three to five times, and Figures 1–5 show the results from one representative experiment. Statistical differences were analysed using Student's t-test, and a value of $P < 0.05$ was considered significant.

3. Results

3.1. BSE Inhibits RANKL-Induced Osteoclast Differentiation. To determine the effect of BSE on RANKL-mediated osteoclastogenesis, the BMMs were incubated with different concentrations of BSE followed by RANKL (10 ng/ml) treatment. The BMMs induced numerous TRAP-positive multinucleated osteoclast cells (TRAP+ MNCs) by RANKL in the control group (vehicle treatment), but BSE attenuated the formation of TRAP+ MNCs in a dose-dependent manner (Figure 1(a)). The inhibitory effect was confirmed by counting the number of TRAP+ MNCs (Figure 1(b); left panel) and measuring TRAP activity (Figure 1(b); right panel). Since the cellular cytotoxicity of BSE in the survival of the BMMs could affect RANKL-induced osteoclast differentiation, its effect was examined using the CCK-8 assay. As shown in Figure 1(c), no cytotoxicity of BSE was observed at the indicated dose. These results show that BSE significantly inhibited RANKL-mediated osteoclast differentiation without apparent cytotoxicity.

3.2. BSE Attenuates RANKL-Induced Expression of c-Fos and NFATc1 during Osteoclastogenesis. The inhibitory effect of BSE on osteoclast differentiation was examined by evaluating the expression level of several osteoclastogenesis-associated genes, including transcriptional factors. As shown in Figure 2(a), the mRNA expression levels of osteoclastogenesis-related transcription factors, such as c-Fos and NFATc1, were induced by RANKL, but these inductions were significantly inhibited by treatment with BSE. In addition, BSE also strongly attenuated the mRNA induction of c-Fos/NFATc1-dependent molecules, such as TRAP and OSCAR. Western blot analysis further revealed that the RANKL-induced translational expression of both c-Fos and NFATc1 was strongly inhibited by treatment with BSE (Figure 2(b)). Taken together, these results suggest that the antiosteoclastogenesis activity of BSE could arise from its potential to inhibit the expression of c-Fos/NFATc1, the early-stage transcription factor that is required for osteoclast differentiation.

3.3. BSE Contributes to RANKL-Mediated NF-κB/IκB Signaling Pathways. To clarify the mode of antiosteoclastic action by BSE, we investigated whether or not BSE could affect the activation of the RANKL-mediated signaling molecules associated with the regulation of c-Fos/NFATc1 expression, which are master transcription factors required for osteoclast differentiation. As shown in Figure 3, RANKL stimulated degradation of IκB and the activation of RAC-Alpha Serine/Threonine-Protein Kinase (AKT) and MAP kinases, including extracellular signal-regulated kinase (ERK), c-Jun N-terminal kinase (JNK), and p38, but BSE only blocked the RANKL-induced degradation of IκB. These results demonstrate that attenuation of IκB degradation could be involved in the antiosteoclastogenic action of BSE.

3.4. BSE Inhibits Osteoclast Differentiation in the Late Stage Associated with Cell Fusion as well as in the Early Stages. To better understand when BSE inhibits osteoclast differentiation, we examined the antiosteoclastogenic activity of BSE by treating the cells at four time points, as shown in Figure 4(a). Treatment with BSE for 24 hrs moderately inhibited the RANKL-induced formation of TRAP+ MNCs in the early-to-late stages of osteoclastogenesis (Figure 4(b)). Moreover, TRAP activity was also attenuated by the addition of BSE (Figure 4(c)). Interestingly, the presence of BSE (3 μg/ml) from day 3 to day 4 dramatically repressed TRAP+ MNCs formation with >10 nuclei giant osteoclasts (Figure 4(b), 3-4 d) and reduced the number of fused cells (Figure 4(d)). We confirmed the inhibitory effect of BSE on the monocyte TRAP+ cells into giant multinucleated osteoclasts by evaluating the mRNA expression level of DC-STAMP, which is an essential factor for osteoclast fusion. BSE strongly inhibited the RANKL-induced mRNA expression of DC-STAMP (Figure 4(e)). These results indicate that the antiosteoclastogenic effect of BSE could be due to its potential to inhibit multistep response in the early, middle, and late stages of osteoclast differentiation.

3.5. BSE Prevents the Bone-Resorbing Function of Mature Osteoclasts. Next, to investigate whether BSE has the potential to inhibit the survival and the bone-resorbing activity of mature osteoclasts, we performed resorption-related gene expression, mature osteoclast counting, and a bone pit formation assay. As shown in Figure 5(a), BSE significantly

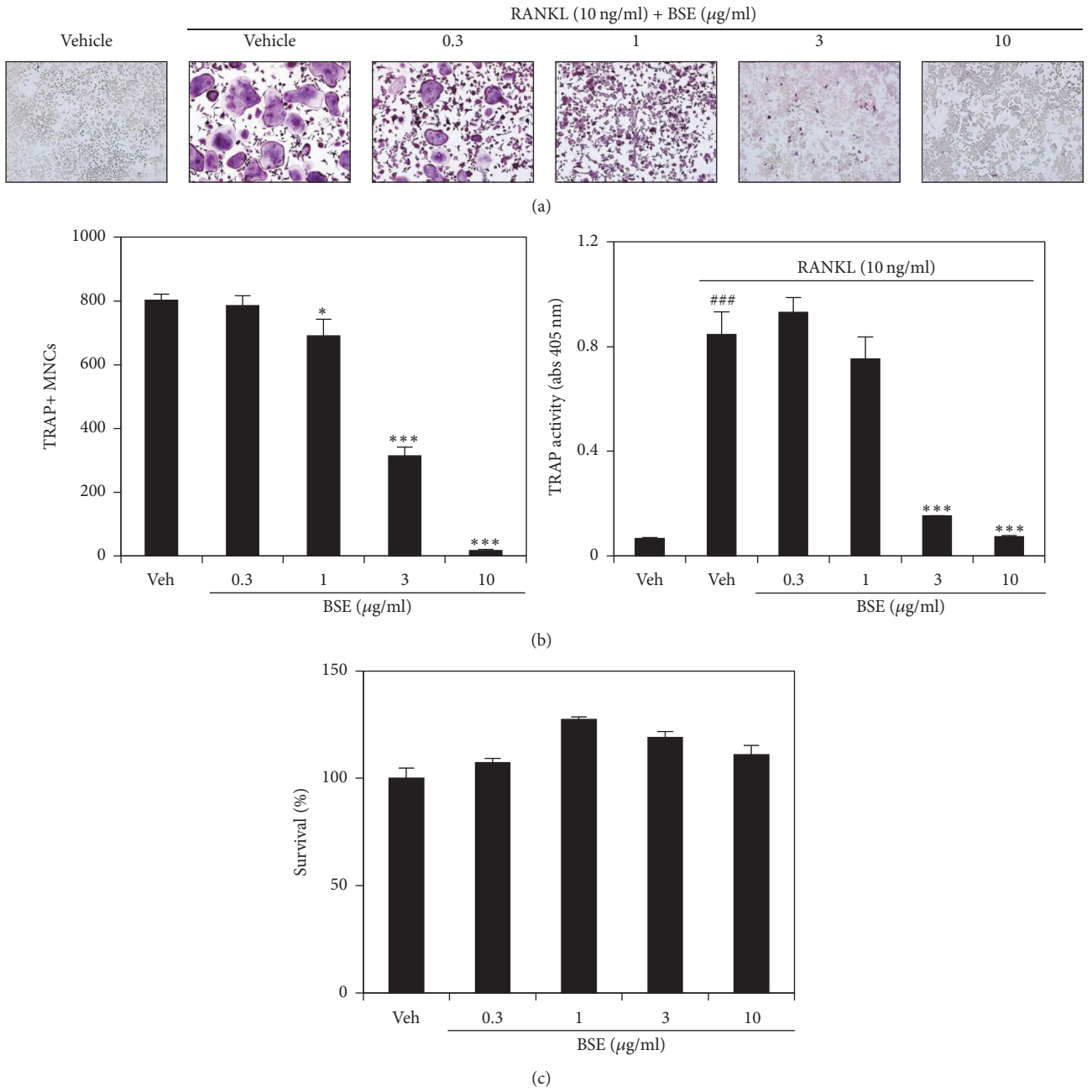

Figure 1: BSE impairs RANKL-induced osteoclast differentiation. (a) The BMMs were cultured for 4 days in the presence of RANKL (10 ng/ml) and M-CSF (30 ng/ml) with either the vehicle (prethanol) or the indicated concentration of BSE. Multinucleated osteoclasts were visualised using TRAP staining. (b) TRAP+ MNCs were counted (left panel) and TRAP activity was measured (right panel). $^{###}P < 0.001$ (versus the control); $^{*}P < 0.05$; $^{***}P < 0.001$ (versus the RANKL-treated group). (c) The effect of BSE on the viability of BMMs was evaluated using the CCK-8 assay. Data are expressed as mean ± SD and are representative of at least three experiments.

inhibited the RANKL-mediated mRNA induction of cathepsin K, which plays a role in bone resorption. We then confirmed the effect of BSE on the RANKL-induced bone resorptive function of mature osteoclasts in a coculture system of BMMs and primary osteoblast cells. When the purified mature osteoclasts from the coculture were replated on a bone biomimetic synthetic surface and cultured with/without BSE for 1 day, no significant difference was observed between the BSE-treated cells and the control group in terms of TRAP+ MNCs formation (Figure 5(b); upper panel) and the number of TRAP+ MNCs (Figure 5(c)). However, the addition of BSE strongly inhibited the areas of resorption formation (Figure 5(b); bottom panel) as measured using the resorbing bone pit assay (Figure 5(d)). These results revealed that

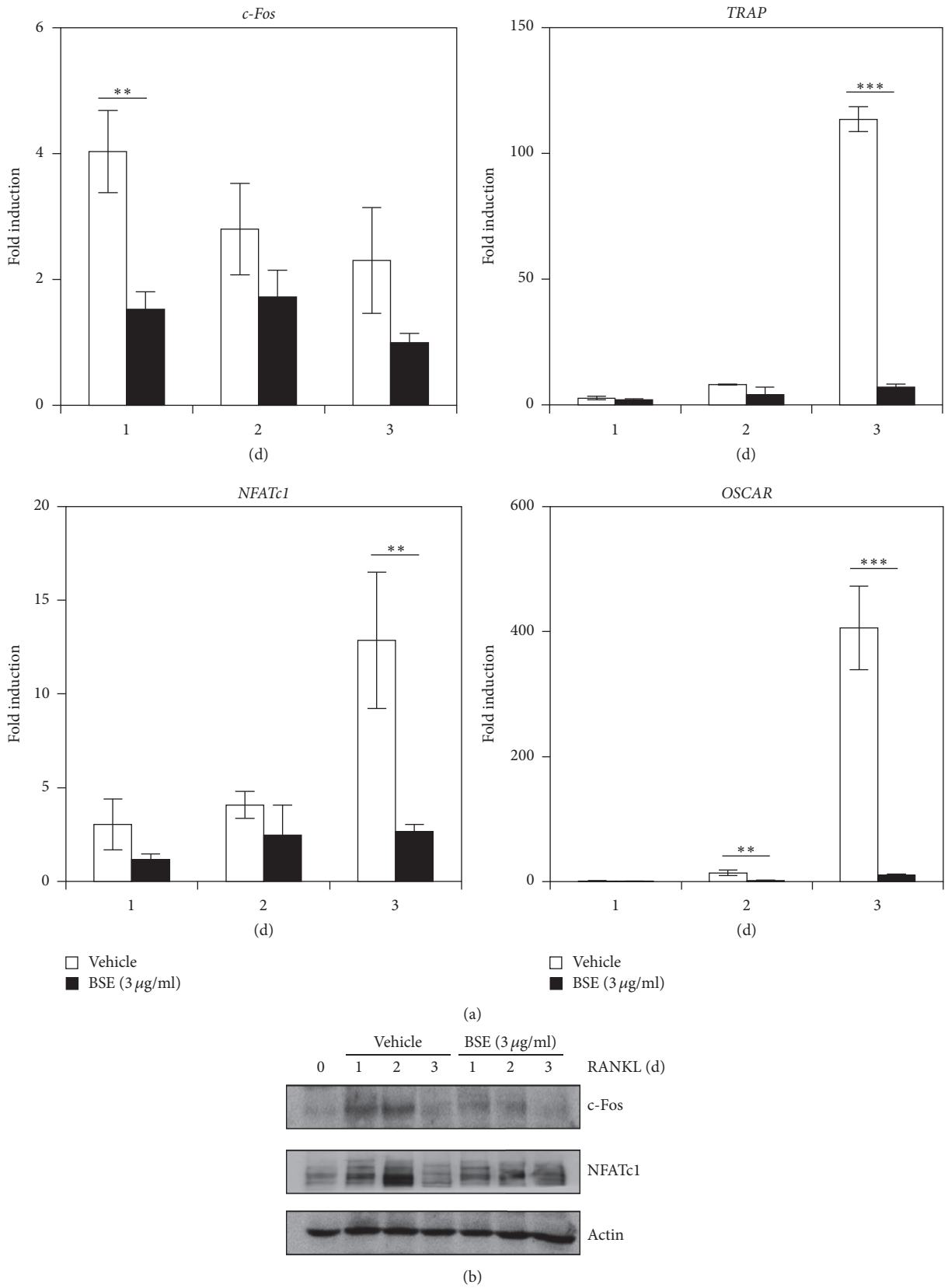

Figure 2: BSE inhibits the RANKL-mediated expression level of c-Fos/NFATc1. (a) The BMMs were stimulated with RANKL (10 ng/ml) and M-CSF (30 ng/ml) in the presence or absence of BSE (3 μg/ml) for the indicated times. Total RNA was then isolated using TRIzol reagent, and the mRNA expression levels were evaluated using real-time PCR. GAPDH was used as the internal control. $^{**}P < 0.01$; $^{***}P < 0.001$ (versus the vehicle control). (b) The effect of BSE on the protein expression level of RANKL-induced transcription factors was evaluated using Western blot analysis. Actin was used as the internal control. Data are representative of at least three experiments.

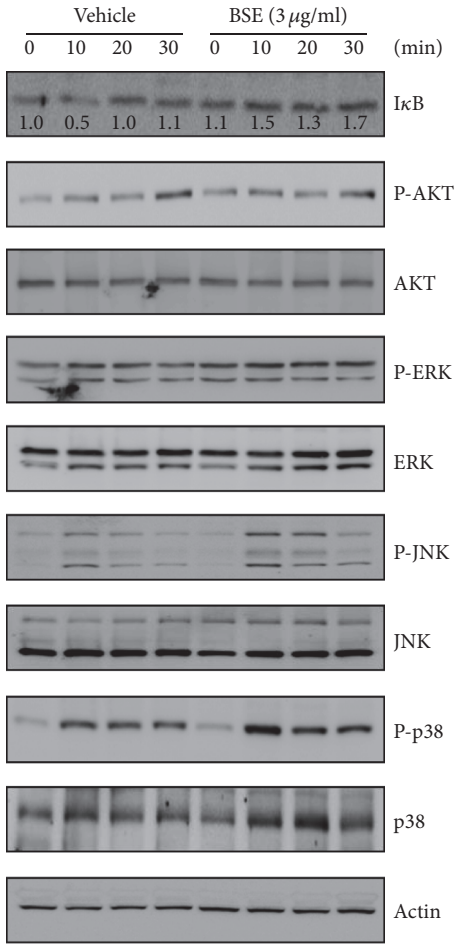

Figure 3: BSE attenuates RANKL-induced degradation of IκB signaling molecules. In the condition of serum starvation for 1 hr, the BMMs were pretreated with or without BSE (3 μg/ml) for 1 hr prior to RANKL stimulation (10 ng/ml) at the indicated time periods. Then, the expression levels of the signaling molecules were evaluated using Western blot analysis. The indicated densitometric values were obtained using Multi Gauge version 3 software. One representative result obtained from three independent experiments yielding similar results is shown.

BSE could prevent the bone resorptive function of mature osteoclasts without any alterations in the cell survival of the giant multinucleated osteoclasts.

4. Discussion

Antiosteoclastic agents have become the therapeutic mainstay for treating osteoporosis. However, the most common antiresorptive agents, such as bisphosphonates, also carry the risk of side effects, such as bisphosphonate-mediated osteonecrosis of the jaw [30] and atypical femoral fractures [31]. Consequently, the use of antiosteoclastic agents is limited due to concerns about their long-term safety. Therefore, new, safe therapeutic agents are urgently needed for the long-term management of bone disease.

Plant-based natural products have traditionally yielded a variety of therapeutic agents. Generally, healthy nutrients or foods with pharmaceutical properties are both effective and safe for the long-term administration of a variety of disorders. Recently, studies have attempted to identify natural products or healthy foods that can prevent and/or treat osteoporosis with minimal adverse effects [32].

As a major food crop for humans, barley is the second most commonly consumed grain in Korea, and it is recognised as a safe and healthy food to consume. Several studies have shown that BSE and its components exhibit antioxidant activities, decrease blood glucose and cholesterol levels, and protect against liver injury [33–36]. Nonetheless, the antiresorptive activity and mode of action of BS in bone metabolic diseases have not been revealed. This current study is the first to report on the antiosteoclastogenesis and inhibition of bone-resorbing activity of BSE.

The differentiation of osteoclasts from hematopoietic stem cells in bone marrow is specifically regulated by RANKL [37]. RANKL signaling triggers osteoclast formation, which is considered to be an important target for preventing pathological bone loss. In this study, BSE attenuated the RANKL-related differentiation of BMMs into osteoclasts in a dose-dependent manner without any cytotoxicity in concentrations up to 10 μg/ml.

RANKL stimulates transcription factors, such as c-Fos and NFATc1, during osteoclast differentiation. As activator protein-1 (AP-1) family members, c-Fos and NFATc1 play a major role in the regulation of molecules for osteoclast differentiation. An important role for c-Fos in the process of osteoclast differentiation has been clarified in c-Fos knockout mice [38]. The c-Fos-deficient mice had osteopetrosis due to a cell-autonomous defect in osteoclast differentiation [39]. Furthermore, Takayanagi et al. [40] reported that NFATc1-deficient embryonic stem cells do not differentiate into mature osteoclasts, even in the presence of RANKL. As major transcription factors, c-Fos and NFATc1 are also functionally linked together. Particularly, c-Fos is essential for RANKL-induced expression of NFATc1. c-Fos is expressed in the early stages of osteoclast differentiation, and it regulates NFATc1 gene expression by binding to the promoter region of NFATc1 [40]. NFATc1 is expressed in the middle or late stages of osteoclastogenesis, and it regulates osteoclast-mediated genes, such as TRAP, and OSCAR [9, 41]. Therefore, c-Fos and NFATc1 are master regulators for RANKL-induced osteoclast differentiation. In this study, two transcription factors such as c-Fos and NFATc1 inhibited the expression of the transcriptional and translational levels by BSE treatment during osteoclast differentiation. In addition, the inhibitory effect of BSE via downregulation of c-Fos and NFATc1 was confirmed by evaluating the transcriptional expression levels of c-Fos/NFATc1-dependent genes, such as TRAP and OSCAR. These results suggest that c-Fos/NFATc1, as a main transcriptional marker of osteoclastogenesis, is involved in BSE's inhibitory effect on osteoclast differentiation.

The binding of RANKL to its receptor RANK activates various signaling pathways, including NF-κB, PI3K/AKT, and MAP kinases, consisting of p38, ERK, and JNK, in the early stage of osteoclastogenesis [37, 42]. It is known that

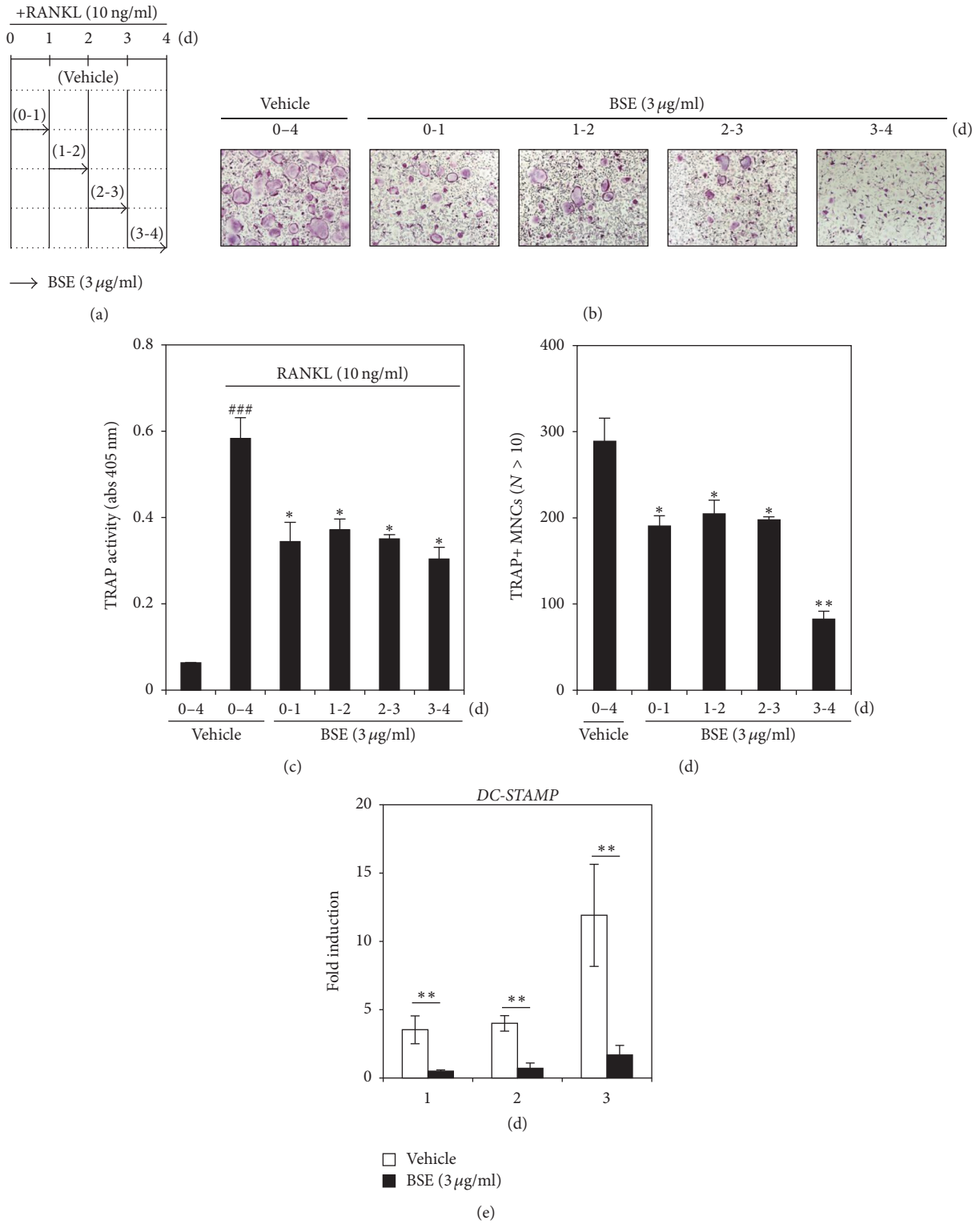

Figure 4: BSE also inhibits RANKL-mediated cell fusion during osteoclastogenesis. (a) Based on the exposure schedule, the BMMs were cultured with BSE (3 ug/ml) for various times periods (the indicated black arrow) in the presence of M-CSF (30 ng/ml) and RANKL (10 ng/ml). (b) After the BMMs differentiated into osteoclasts (as described in (a)), the cells were fixed, permeabilised, and stained with TRAP. TRAP+ MNCs formation was photographed under a light microscope. Each exposure period of BSE was indicated as "0–4" for the vehicle. "0-1" for 0-1 day, "1-2" for 1-2 days, "2-3" for 2-3 days, and "3-4" for 3-4 days. (c) TRAP activity was measured at 405 nm. $^{###}P < 0.001$ (versus the control); $^{*}P < 0.05$ (versus the RANKL-treated control). (d) The number of TRAP+ MNCs (nuclei > 10) was counted. $^{*}P < 0.05$; $^{**}P < 0.01$ (versus the RANKL-treated group). (e) The effect of BSE on the mRNA expression of DC-STAMP was analysed using real-time PCR, as described in Figure 2(a). HPRT was used as the internal control. White column (vehicle-treated); black column (3 μg/ml BSE-treated), $^{**}P < 0.01$ (versus the vehicle control). Data are representative of at least three experiments.

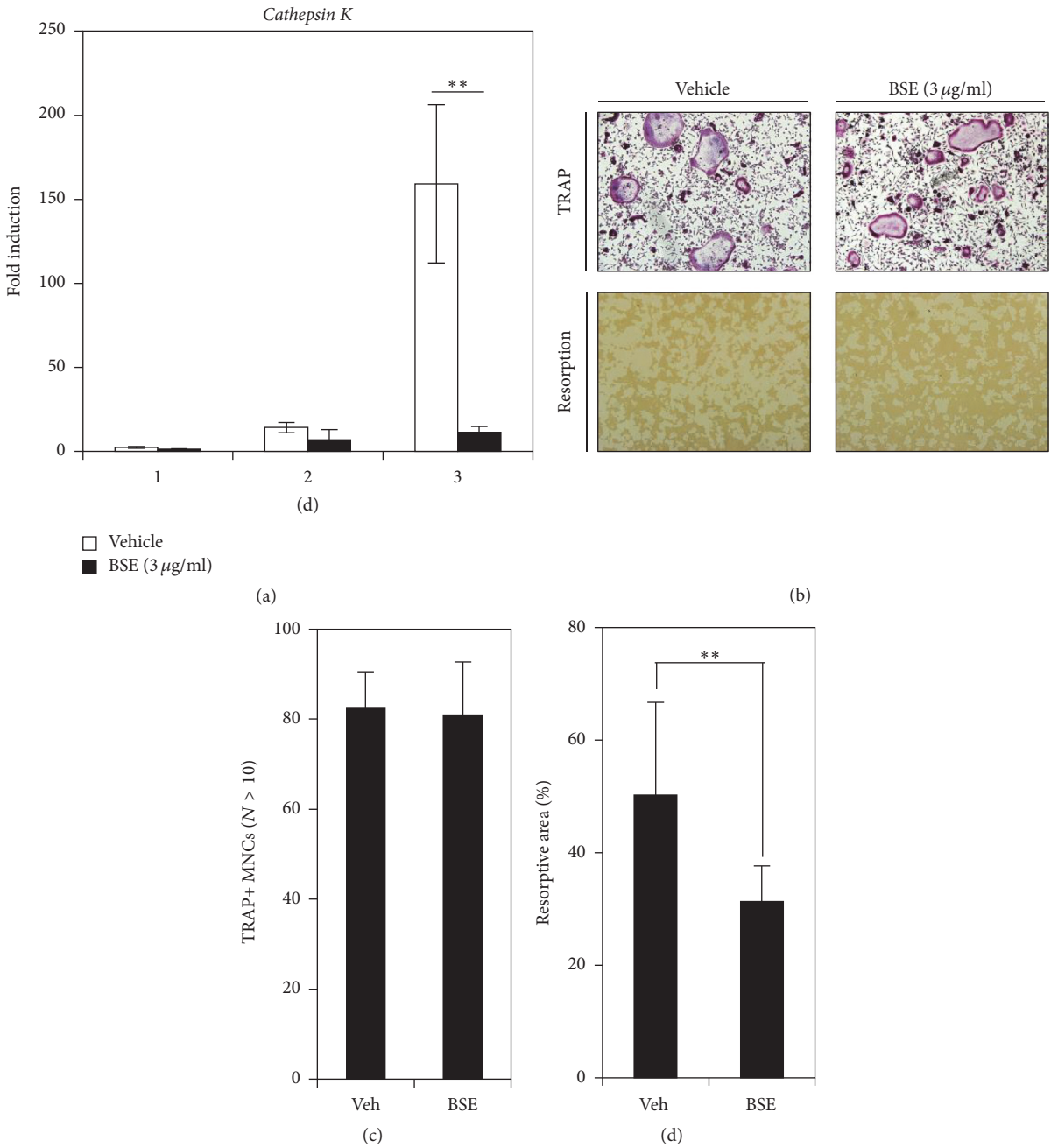

Figure 5: BSE impairs the osteoclastic function of giant multinucleated cells. (a) The mRNA expression of cathepsin K was evaluated during osteoclast differentiation in the absence or presence of BSE (3 μg/ml) using real-time PCR. The relative fold change of the mRNA expression level is presented in comparison to the control (no RANKL-treated). HPRT was used as the internal control. $^{**}P < 0.01$ (versus the vehicle control). (b) The mature osteoclasts were plated on bone biomimetic synthetic surface and treated for 24 hrs with BSE (3 μg/ml). The cells were fixed, permeabilised, and stained with TRAP. TRAP+ MNCs formation was visualised under a light microscope (top images). The resorption areas were removed from the cells and photographed under a light microscope (bottom images). (c-d) The form (as visualised in (b)) was counted as the number of TRAP+ MNCs (nuclei > 10; (c)), and the resorptive areas (%) were quantified using the Image*J* program (d). $^{**}P < 0.01$ (versus the vehicle control). One representative result achieved from three independent experiments yielding similar results is shown.

the expression of c-Fos/NFATc1 requires assembly of NF-κB, PI3K/AKT, and MAP kinase signaling [40, 43–45]. In this present study, the pathways for the PI3K/AKT and MAP kinases were not affected by BSE. However, BSE prevented the alternation of the RANKL-induced degradation of IκB signaling molecules, which leads to NF-κB activation. IκB is a member of a family of cellular proteins that function to inhibit NF-κB molecules. IκB inhibits NF-κB by

masking the nuclear localisation signals of NF-κB proteins and keeping them sequestered in an in-active state in the cytoplasm [46]. In IKK-knockout mice, the upstream IκB die at birth as a result of severe epidermal defects; however, analysis of the embryonic osteoclasts (E18.5 days postcoitus) revealed reduced numbers of multinucleated osteoclasts with altered morphology [47]. Additionally, NF-κB p50/p52 double knockout mice display defects of osteoclast differentiation and severe osteopetrosis because c-Fos/NFATc1 was not induced by RANKL [48]. These reports indicated that the NF-κB/IκB signaling pathway could have the potential to regulate osteoclast differentiation through c-Fos/NFATc1 expression. In this present study, the inhibitory effect of BSE on osteoclastogenesis could result from its potential ability to attenuate the NF-κB/IκB-c-fos/NFATc1 signaling axis at the early stage of osteoclast differentiation.

Osteoclast differentiation is a multistep progressive process that involves cell proliferation, commitment, migration, fusion, and maturation [49, 50]. Monocyte/macrophage precursors derived from hematopoietic stem cells in the bone marrow become preosteoclasts that then migrate and fuse to form giant multinucleated osteoclasts. In this regard, we next investigated whether the inhibitory effect of BSE affected some of the stages of osteoclast differentiation. To determine this, we reevaluated the antiosteoclastogenic activity of BSE by treating cells at each osteoclastogenesis stage. Interestingly, the TRAP+ MNCs formation by BSE was suppressed during the early, middle, and late stages of osteoclast differentiation.

Cell-cell fusion is essential for the formation and maturation of multinucleated osteoclasts; this process involves cellular fusion molecules, such as DC-STAMP. In osteoclastogenesis, DC-STAMP has been reported to be essential for cell-to-cell fusion of preosteoclasts, and it is preferentially expressed in the late stage [51–53]. Osteoclasts derived from DC-STAMP-deficient mice were found to abrogate multinucleated osteoclast formation and increase bone mass [54]. Additionally, DC-STAMP contains multiple NFATc1 binding sites in promoter regions, and it is regulated by NFATc1 transcription factor [55]. As mentioned earlier, we found that the mRNA expression levels of DC-STAMP and NFATc1 were inhibited by BSE during osteoclast differentiation. Taken together, these results suggest that BSE with antiosteoclastogenic activity is involved in osteoclast differentiation from the initial phase of osteoclastogenesis to the terminal phase.

Bone resorption is a unique function of osteoclasts, and it plays a central role in the formation of the skeleton and the regulation of its mass, which is involved in the matrix degradation of the organic and inorganic phases of bone [56]. In this progression, active proteases released from osteoclasts into the resorption lacunae are known to be involved in matrix degradation, and it has been reported that cysteine proteinases play a vital role in this process [57, 58]. Cathepsin K is a type of lysosomal cysteine protease, such as a proteolytic enzyme, and it is abundantly expressed in mature osteoclasts. It can degrade the protein components of the demineralised bone matrix, most notably type-1 collagen [59–61]. In addition, a study of cathepsin K-deficient mice found impaired bone loss via reduction of bone resorption and an increased bone formation rate in comparison to the control [62, 63]. RANKL-mediated cathepsin K expression has been shown to be regulated by NFATc1 [64]. Thus, induction of cathepsin K by NFATc1 is responsible for the degradation of the collagen matrix by osteoclasts. In our present study, the presence of BSE was associated with inhibition of the cathepsin K expression level and the anti-bone-resorbing activity of mature osteoclasts.

5. Conclusions

To the best of our knowledge, this is the first study to have shown the potential of a natural food, such as BSE, to inhibit osteoclast differentiation and bone-resorbing activity in the early-to-late stages of osteoclastogenesis, although additional experiments are needed to substantiate the identification of the pharmaceutical components in BSE for antiosteoclastogenic activity. BSE inhibits RANKL-induced osteoclastogenic activity by preventing IκB degradation and c-Fos/NFATc1 expression. Consequently, the alteration of IκB/c-Fos/NFATc1 could lead to the decreased expression of the genes required for bone-resorbing activity and cell fusion, such as DC-STAMP and cathepsin K. Moreover, BSE prevented the bone-resorbing activity of mature osteoclasts. Finally, our results suggest that the potential antiresorptive property of BSE might be developed as a functional food and pharmacological agent to improve bone health and to treat osteoclast-mediated bone metabolic disorders, including osteoporosis.

Conflicts of Interest

The authors have declared no conflicts of interest.

Authors' Contributions

Sik-Won Choi and Shin-Hye Kim contributed equally to this study.

Acknowledgments

This work was conducted with the support of the Cooperative Research Program for Agriculture Science & Technology Development (project title: Study of Metabolites and New Materials for Improvement of Lifestyle Related Disease on Rice and Barley, Project no. PJ00925701) of the Rural Development Administration (RDA), Korea.

References

[1] S. C. Manolagas and A. M. Parfitt, "What old means to bone," *Trends in Endocrinology and Metabolism*, vol. 21, no. 6, pp. 369–374, 2010.

[2] G. A. Rodan and T. J. Martin, "Therapeutic approaches to bone diseases," *Science*, vol. 289, no. 5484, pp. 1508–1514, 2000.

[3] S. Khosla and B. L. Riggs, "Pathophysiology of age-related bone loss and osteoporosis," *Endocrinology and Metabolism Clinics of North America*, vol. 34, no. 4, pp. 1015–1030, 2005.

[4] X. Feng and J. M. McDonald, "Disorders of bone remodeling," *Annual Review of Pathology*, vol. 6, pp. 121–145, 2011.

[5] E. Chrischilles, T. Shireman, and R. Wallace, "Costs and health effects of osteoporotic fractures," *Bone*, vol. 15, no. 4, pp. 377–386, 1994.

[6] "Osteoporosis prevention, diagnosis, and therapy," JAMA, 2001.

[7] X. Feng, "RANKing intracellular signaling in osteoclasts," *IUBMB Life*, vol. 57, no. 6, pp. 389–395, 2005.

[8] L. Galibert, M. E. Tometsko, D. M. Andersen, D. Cosman, and W. C. Dougall, "The involvement of multiple tumor necrosis factor receptor (TNFR)-associated factors in the signaling mechanisms of receptor activator of NF-κB, a member of the TNFR superfamily," *Journal of Biological Chemistry*, vol. 273, no. 51, pp. 34120–34127, 1998.

[9] H. Takayanagi, "Osteoimmunology: shared mechanisms and crosstalk between the immune and bone systems," *Nature Reviews Immunology*, vol. 7, no. 4, pp. 292–304, 2007.

[10] H. Takayanagi, "Inflammatory bone destruction and osteoimmunology," *Journal of Periodontal Research*, vol. 40, no. 4, pp. 287–293, 2005.

[11] I. Nakamura, N. Takahashi, E. Jimi, N. Udagawa, and T. Suda, "Regulation of osteoclast function," *Modern Rheumatology*, vol. 22, no. 2, pp. 167–177, 2012.

[12] S. Hooshmand and B. H. Arjmandi, "Viewpoint: dried plum, an emerging functional food that may effectively improve bone health," *Ageing Research Reviews*, vol. 8, no. 2, pp. 122–127, 2009.

[13] T.-H. Huang, R. C. Mühlbauer, C.-H. Tang et al., "Onion decreases the ovariectomy-induced osteopenia in young adult rats," *Bone*, vol. 42, no. 6, pp. 1154–1163, 2008.

[14] X. Zhang, X.-O. Shu, H. Li et al., "Prospective cohort study of soy food consumption and risk of bone fracture among postmenopausal women," *Archives of Internal Medicine*, vol. 165, no. 16, pp. 1890–1895, 2005.

[15] R. C. Mühlbauer, A. Lozano, A. Reinli, and H. Wetli, "Various selected vegetables, fruits, mushrooms and red wine residue inhibit bone resorption in rats," *Journal of Nutrition*, vol. 133, no. 11, pp. 3592–3597, 2003.

[16] J. Zhang, X. Xiao, Y. Dong, L. Shi, T. Xu, and F. Wu, "The anti-obesity effect of fermented barley extracts with *Lactobacillus plantarum* dy-1 and *Saccharomyces cerevisiae* in diet-induced obese rats," *Food & Function*, vol. 8, no. 3, pp. 1132–1143, 2017.

[17] S. Gul, S. Ahmed, N. Kifli et al., "Multiple pathways are responsible for anti-inflammatory and cardiovascular activities of Hordeum vulgare L.," *Journal of Translational Medicine*, vol. 12, no. 1, 2014, article 316.

[18] K.-C. Choi, J.-M. Hwang, S.-J. Bang et al., "Methanol extract of the aerial parts of barley (Hordeum vulgare) suppresses lipopolysaccharide-induced inflammatory responses in vitro and in vivo," *Pharmaceutical Biology*, vol. 51, no. 8, pp. 1066–1076, 2013.

[19] J. G. Shah, B. G. Patel, S. B. Patel, and R. K. Patel, "Antiurolithiatic and antioxidant activity of Hordeum vulgare seeds on ethylene glycol-induced urolithiasis in rats," *Indian Journal of Pharmacology*, vol. 44, no. 6, pp. 672–677, 2012.

[20] A. Kamimura and T. Takashashi, "Procyanidin B-3, isolated from barley and identified as a hair-growth stimulant, has the potential to counteract inhibitory regulation by TGF-β1," *Experimental Dermatology*, vol. 11, no. 6, pp. 532–541, 2002.

[21] J. R. Lupton, M. C. Robinson, and J. L. Morin, "Cholesterol-lowering effect of barley bran flour and oil," *Journal of the American Dietetic Association*, vol. 94, no. 1, pp. 65–70, 1994.

[22] M. J. Park, J.-E. Ra, K. H. Seo et al., "Identification and evaluation of flavone-glucosides isolated from barley sprouts and their inhibitory activity against bacterial neuraminidase," *Natural Product Communications*, vol. 9, no. 10, pp. 1469–1472, 2014.

[23] W. D. Seo, H. J. Yuk, M. J. Curtis-Long et al., "Effect of the growth stage and cultivar on policosanol profiles of barley sprouts and their adenosine 5′-monophosphate-activated protein kinase activation," *Journal of Agricultural and Food Chemistry*, vol. 61, no. 5, pp. 1117–1123, 2013.

[24] S.-W. Choi, J.-T. Yeon, B. J. Ryu et al., "Repositioning potential of pak4 to osteoclastic bone resorption," *Journal of Bone and Mineral Research*, vol. 30, no. 8, pp. 1494–1507, 2015.

[25] J.-T. Yeon, K.-J. Kim, S. W. Chun et al., "KCNK1 inhibits osteoclastogenesis by blocking the Ca2+ oscillation and JNK-NFATc1 signaling axis," *Journal of Cell Science*, vol. 128, no. 18, pp. 3411–3419, 2015.

[26] S. Rozen and H. Skaletsky, "Primer3 on the WWW for general users and for biologist programmers," *Methods in Molecular Biology*, vol. 132, pp. 365–386, 2000.

[27] K. J. Livak and T. D. Schmittgen, "Analysis of relative gene expression data using real-time quantitative PCR and the $2^{-\Delta\Delta C_T}$ method," *Methods*, vol. 25, no. 4, pp. 402–408, 2001.

[28] S. Choi, K. Lee, J. H. Lee et al., "Suppression of Akt-HIF-1α signaling axis by diacetyl atractylodiol inhibits hypoxia-induced angiogenesis," *BMB Reports*, vol. 49, no. 9, pp. 508–513, 2016.

[29] S.-W. Choi, Y.-J. Son, J.-M. Yun, and S. H. Kim, "Fisetin inhibits osteoclast differentiation via downregulation of p38 and c-Fos-NFATc1 signaling pathways," *Evidence-Based Complementary and Alternative Medicine*, vol. 2012, Article ID 810563, 9 pages, 2012.

[30] C. Dannemann, K. W. Grätz, M. O. Riener, and R. A. Zwahlen, "Jaw osteonecrosis related to bisphosphonate therapy. A severe secondary disorder," *Bone*, vol. 40, no. 4, pp. 828–834, 2007.

[31] R. P. H. Meier, T. V. Perneger, R. Stern, R. Rizzoli, and R. E. Peter, "Increasing occurrence of atypical femoral fractures associated with bisphosphonate use," *Archives of Internal Medicine*, vol. 172, no. 12, pp. 930–936, 2012.

[32] A. Scalbert, C. Manach, C. Morand, and C. Remesy, "Dietary polyphenols and the prevention of diseases," *Critical Reviews in Food Science and Nutrition*, vol. 45, no. 4, pp. 287–306, 2005.

[33] Y.-H. Lee, J.-H. Kim, S. H. Kim et al., "Barley sprouts extract attenuates alcoholic fatty liver injury in mice by reducing inflammatory response," *Nutrients*, vol. 8, no. 7, article no. 440, 2016.

[34] A. R. Byun, H. Chun, J. Lee, S. W. Lee, H. S. Lee, and K. W. Shim, "Effects of a dietary supplement with barley sprout extract on blood cholesterol metabolism," *Evidence-based Complementary and Alternative Medicine*, vol. 2015, Article ID 473056, 7 pages, 2015.

[35] A. Takano, T. Kamiya, H. Tomozawa et al., "Insoluble fiber in young barley leaf suppresses the increment of postprandial blood glucose level by increasing the digesta viscosity," *Evidence-Based Complementary and Alternative Medicine*, vol. 2013, article 137871, 10 pages, 2013.

[36] J. A. Benedet, H. Umeda, and T. Shibamoto, "Antioxidant activity of flavonoids isolated from young green barley leaves toward biological lipid samples," *Journal of Agricultural and Food Chemistry*, vol. 55, no. 14, pp. 5499–5504, 2007.

[37] W. J. Boyle, W. S. Simonet, and D. L. Lacey, "Osteoclast differentiation and activation," *Nature*, vol. 423, no. 6937, pp. 337–342, 2003.

[38] A. Arai, T. Mizoguchi, S. Harada et al., "Fos plays an essential role in the upregulation of RANK expression in osteoclast precursors within the bone microenvironment," *Journal of Cell Science*, vol. 125, part 12, pp. 2910–2917, 2012.

[39] A. Fleischmann, F. Hafezi, C. Elliott et al., *Fra-1 replaces c-Fos-dependent functions in mice, Genes development*, vol. 14.

[40] H. Takayanagi, S. Kim, T. Koga et al., "Induction and activation of the transcription factor NFATc1 (NFAT2) integrate RANKL signaling in terminal differentiation of osteoclasts," *Developmental Cell*, vol. 3, no. 6, pp. 889–901, 2002.

[41] A. Rao, C. Luo, and P. G. Hogan, "Transcription factors of the NFAT family: regulation and function," *Annual Review of Immunology*, vol. 15, pp. 707–747, 1997.

[42] H. C. Blair, L. J. Robinson, and M. Zaidi, "Osteoclast signalling pathways," *Biochemical and Biophysical Research Communications*, vol. 328, no. 3, pp. 728–738, 2005.

[43] N. Kobayashi, Y. Kadono, A. Naito et al., "Segregation of TRAF6-mediated signaling pathways clarifies its role in osteoclastogenesis," *EMBO Journal*, vol. 20, no. 6, pp. 1271–1280, 2001.

[44] B. R. Wong, D. Besser, N. Kim et al., "TRANCE, a TNF family member, activates Akt/PKB through a signaling complex involving TRAF6 and c-Src," *Molecular Cell*, vol. 4, no. 6, pp. 1041–1049, 1999.

[45] B. R. Wong, R. Josien, S. Y. Lee, M. Vologodskaia, R. M. Steinman, and Y. Choi, "The TRAF family of signal transducers mediates NF-κB activation by the TRANCE receptor," *The Journal of Biological Chemistry*, vol. 273, no. 43, pp. 28355–28359, 1998.

[46] M. D. Jacobs and S. C. Harrison, "Structure of an IκBα/NF-κB complex," *Cell*, vol. 95, no. 6, pp. 749–758, 1998.

[47] M. L. Chaisson, D. G. Branstetter, J. M. Derry et al., "Osteoclast differentiation is impaired in the absence of inhibitor of κB kinase α," *Journal of Biological Chemistry*, vol. 279, no. 52, pp. 54841–54848, 2004.

[48] V. Iotsova, J. Caamaño, J. Loy, Y. Yang, A. Lewin, and R. Bravo, "Osteopetrosis in mice lacking NF-κB1 and NF-κB2," *Nature Medicine*, vol. 3, no. 11, pp. 1285–1289, 1997.

[49] M. Asagiri and H. Takayanagi, "The molecular understanding of osteoclast differentiation," *Bone*, vol. 40, no. 2, pp. 251–264, 2007.

[50] T. Suda, N. Takahashi, N. Udagawa, E. Jimi, M. T. Gillespie, and T. J. Martin, "Modulation of osteoclast differentiation and function by the new members of the tumor necrosis factor receptor and ligand families," *Endocrine Reviews*, vol. 20, no. 3, pp. 345–357, 1999.

[51] R. Islam, H.-S. Bae, W.-J. Yoon et al., "Pin1 regulates osteoclast fusion through suppression of the master regulator of cell fusion DC-STAMP," *Journal of Cellular Physiology*, vol. 229, no. 12, pp. 2166–2174, 2014.

[52] C. Zhang, C. Dou, J. Xu, and S. Dong, "DC-STAMP, the key fusion-mediating molecule in osteoclastogenesis," *Journal of Cellular Physiology*, vol. 229, no. 10, pp. 1330–1335, 2014.

[53] N. Courtial, J. J. Smink, O. N. Kuvardina, A. Leutz, J. R. Göthert, and J. Lausen, "Tal1 regulates osteoclast differentiation through suppression of the master regulator of cell fusion DC-STAMP," *FASEB Journal*, vol. 26, no. 2, pp. 523–532, 2012.

[54] M. Yagi, T. Miyamoto, Y. Sawatani et al., "DC-STAMP is essential for cell-cell fusion in osteoclasts and foreign body giant cells," *Journal of Experimental Medicine*, vol. 202, no. 3, pp. 345–351, 2005.

[55] T. Miyamoto, "The dendritic cell-specific transmembrane protein DC-STAMP is essential for osteoclast fusion and osteoclast bone-resorbing activity," *Modern Rheumatology*, vol. 16, no. 6, pp. 341–342, 2006.

[56] S. L. Teitelbaum, "Bone resorption by osteoclasts," *Science*, vol. 289, no. 5484, pp. 1504–1508, 2000.

[57] A. Erlebacher, E. H. Filvaroff, S. E. Gitelman, and R. Derynck, "Toward a molecular understanding of skeletal development," *Cell*, vol. 80, no. 3, pp. 371–378, 1995.

[58] V. Everts, J. Delaissé, W. Korper, A. Niehof, G. Vaes, and W. Beertsen, "Degradation of collagen in the bone-resorbing compartment underlying the osteoclast involves both cysteine-proteinases and matrix metalloproteinases," *Journal of Cellular Physiology*, vol. 150, no. 2, pp. 221–231, 1992.

[59] T. Ishikawa, M. Kamiyama, N. Tani-Ishii et al., "Inhibition of osteoclast differentiation and bone resorption by cathepsin k antisense oligonucleotides," *Molecular Carcinogenesis*, vol. 32, no. 2, pp. 84–91, 2001.

[60] B. D. Gelb, G.-P. Shi, H. A. Chapman, and R. J. Desnick, "Pycnodysostosis, a lysosomal disease caused by cathepsin K deficiency," *Science*, vol. 273, no. 5279, pp. 1236–1238, 1996.

[61] D. Brömme, K. Okamoto, B. B. Wang, and S. Biroc, "Human cathepsin O_2, a matrix protein-degrading cysteine protease expressed in osteoclasts: functional expression of human cathepsin O_2 in Spodoptera frugiperda and characterization of the enzyme," *Journal of Biological Chemistry*, vol. 271, no. 4, pp. 2126–2132, 1996.

[62] P. Leung, M. Pickarski, Y. Zhuo, P. J. Masarachia, and L. T. Duong, "The effects of the cathepsin K inhibitor odanacatib on osteoclastic bone resorption and vesicular trafficking," *Bone*, vol. 49, no. 4, pp. 623–635, 2011.

[63] V. Everts, D. C. Aronson, and W. Beertsen, "Phagocytosis of bone collagen by osteoclasts in two cases of pycnodysostosis," *Calcified Tissue International*, vol. 37, no. 1, pp. 25–31, 1985.

[64] M. Matsumoto, M. Kogawa, S. Wada et al., "Essential role of p38 mitogen-activated protein kinase in cathepsin K gene expression during osteoclastogenesis through association of NFATc1 and PU.1," *The Journal of Biological Chemistry*, vol. 279, no. 44, pp. 45969–45979, 2004.

Hindawi
Evidence-Based Complementary and Alternative Medicine
Volume 2017, Article ID 2109249, 10 pages
https://doi.org/10.1155/2017/2109249

Research Article

Pingmu Decoction Induces Orbital Preadipocytes Apoptosis In Vitro

Yali Zhang,[1] Hong Li,[2] Long Gao,[2] Xia Zhang,[2] and RuiFang Xie[3]

[1]*Department of Gastroenterology, Long Hua Hospital Affiliated to Shanghai University of Traditional Chinese Medicine, The Institute of Digestive Disease Affiliated to Shanghai University of Traditional Chinese Medicine, South Wan Ping Road No. 725, Shanghai 200032, China*
[2]*Department of Endocrinology, Long Hua Hospital Affiliated to Shanghai University of Traditional Chinese Medicine, South Wan Ping Road No. 725, Shanghai 200032, China*
[3]*Department of Pharmacy, Long Hua Hospital Affiliated to Shanghai University of Traditional Chinese Medicine, South Wan Ping Road No. 725, Shanghai 200032, China*

Correspondence should be addressed to Hong Li; shanhongli@126.com

Received 1 November 2016; Revised 23 February 2017; Accepted 20 March 2017; Published 18 April 2017

Academic Editor: Pradeep Kumar

Pingmu Decoction is the Traditional Chinese Medicine which has treated Graves' Ophthalmopathy (GO) in the inactive stage for more than ten years. This study was to explore the mechanism of Pingmu Decoction of inhibiting preadipocytes in GO patients from differentiating into mature adipocytes. Human orbital preadipocytes were isolated and cultured through tissue explant method. Orbital preadipocytes were induced into mature adipocytes. The medicinal serum was prepared from rats. The cells were treated with medicinal serum which were divided into three groups, low dose group (5%), medium dose group (10%), and high dose group (20%). The cells viabilities were observed by Oil Red O staining, MTT method, and Annexin V/propidium iodide (PI) double staining. Effect of Pingmu Decoction on cell apoptosis rate of orbital matured adipocytes was measured by flow cytometry. The genes Fas and Fas L from cell groups were tested by RT-PCR and Western blotting. The expression of master adipogenic transcription factors, including peroxisome proliferation-activity receptor (PPAR) γ and CCAAT/enhancer binding protein (C/EBP) α, was tested by Western blotting. Pingmu Decoction could reduce orbital preadipocytes viability and induce apoptosis of mature adipocyte via Fas/Fas L signaling pathway. Pingmu Decoction reduced lipid accumulation and downregulated the expression of PPAR γ and C/EBP α. Pingmu Decoction may play a therapeutic effect by reducing the accumulation of orbital adipocytes.

1. Introduction

Graves' Ophthalmopathy (GO), also known as thyroid-associated ophthalmopathy, is an autoimmune disease characterized by invasion of retrobulbar and orbital tissues [1, 2]. About 20–50% of GO patients also present clinically with Graves' Disease (GD), which is characterized by diffuse goiter with hyperthyroidism [3–5]. In recent years, the incidence of GD has undergone an annual increase due to the influence of hereditary and environmental factors that contribute to autoimmune disorders [6]. GO affects adults worldwide and has become one of the major causes of blindness. However, the etiology and pathogenesis of GO have not been completely defined. An increase in orbital adipose tissue content may increase the orbital pressure and lead to proptosis. Thus, abnormal proliferation of orbital adipose tissue and the occurrence of fat in GO play an important role in disease development [7, 8]. Furthermore, an increase in orbital preadipocyte volume and quantity may lead to the characteristic increase in adipose tissues [9]. Recent studies have confirmed that preadipocytes that reside in orbital tissues of patients can transform into fatty cells under certain conditions and contribute to the development of GO [10, 11]. Therefore, an imbalance in the proliferation, differentiation, and apoptosis of orbital preadipocytes may be the main factor regulating orbital exenteration increase, orbital pressure increase, and the occurrence of proptosis in patients with GO.

GO can be divided into active and inactive stages according to its development. In the inactive stage, the clinical curative effect is not very good, with no available specific and effective methods of treatment by Western medicine. Pingmu Decoction has been used in Chinese medicine to treat GO in the inactive stage for more than ten years, with good clinical curative effects. A preliminary experimental study demonstrated that serum from rats treated with Pingmu Decoction and its components can act on orbital preadipocytes from patients with GO in the inactive period. Pingmu Decoction serum promotes the apoptosis of adipocytes and reduces the accumulation of orbital adipocytes by increasing the expression of Caspase-3, Caspase-8, and Caspase-9 protein [12]. However, its apoptotic effect on differentiated adipocytes from GO patients remains uncharacterized. Intracellular pathways mediated by Fas/Fas L in mammals can induce apoptosis [13, 14]. We cultured orbital preadipocytes from patients by the tissue explant method and differentiated them into orbital adipocytes. The effect and molecular mechanism of Pingmu Decoction on the apoptosis of orbital adipocytes were explored by a variety of methods.

2. Materials and Methods

2.1. Experimental Animals and Drugs. Six-week-old specific pathogen-free male Sprague-Dawley rats weighing 200 ± 10 g were purchased from Shanghai Silaike Experimental Animal Co. Ltd. (certification number SCXK (Hu) 2012-0002). Animal experiment ethical approval was obtained from the Affiliated Long Hua Hospital of Shanghai University of Traditional Chinese Medicine.

Pingmu Decoction was composed of 30 g of Huangqi *(Astragalus membranaceus)*, 15 g of Xianlingpi *(Herba Epimedii)*, 15 g of Chuanxiong *(Ligusticum wallichii)*, 15 g of Baijiezi *(Brassica alba Boiss.)*, 15 g of stir-baked Biejia (Carapax Trionycis), and 30 g of Cheqianzi *(Semen plantaginis)*. These herbs were provided by the Chinese Medicine Pharmacy of the Affiliated Long Hua Hospital of Shanghai University of Traditional Chinese Medicine (TCM). The Decoction of the above herbs was prepared twice according to the original formula and then filtered and concentrated in a combined liquor. The dose of rat administration is based on the human mouse equivalent dosage conversion according to the textbook *Pharmacology and Pharmacology Experiment of TCM* (edited by Zhang Dafang, Shanghai Science and Technology Press, 2002). The crude drug (4 g/mL) was stored at 4°C.

2.2. GO Patients. Four cases (4 eyes) of postbulbar adipose tissues from GO inpatients were collected from Shanghai EENT Hospital. Of the four GO cases in this study, two female and two male patients (age ranging from 25 to 48 years old) had a GO history of three to eight years. Diagnostic criteria of GO were in accordance with the clinical score standards described in the *Chinese Guideline for Diagnosis and Treatment of Thyroid Disease* published in 2008. The clinical activity score (CAS) of GO in clinical practice was based on the clinical score standards of *Chinese Guideline for Diagnosis and Treatment of Thyroid Disease*, including spontaneous retrobulbar pain, pain with eye movement, eyelid erythema, conjunctival hyperemia, chemosis, swollen lacrimal caruncle, and swollen eyelid. Each symptom accounted for one point, and the total score obtained was up to seven in each case. The inactive phase of GO referred to active exophthalmos with the clinical score of <3. Classification of exophthalmos in this study was in accordance with the classification criteria of GO proposed by the American Thyroid Association (ATA). The patients were confirmed to have GO paralleled orbital decompression by the Ophthalmology Department at Shanghai EENT Hospital. All patients were in the GO inactive stage, which is in line with the diagnostic criteria. Other diseases, such as autoimmune diseases and cancer, were ruled out. Approval was obtained from the Medical Ethical Committee and patient consent was obtained in writing prior to collection of tissue samples.

2.3. Medicinal Serum Preparation. The Sprague-Dawley rats were randomly divided into 2 groups with 5 rats per group. The rats in the Pingmu Decoction group were given 15 mL/kg Pingmu Decoction, and the rats in the control group were given an equal volume of distilled water by intragastric administration twice a day for 3 days. The final concentrations of medicinal serum (final concentration = volume added to serum/total volume × 100%) were 5% (low dose), 10% (medium dose), and 20% (high dose).

Blood was collected from the abdominal aortae of the rats under ether anesthesia 1.5 h after the last administration. The blood was incubated for 2 h at 4°C and then centrifuged at 4°C at 3000 rpm/min for 15 min. The sera from each group of mice were combined and inactivated for 30 min at 56°C in a water bath, filtered with 0.22 μm aperture micropore film, packed with frozen pipes, and stored at −20°C.

2.4. Culture of Primary Cells from Patient Tissue. Sterilized orbital adipose tissues from the operating table were washed 3 times with sterile phosphate buffer solution (PBS) to remove the blood and then were placed into culture bottles containing complete medium. As soon as possible after transfer to the laboratory (within 4 h) the tissues were processed for experimentation at room temperature. Human orbital preadipocytes were cultured by the tissue explant method. The adipose tissue with visible connective tissue or blood clots was removed and the remaining tissue was harvested into Petri dishes with D-Hank's solution. The tissues were cut into pieces of approximately 1 mm × 1 mm × 1 mm in size with ophthalmic scissors and were seeded evenly at the bottom of culture bottles. Then the bottles were gently turned upside down, and 2 mL complete culture solution was added. The bottles were placed askew into an incubator with 5% CO_2 at 37°C for culturing. After the tissue explants adhered tightly to the culture bottle, 5 mL complete culture solution was added, and the solution was replaced with fresh solution every 2-3 d. At 80% confluence, the cells were passaged 1 : 3 (every 3-4 d). Cells were used in experiments after 3–6 generations. The morphology and growth status of the cultured primary cells were observed every day. Oil Red O staining and microscopic photography were performed to assess the formation of lipid droplets. Healthy preadipocytes

were seeded at a density of 3–5 × 10^7/L on coverslips in a 6-well plate. When they approached confluence, the cells were fixed in 4% paraformaldehyde for 10 minutes at normal temperature and stained by indirect immunofluorescent assay. The prepared cell slides were washed 3 times with PBS for 3 minutes, incubated for 1 h at 37°C with PBS containing 2% bovine serum albumin and Pref-1 antibody (diluted 1 : 100), and then incubated at 4°C overnight. After 4 washes with PBS for 5 minutes, FITC-secondary antibody (diluted 1 : 500) was added for 30 min at room temperature in darkness and the slides were washed 4 times with PBS for 5 minutes. The slides were then stained with 5 μg/mL DAPI for 2 min, and antiquenching mounting medium was added before examination under a fluorescent inverted microscope.

2.5. Identification of Mature Adipocytes. Healthy preadipocytes were seeded at a density of 1 × 10^5 in 6-well plates. After the cells adhered, the medium was replaced with Differentiation Medium I containing Dexamethasone (1 μmol/L), IBMX (0.2 mmol/L) and insulin (10 μg/mL) to induce differentiation. After 4 days, the medium was replaced with Differentiation Medium II, which has no Dexamethasone and IBMX, and the cells were cultured for 4 additional days. Then medium was replaced with complete medium and the cells were cultured for 8 d, with the medium replaced every 2 d. The entire differentiation period was 16 d.

After differentiation, the mature adipocytes were washed 3 times with PBS and fixed with 4% paraformaldehyde for 10 minutes. The excess liquid was removed by aspiration, and Oil Red O solution was added. The cells were rinsed with 75% ethanol to facilitate observation. The resulting orange lipid droplets were observable for 10 min under the fluorescent inverted microscope.

2.6. Cell Viability Assessment by the MTT Method. Cells in the logarithmic phase were digested with trypsin to produce a monocell suspension in complete culture medium. The cells were seeded in 96-well plates at about 10000 cells/200 μL per well. Then the 96-well plates were cultured in 5% CO_2 in an incubator at 37°C. The cells in each group (group 1: control group, group 2: Pingmu Decoction low dose group, group 3: Pingmu Decoction medium dose group, group 4: Pingmu Decoction high dose group, and group 5: Dexamethasone group) were cultured for 24 h, 48 h, 72 h, and 96 h. A zero control (culture media, MTT, and DMSO) and a blank control (cells, culture medium without serum, MTT, and DMSO) were also assayed in triplicate. After 4 additional days of culture, 20 μL MTT solution (5 mg/mL in PBS) was added to each well. The culture supernatant was carefully aspirated, and then 150 μL DMSO was added to each well with low speed oscillation to allow the crystals to dissolve adequately. The optical density value of each group was measured at 490 nm, and a cell growth curve was drawn using time as the x-axis and light absorption as the y-axis.

2.7. Apoptosis Assessment by the Annexin V/Propidium Iodide (PI) Double Staining Method. Cells treated with different amounts of Pingmu Decoction serum were cultured for 2 d. The cell culture medium in each well of a 6-well plate was aspirated, and 400 μL trypsin was added. After 3 min, 1 mL complete culture medium was added to terminate the digestion and the nonadherent cells were collected. The wells were washed with 500 μL culture media to recover all of the cells, and cells from both washes were combined and centrifuged at 2000 rpm/min for 5 min. The supernatant was discarded, and the cells were washed with chilled sterile PBS, resuspended in PBS, counted, and adjusted to 1 × 10^6/mL. The cell suspensions were collected, mixed gently with 5 μL Annexin V-FITC, and incubated at room temperature for 15 min in darkness. Then 5 μL PI staining solution was added gently, and the cells were incubated in an ice bath in darkness for 5 min. Flow cytometry was performed immediately after adding 300 μL binding buffer.

2.8. Real-Time PCR Assessment of Fas and Fas L mRNA Expression. Total mRNA was extracted by the Trizol method. The samples (2 μL per well) were plated, with DEPC water as the background. Then the sample concentration was assessed using a micro reader. RNA of sufficient purity (A260/A280 value 1.8–2) was used for subsequent experimentation. The concentrations were adjusted to 1 μg/μL, and then mRNA was heat-denatured for 5 min at 65°C, cooled immediately, and reverse transcribed to cDNA using the Sensiscript RT Kit. Reverse transcription was performed in a 20 μL volume (9 μL nuclease-free water, 4 μL 5x RT Buffer, 1 μL RT Enzyme, 1 μL Primer Mix, and 5 μL cDNA). Reaction conditions were as follows: 37°C for 15 min, 98°C for 5 min, and 4°C for 5 min.

For PCR, the primer sequences selected were designed based on the information in GenBank. The upstream and downstream sequences of the primers and predicted product size were as follows: Fas: 5′-TTCTGCCATAAGCCCTGTCC-3′ and 5′-CTAAGCCATGTCCTTCATCACAC-3′ (169 bp); Fas L: 5′-GGATGTTTCAGCTCTTCCACCTAC-3′ and 5′-TGTTAAATGGGCCACTTTCCTC-3 (152 bp); GAPDH: 5′-GCACCGTCAAGGCTGAGAAC-3′ and 5′-TGGTGAAGACGCCAGTGGA-3′ (138 bp). Real-time PCR reactions (50 μL total) included 5 μL cDNA sample, 2 μL upstream primers (10 μM), 2 μL downstream primers (10 μM), 16 μL distilled water, and 25 μL SYBR Green. The conditions of PCR amplification were 95°C for 15 s, 60°C for 15 s, and 72°C for 45 s (40 cycles). The relative quantity of the target genes was determined by the comparative Ct value/$2^{-\Delta\Delta Ct}$ method with GAPDH as control.

2.9. Assessment of Fas, Fas L, PPAR γ, and C/EBP α Protein Expression by Western Blotting. Cells were cultured for 2 d under different conditions (control group, Pingmu Decoction low, moderate, and high dose group, and Dexamethasone group). 2 × 10^6 adipocytes were washed twice with PBS, and 100 μL precooling protein lysis buffer (50 mM Tris-HCl, 150 mM NaCl, 0.02% NaN_3, 1% Triton X-100, 1 mM PMSF, 1 μg/mL aprotinin, and 1 μg/mL leupeptin) was added to the plates on ice for 10–20 min. The cells were then scraped and collected into EP tubes at 12000 rpm for 5 min at 4°C. Then the supernatants were transferred into another centrifuge tube, and a small amount of supernatant was used for protein quantitation by the Bradford Assay. Fifty microliters of protein from each sample was separated by SDS-PAGE,

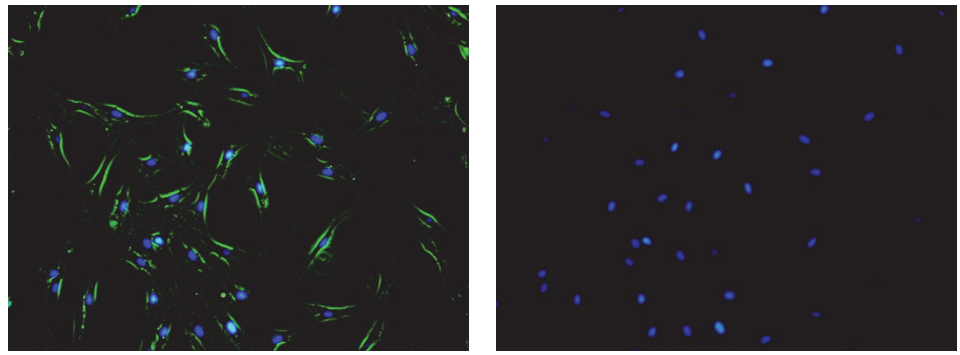

(a) (b)

Figure 1: Verification of Pref-1 expression by preadipocytes. Positive Pref-1 expression by preadipocytes was confirmed by indirect immunofluorescent assay (a-b). Merged image of Pref-1 stain (green) and nuclear stain (blue) (a). Nucleus was stained by DAPI (blue) (b).

and after transfer, PVDF membranes were incubated at 4°C overnight with primary antibody against Fas, Fas L, PPAR γ, or C/EBP α (1 : 1000; diluted in TBST). Fluorescence-labeled secondary antibody (1 : 2000) was added after washing, and the membranes were incubated for 2 h at room temperature. The membranes were rinsed with TBST. ECL luminescence reagents (reagent A mix with equal volume of reagent B) were added, and the membranes were dynamically integrated on a gel imaging instrument for 5–15 min with analysis by Gel-Pro analysis software.

2.10. Statistical Analysis. Statistical analysis was performed using SPSS 18.0 software. Data measurement was expressed as mean values ± standard deviation. Normal distribution and homogeneity of variance assessments were carried out first. For experimental data that met the criteria, comparisons between multiple groups were performed using single-factor analysis of variance (analysis of variance, ANOVA); and comparisons among groups were performed using LSD-t (least significant difference-t). For experimental data that did not meet the normal distribution and homogeneity of variance criteria, nonparametric tests were adopted. $P < 0.05$ was considered statistically significant.

3. Results

3.1. Primary Culture of Preadipocytes, Growth Characteristics after Passage, and Morphological Observation. To determine the molecular effects of Pingmu Decoction on orbital adipocytes from GO patients, we collected tissue from patients undergoing surgery. Cells cultured from the tissue samples emerged from the tissue block on the fourth day and were spindle shaped with oval or near-circular nuclei. The cells morphology was close to that of fibrocytes, with gradual proliferation of cells. After passaging, the preadipocytes gradually arranged themselves and grew 3-4 d before requiring subsequent passage. In this study, orbital adipose tissue from 4 cases of GO was cultured, and cells emerged from the adipose tissue block in all cases within 4-5 d. The cells were passaged when they reached confluence (within 9-10 d) under the sterile conditions. Subsequently, the cells were passaged once every 3-4 d.

3.2. Identification of Preadipocytes. To verify that the cultured cells represented preadipocytes, we performed immunofluorescent staining assays with Pref-1 antibody. The membranes of the cultured preadipocytes positively expressed Pref-1 (green fluorescence) as identified by indirect immunofluorescent assay (Figures 1(a) and 1(b)). Based on this finding, it can be verified that the cultured primary cells were preadipocytes.

3.3. Induction of Differentiation of Preadipocytes and the Effects of Pingmu Decoction on Differentiation. To induce differentiation of the preadipocytes into mature adipocytes, we cultured them in differentiation liquid. The cells retracted, the cell space became larger, and proliferation stopped gradually. Furthermore, the morphology of the cells gradually changed to oval or nearly circular, and the volume of the cells gradually increased. An obvious change in morphology was generally observed after a week or so. Lipid granules presented as fat droplets in the cytoplasm as observed under the light microscope. On the 8th day of the differentiation, the cells swelled prominently and their shape became short or polygonal. Fat droplets became enlarged and gradually increased in number as observed by Oil Red O staining. On the 16th day of the differentiation, the cell differentiation was close to 80–90% complete, and the nuclei shifted to one side. Fat droplets in the cytoplasm stained red with Oil Red O and could be seen under the inverted microscope (Figure 2(a)). Based on this finding, it could be verified that the preadipocytes were successfully differentiated as mature adipocytes.

Next, we treated the mature adipocytes with three different doses of Pingmu Decoction serum (low, 5%; medium, 10%; and high, 20%). As a control, cells were untreated (blank) or treated with 30 μg/mL Dexamethasone (Dexa). The results demonstrate that Pingmu Decoction serum can inhibit differentiation (Figures 2(b)–2(f)). These findings suggest that the explanted preadipocytes can be differentiated, but that exposure with Pingmu Decoction serum during the differentiation blocks maturation.

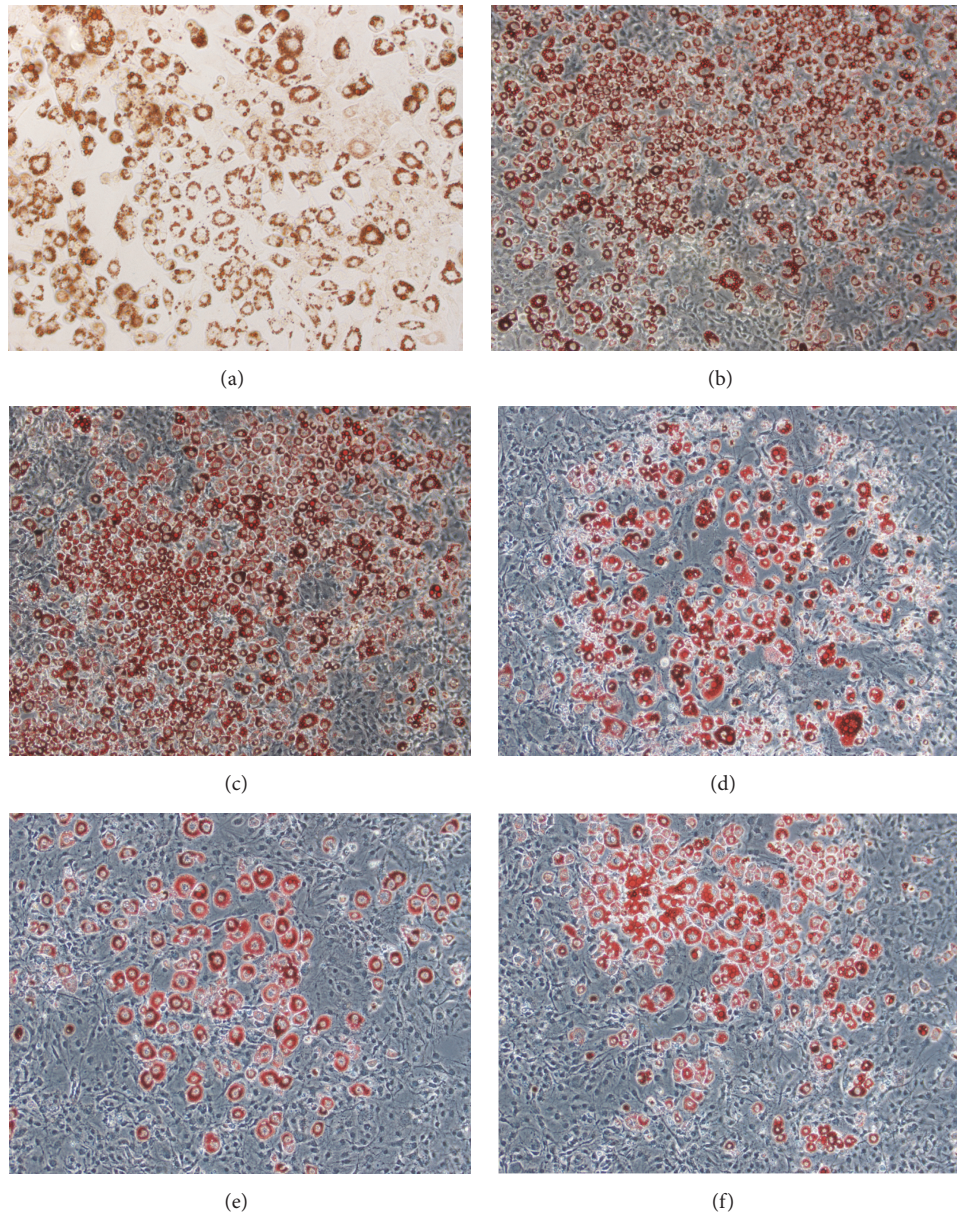

Figure 2: Fat accumulation in mature adipocytes. Lipid droplets in adipocytes were stained with Oil Red O. Staining was performed for normal mature adipocytes (a) and for preadipocytes treated with or without Pingmu Decoction serum during differentiation as indicated (b–f). Blank, blank control group; Dexa, Dexamethasone group; Pingmu low, Pingmu Decoction low dose group; Pingmu moderate, Pingmu Decoction medium dose group; Pingmu high, Pingmu Decoction high dose group.

3.4. Effect of Pingmu Decoction Serum on Cell Viability. To further explore the effects of Pingmu Decoction serum, we treated differentiated adipocytes for up to 96 h. The growth curves of the Pingmu Decoction low, moderate, and high groups, compared with the Blank and Dexa groups, were significantly reduced, which indicates that the cell viability was decreased (Figure 3). There were no significant differences between the Blank and Dexa groups. The OD values of each Pingmu Decoction group compared with the control group were decreased at 48 h ($P < 0.05$). The OD values were further decreased in the Pingmu Decoction groups at 96 h, with the most dramatic decrease observed for the medium dose group ($P < 0.05$). These results verify the time-dependent effect of Pingmu Decoction serum in suppressing the growth of adipocytes from GO patients.

3.5. Effect of Pingmu Decoction Serum on Apoptosis of Mature Adipocytes. To determine whether the decrease in cell viability by Pingmu Decoction serum occurs at the level of apoptosis, we performed flow cytometry of cells assessed by Annexin V/PI double staining. The results show that the early and total apoptosis rates of mature adipocytes were 0.65% and 1.53% in the blank control group. However, the cell apoptosis of each Pingmu Decoction group was increased ($P < 0.05$),

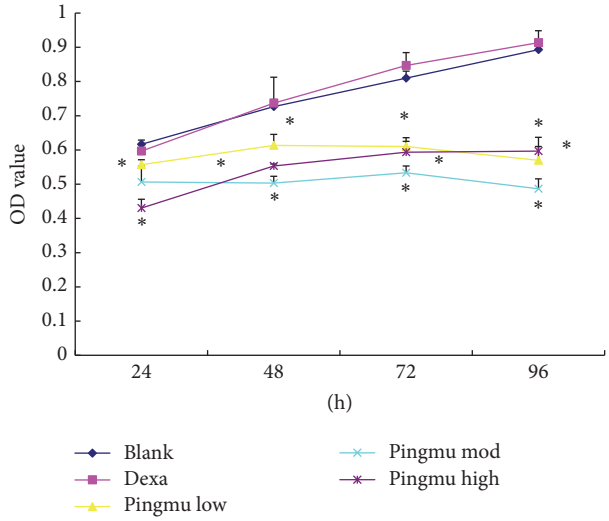

Figure 3: MTT cell viability assay of control adipocytes and adipocytes treated with Pingmu Decoction serum. Blank, blank control group; Dexa, Dexamethasone group; Pingmu low, Pingmu Decoction low dose group; Pingmu moderate, Pingmu Decoction medium dose group; Pingmu high, Pingmu Decoction high dose group. $^{*}P < 0.05$ versus the blank control group ($n = 3$ per group).

with the early and total apoptosis rates in the Pingmu Decoction medium dose group being the highest (Figure 4). There were no significant differences between Dexa and blank groups. There were statistical differences between the medium dose group and low dose group ($P < 0.05$), but not the high dose group, in the early apoptosis rate. These results suggest that Pingmu Decoction serum induces apoptosis of mature GO adipocytes, with the most dramatic effect occurring at the medium dose.

3.6. Effect of Pingmu Decoction Serum on the Expression of Fas and Fas L mRNA. To further verify the apoptotic effect of Pingmu Decoction serum and to determine whether the effect might be explained by alterations in the expression of the apoptosis modulators Fas and Fas L, we performed RT-PCR. The relative expression of Fas mRNA in adipocytes from each Pingmu Decoction group was higher than blank control group (low: 1.37-fold increase; medium: 1.50-fold increase; high: 1.42-fold increase), and the difference between the low dose group and the blank group was statistical ($P < 0.05$). Furthermore, the relative expression quantity of Fas L mRNA in adipocytes from each Pingmu Decoction was higher than blank control ($P < 0.05$) (low: 1.32-fold increase; medium: 1.46-fold increase; high: 1.42-fold increase) (Figure 5). There were no significant differences in the expression of Fas or Fas L mRNA between the Blank and Dexa groups.

3.7. Effect of Pingmu Decoction Serum on the Expression of Fas and Fas L Protein. The protein expression of Fas and Fas L was further assessed by Western blotting. Compared with the blank control group, the Fas and Fas L expression of each Pingmu Decoction group was increased statistically ($P < 0.05$) (Figure 6). Among the Pingmu Decoction groups, the low dose group had the highest expression of Fas but the lowest expression of Fas L, and the high dose group has the lowest expression of Fas but the highest expression of Fas L. There was no significant difference between the Blank and Dexa groups. These results verify the RT-PCR results suggesting that Pingmu Decoction may induce apoptosis of GO adipocytes by increasing Fas/Fas L signaling but suggest that the relationship may not be strictly dose-dependent.

3.8. Pingmu Decoction Decreases Protein Expression of Adipogenic Transcription Factors. To identify the effect of Pingmu Decoction on adipogenic transcription factors, the protein expression of PPAR γ and C/EBP α was further assessed by Western blotting. Compared with the blank control group, the PPAR γ and C/EBP α expression of each Pingmu Decoction group was decreased statistically ($P < 0.05$) (Figure 7). Among the Pingmu Decoction groups, there was no significant difference. And also there was no significant difference between the Blank and Dexa groups.

4. Discussion

The clinical symptoms of patients with GO are caused by a shift in the balance between limited orbital volume and increasing amounts of the orbital adipose tissue [15]. The increase in orbital adipose tissue can directly increase orbital pressure. The abnormal proliferation of orbital adipose tissue and fat accumulation play a major role in the occurrence and development of GO. Accordingly, the role of orbital adipose tissue in GO has received increasing attention [16–18]. CT examination has indicated that the increase in orbital fat in GO is consistent with the degree of exophthalmos and inconsistent with orbital muscle enlargement [19]. Potgieser and others [20] have demonstrated that the increase in extraocular muscle volume in GO is obviously lower than the increase in orbital adipose tissue volume, and the correlation coefficient between total orbital adipose volume and the degree of exophthalmos is higher than the correlation coefficient between extraocular muscle volume and exophthalmos. Kumar and others [21] found evidence of new adipose tissue in GO patients. Furthermore, some GO patients with obvious exophthalmos are observed to only manifest with an increase in the retrobulbar adipose tissue, without the enlargement of extraocular muscle. Patients with this variety of GO mainly manifest with exophthalmos, which will affect appearance. In this case, the patients' total cross-sectional area of extraocular muscle is not large [22, 23].

To examine the mechanisms of growth control in adipocytes by Pingmu Decoction serum, we cultured preadipocytes. Preadipocytes were shown to be cultured successfully by the tissue explant method in this study. Cells emerged from the adipose tissue block on the 4th day. The primary cells were spindle shaped with oval or near-circular nuclei, which is similar to the morphology of fibroblasts under the microscope. The cells proliferated gradually at first and then proliferated more rapidly after passage. We verified the identification of human preadipocytes from the primary culture of orbital adipose tissue by staining for Pref-1, a

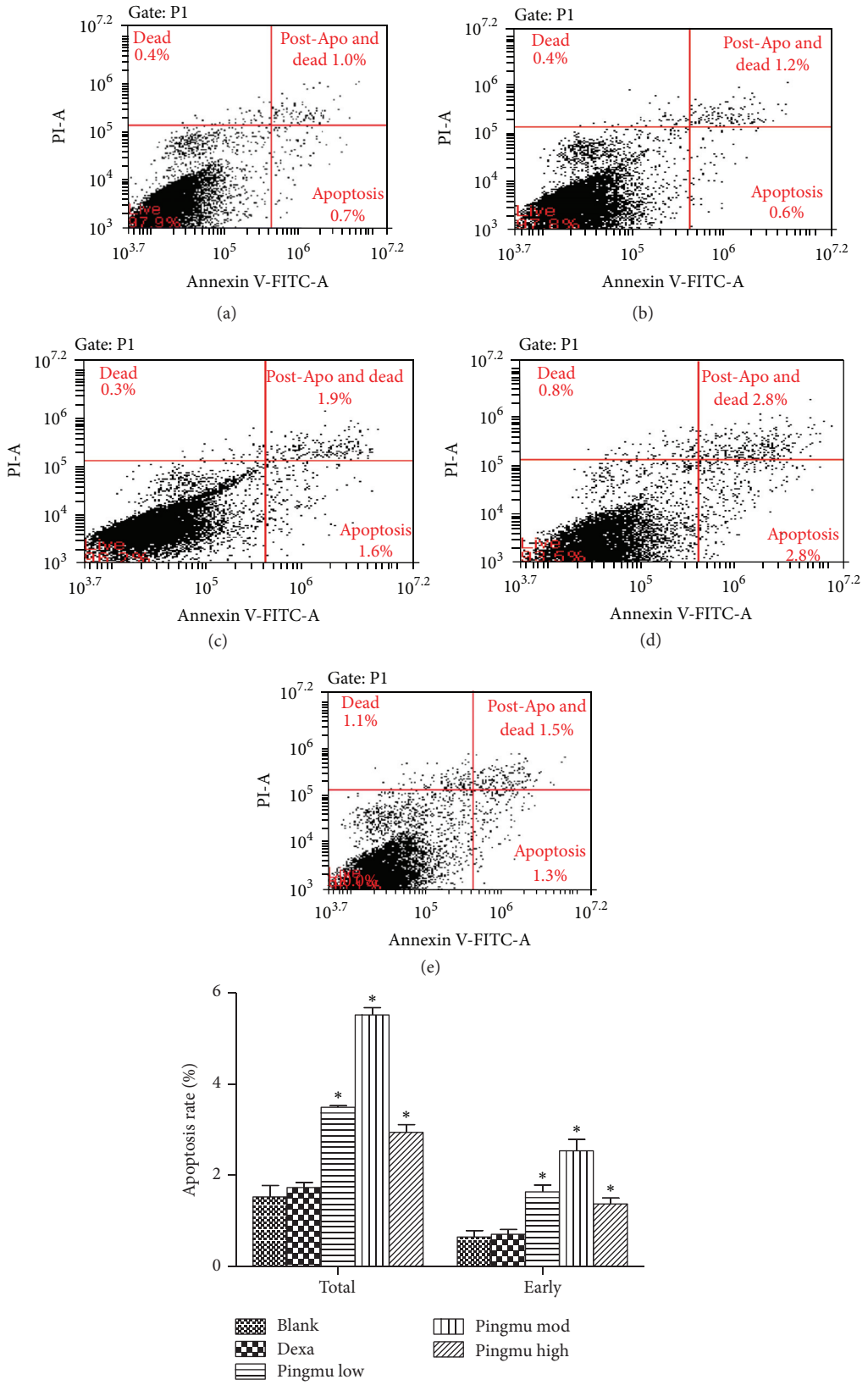

Figure 4: Apoptosis rates of the matured adipocytes treated with Pingmu Decoction serum. Apoptosis rates were determined by Annexin V/PI staining and flow cytometry. Blank control group (a); Dexamethasone group (b); Pingmu Decoction low dose group (c), Pingmu Decoction medium dose group (d); Pingmu Decoction high dose group (e). $^{*}P < 0.05$ versus the blank control group ($n = 3$ per group).

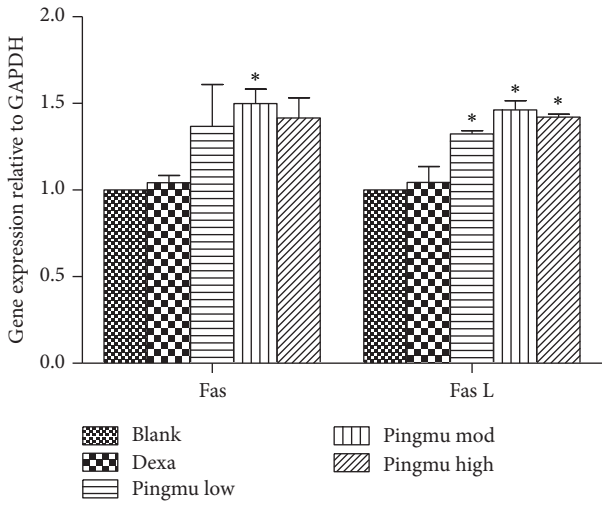

Figure 5: Effect of Pingmu Decoction serum on the expression of Fas and Fas L mRNA. Expression was quantified by RT-PCR. Blank, blank control group; Dexa, Dexamethasone group; Pingmu low, Pingmu Decoction low dose group; Pingmu moderate, Pingmu Decoction medium dose group; Pingmu high, Pingmu Decoction high dose group. $^{*}P < 0.05$ versus the blank control group ($n = 3$ per group).

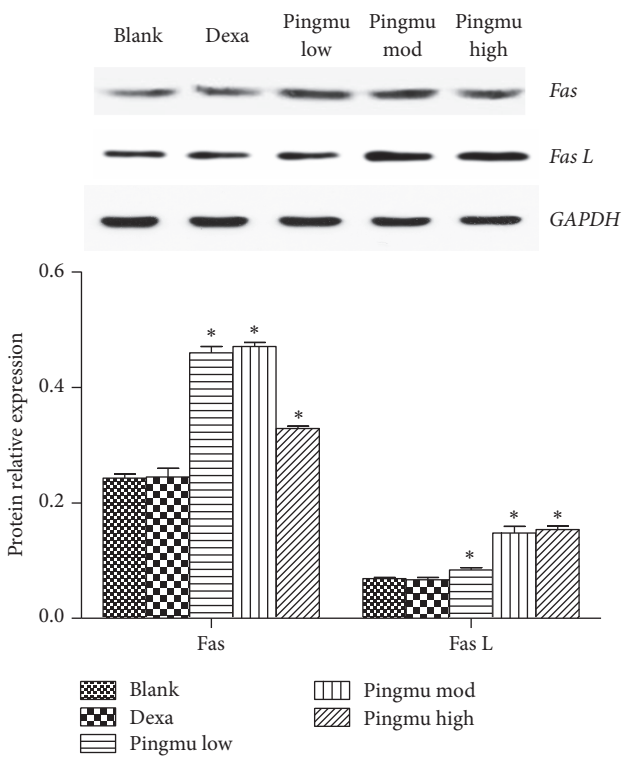

Figure 6: Effect of Pingmu Decoction serum on the expression of Fas and Fas L protein. Protein expression was quantified by Western blotting. Blank, blank control group; Dexa, Dexamethasone group; Pingmu low, Pingmu Decoction low dose group; Pingmu moderate, Pingmu Decoction medium dose group; Pingmu high, Pingmu Decoction high dose group. $^{*}P < 0.05$ versus the blank control group ($n = 3$ per group).

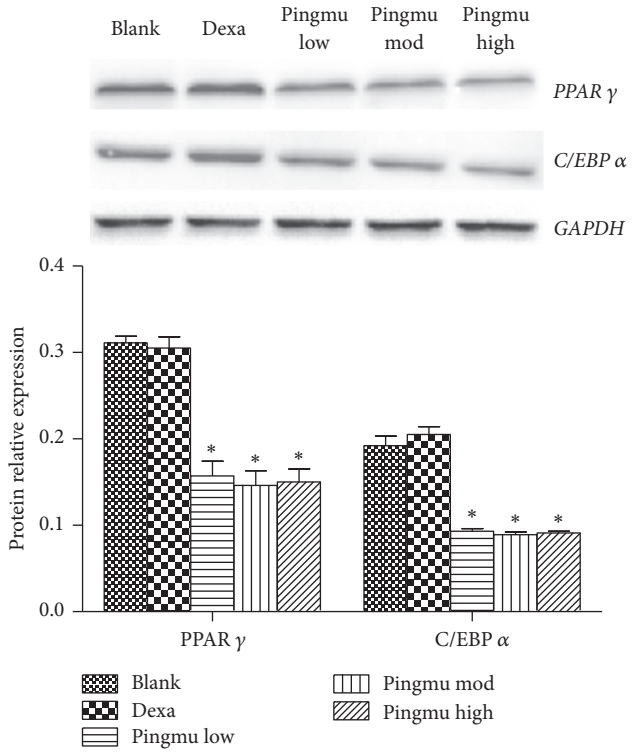

Figure 7: Effect of Pingmu Decoction serum on the expression of PPAR γ and C/EBP α protein. Protein expression was quantified by Western blotting. Blank, blank control group; Dexa, Dexamethasone group; Pingmu low, Pingmu Decoction low dose group; Pingmu moderate, Pingmu Decoction medium dose group; Pingmu high, Pingmu Decoction high dose group. $^{*}P < 0.05$ versus the blank control group ($n = 3$ per group).

marker expressed preferentially in preadipocytes, rather than mature adipocytes. Pref-1 inhibits the differentiation of the preadipocytes and reduces the generation of fat [24], and glucocorticoid can promote the differentiation of the adipocytes by inhibiting the expression of Pref-1 [25]. Our examination revealed that Pref-1 was positively expressed in cultured cells, which verifies that these cells were preadipocytes. Oil Red O staining, a specific method for staining lipid droplets, also was used to confirm that preadipocytes could be differentiated into mature adipocytes, which further validates our isolation and culture methods.

The effects of Pingmu Decoction on cell viability were assessed by MTT assay. Our results show that the cell viability of preadipocytes could be reduced by Pingmu Decoction serum at low medium and high doses at 48 h, with the most significant effects observed with the medium dose and at 96 h. The results of flow cytometry revealed that the early and total apoptosis rates of matured adipocytes were also increased obviously for cells exposed to Pingmu Decoction serum ($P < 0.05$), with the most dramatic effects in the medium and low dose groups. These results suggest that Pingmu Decoction can promote the apoptosis of adipocytes from GO patients. In these experiments, the medium dose, which was designed to reflect the prescribed human dose, was most effective.

However, additional experiment with a more narrow range of doses might verify a dose-effect relationship.

We also demonstrated that Pingmu Decoction serum mediates an increase in Fas and Fas L, which was shown both at the level of mRNA and protein. Thus, the mechanism by which Pingmu Decoction serum may act to promote cell death could involve the activation of death receptor apoptosis mediated by Fas and Fas L expression. While the current study was limited in the availability of primary tissues, future experimentation should be performed to investigate the responsiveness of the primary adipocytes to Fas L, as well as the Fas L concentration in the orbital locale of patients as compared to healthy subjects. Pingmu Decoction reduced lipid accumulation and downregulated the expression of PPAR γ and C/EBP α. Icariin is the main constituent of Herba Epimedii. Han et al. found that Icariin can inhibit the adipocyte differentiation through downregulation of the adipogenic transcription factors [26]. Zhang et al. show that Icariin could inhibit adipogenic differentiation of BMSCs in the osteoblast-osteoclast coculture [27]. And Icariin can also inhibit the adipogenic transdifferentiation of osteoblasts [28]. However, despite experimental limitations, our study is consistent with the possibility that Pingmu Decoction reduces the accumulation of orbital adipocytes in the inactive stage of GO to play a therapeutic role, and this effect is likely to be explained by increased Fas/Fas L expression and increased apoptosis.

In this study, we used standardized methods to produce the Pingmu Decoction serum. Components used to make the Pingmu Decoction were produced in factories that adhere to TCM good manufacturing practice. Additionally, our protocols followed methods that are used in clinical application as described in the *Pharmacology and Pharmacological Experiments with Traditional Chinese Medicine* [29]. However, as for any form of herbal medicine, batches of Pingmu Decoction may vary according to the source. For this reason, future studies should be done to verify the findings using Pingmu Decoction from other sources.

5. Conclusion

Our results show that Pingmu Decoction can reduce the cell viability of orbital preadipocytes and inhibit their differentiation into adipocytes. This effect may be mediated by the activation of Fas and Fas L by the death signaling pathway to promote the apoptosis of matured adipocytes. These results suggest a therapeutic mechanism for Pingmu Decoction in reducing the accumulation of orbital adipocytes in GO.

Conflicts of Interest

The authors declare that there are no conflicts of interest regarding the publication of this paper.

Acknowledgments

This study is supported by Grants from the National Natural Science Foundation of China (Grant no. 81373617).

References

[1] J. Shen, Z. Li, W. Li et al., "Th1, Th2, and Th17 cytokine involvement in thyroid associated ophthalmopathy," *Disease Markers*, vol. 2015, Article ID 609593, 6 pages, 2015.

[2] K. P. Cockerham and S. S. Chan, "Thyroid eye disease," *Neurologic Clinics*, vol. 28, no. 3, pp. 729–755, 2010.

[3] S. S. Cury, M. Oliveira, M. T. Síbio et al., "Gene expression of estrogen receptor-alpha in orbital fibroblasts in Graves' ophthalmopathy," *Archives of Endocrinology and Metabolism*, vol. 59, no. 3, pp. 273–276, 2015.

[4] F. Menconi, C. Marcocci, and M. Marinò, "Diagnosis and classification of Graves' disease," *Autoimmunity Reviews*, vol. 13, no. 4-5, pp. 398–402, 2014.

[5] L. Bartalena, "Diagnosis and management of Graves disease: a global overview," *Nature Reviews Endocrinology*, vol. 9, no. 12, pp. 724–734, 2013.

[6] J. Barrio-Barrio, A. L. Sabater, E. Bonet-Farriol, Á. Velázquez-Villoria, and J. C. Galofré, "Graves' ophthalmopathy: VISA versus EUGOGO classification, assessment, and management," *Journal of Ophthalmology*, vol. 2015, Article ID 249125, 16 pages, 2015.

[7] R. S. Bahn, "Current insights into the pathogenesis of graves' ophthalmopathy," *Hormone and Metabolic Research*, vol. 47, no. 10, pp. 773–778, 2015.

[8] S. Virakul, V. A. S. H. Dalm, D. Paridaens et al., "Platelet-derived growth factor-BB enhances adipogenesis in orbital fibroblasts," *Investigative Ophthalmology and Visual Science*, vol. 56, no. 9, pp. 5457–5464, 2015.

[9] J. A. Garrity and R. S. Bahn, "Pathogenesis of graves ophthalmopathy: implications for prediction, prevention, and treatment," *American Journal of Ophthalmology*, vol. 142, no. 1, pp. 147.e2–153.e2, 2006.

[10] A. Antonelli, S. M. Ferrari, S. Frascerra et al., "Peroxisome proliferator-activated receptor-α agonists modulate CXCL9 and CXCL11 chemokines in Graves' ophthalmopathy fibroblasts and preadipocytes," *Molecular and Cellular Endocrinology*, vol. 349, no. 2, pp. 255–261, 2012.

[11] S. Kumar, S. Nadeem, M. N. Stan, M. Coenen, and R. S. Bahn, "A stimulatory TSH receptor antibody enhances adipogenesis via phosphoinositide 3-kinase activation in orbital preadipocytes from patients with Graves' ophthalmopathy," *Journal of Molecular Endocrinology*, vol. 46, no. 3, pp. 155–163, 2011.

[12] H. Li, Y. Wang, and R. Xu, "Pingmu decoction enhances apoptosis of orbital adipocytes derived from patients with Graves' ophthalmophathy," *Molecular Medicine Reports*, vol. 6, no. 6, pp. 1361–1366, 2012.

[13] A. Bossowski, B. Czarnocka, A. Stasiak-Barmuta, K. Bardadin, M. Urban, and J. Dadan, "Analysis of Fas, FasL and Caspase-8 expression in thyroid gland in young patients with immune and non-immune thyroid diseases," *Endokrynologia Polska*, vol. 58, no. 4, pp. 303–313, 2007.

[14] C. Gajate and F. Mollinedo, "Lipid raft-mediated Fas/CD95 apoptotic signaling in leukemic cells and normal leukocytes and therapeutic implications," *Journal of Leukocyte Biology*, vol. 98, no. 5, pp. 739–759, 2015.

[15] P. Janusz, E. Pawlak-Adamska, I. E. Kochanowska, and J. Daroszewski, "The role of adipose tissue in the pathogenesis and clinical manifestation of graves' orbitopathy," *Postepy Higieny i Medycyny Doswiadczalnej*, vol. 67, pp. 1173–1181, 2013.

[16] J. S. Yoon, H. J. Lee, M. K. Chae, and E. J. Lee, "Autophagy is involved in the initiation and progression of graves' orbitopathy," *Thyroid*, vol. 25, no. 4, pp. 445–454, 2015.

[17] M. S. Draman, F. Grennan-Jones, L. Zhang et al., "Effects of prostaglandin F2α on adipocyte biology relevant to graves' orbitopathy," *Thyroid*, vol. 23, no. 12, pp. 1600–1608, 2013.

[18] S. E. Kim, J. H. Lee, M. K. Chae, E. J. Lee, and J. S. Yoon, "The role of sphingosine-1-phosphate in adipogenesis of graves' orbitopathy," *Investigative Ophthalmology and Visual Science*, vol. 57, no. 2, pp. 301–311, 2016.

[19] M. Comerci, A. Elefante, D. Strianese et al., "semiautomatic regional segmentation to measure orbital fat volumes in thyroid-associated ophthalmopathy. A validation study," *The Neuroradiology Journal*, vol. 26, no. 4, pp. 373–379, 2013.

[20] P. W. Potgieser, W. M. Wiersinga, N. I. Regensburg, and M. P. Mourits, "Some studies on the natural history of Graves' orbitopathy: increase in orbital fat is a rather late phenomenon," *European Journal of Endocrinology*, vol. 173, no. 2, pp. 149–153, 2015.

[21] S. Kumar, M. J. Coenen, P. E. Scherer, and R. S. Bahn, "Evidence for enhanced adipogenesis in the orbits of patients with graves' ophthalmopathy," *Journal of Clinical Endocrinology and Metabolism*, vol. 89, no. 2, pp. 930–935, 2004.

[22] H. C. Kim, S. W. Yoon, and H. Lew, "Usefulness of the ratio of orbital fat to total orbit area in mild-to-moderate thyroid-associated ophthalmopathy," *British Journal of Radiology*, vol. 88, no. 1053, Article ID 20150164, 2015.

[23] R. I. Cho, V. M. Elner, C. C. Nelson, and B. R. Frueh, "The effect of orbital decompression surgery on lid retraction in thyroid eye disease," *Ophthalmic Plastic and Reconstructive Surgery*, vol. 27, no. 6, pp. 436–438, 2011.

[24] K.-A. Kim, J.-H. Kim, Y. Wang, and H. S. Sul, "Pref-1 (preadipocyte factor 1) activates the MEK/extracellular signal-regulated kinase pathway to inhibit adipocyte differentiation," *Molecular and Cellular Biology*, vol. 27, no. 6, pp. 2294–2308, 2007.

[25] K. Lee, J. A. Villena, Y. S. Moon et al., "Inhibition of adipogenesis and development of glucose intolerance by soluble preadipocyte factor-1 (Pref-1)," *Journal of Clinical Investigation*, vol. 111, no. 4, pp. 453–461, 2003.

[26] Y. Y. Han, M. Y. Song, M. S. Hwang et al., "Epimedium koreanum Nakai and its main constituent icariin suppress lipid accumulation during adipocytedifferentiation of 3T3-L1 preadipocytes," *Chinese Journal of Natural Medicines*, vol. 14, no. 9, pp. 671–676, 2016.

[27] S. Zhang, P. Feng, G. Mo et al., "Icariin influences adipogenic differentiation of stem cells affected by osteoblast-osteoclast co-culture and clinical research adipogenic," *Biomedicine & Pharmacotherapy*, vol. 88, pp. 436–442, 2017.

[28] D. Zhang, C. Fong, Z. Jia, L. Cui, X. Yao, and M. Yang, "Icariin stimulates differentiation and suppresses adipocytic transdifferentiation of primary osteoblasts through estrogen receptor-mediated pathway," *Calcified Tissue International*, vol. 99, no. 2, pp. 187–198, 2016.

[29] D. F. Zhang, *Pharmacology and Pharmacological Experiments with Traditional Chinese Medicine*, Shanghai Science and Technology Press, Shanghai, China, 2002.